Title

Ketamine and Major Ketamine Metabolites Function as Allosteric Modulators of Opioid Receptors

Journal

Molecular Pharmacology, 106(5)

ISSN

0026-895X

Authors

Gomes, Ivone
Gupta, Achla
Margolis, Elyssa B
et al.

Publication Date

2024-11-01

DOI

10.1124/molpharm.124.000947

Peer reviewed

Ketamine and major ketamine metabolites function as allosteric modulators of opioid receptors

Ivone Gomes[1], Achla Gupta[1], Elyssa B. Margolis[2], Lloyd D. Fricker[3], Lakshmi A. Devi[1,4, 5@]

[1]Department of Pharmacological Sciences, Icahn School of Medicine at Mount Sinai, New York, NY, USA.

[2]UCSF Weill Institute for Neurosciences, Department of Neurology, Neuroscience Graduate Program, University of California, San Francisco, CA, USA

[3]Department of Molecular Pharmacology, Albert Einstein College of Medicine, Bronx, NY USA

[4]Nash Family Department of Neuroscience, Icahn School of Medicine at Mount Sinai, New York, NY, USA.

[5]Department of Psychiatry, Icahn School of Medicine at Mount Sinai, New York, NY, USA

Running title:

Ketamine is an opioid receptor allosteric modulator

[@]**Corresponding author:** Prof. Lakshmi A. Devi
Department of Pharmacological Sciences
Icahn School of Medicine at Mount Sinai
12-70B Icahn Building
One Gustave L. Levy Place
New York, NY10029
e-mail: lakshmi.devi@mssm.edu

Number of text pages: 44
Number of tables: 0 in regular section, supplemental tables: 8
Number of figures: 6 in regular section, supplemental figures: 5
Number of references: 87
Number of words in the Abstract: 248
Number of words in the Introduction: 744
Number of words in the Discussion: 1495

Keywords: Ketamine, opioid receptors, enkephalin, endorphin, dynorphin, morphine

Abbreviations: 6-HNK, 6-hydroxynorketamine; aCSF, artificial cerebrospinal fluid; CTAP, D-Phe-Cys-Tyr-D-Trp-Arg-Thr-Pen-Thr-NH_2; CTOP, D-Phe-Cys-Tyr-D-Trp-Orn-Thr-Pen-Thr-amide; DAMGO, [D-Ala^2, *N*-MePhe^4, Gly-ol]-enkephalin; DOR, delta opioid receptor; Dyn A17, dynorphin A17; DNQX, 6,7-Dinitroquinoxaline-2,3-dione; IPSCs, inhibitory postsynaptic currents; KOR, kappa opioid receptor; Leu-enk, leucine-enkephalin; MDD, major depressive disorder; Met-enk, methionine-enkephalin; MOR, mu opioid receptor; NK, norketamine; NMDA, N-methyl-D-aspartate; PAM, positive allosteric modulator

Conflict of Interest Statement:

"No author has an actual or perceived conflict of interest with the contents of this article."

Abstract:

Ketamine is a glutamate receptor antagonist that was developed over 50 years ago as an anesthetic agent. At subanesthetic doses, ketamine and some metabolites are analgesics and fast-acting antidepressants, presumably through targets other than glutamate receptors. We tested ketamine and its metabolites for activity as allosteric modulators of opioid receptors expressed in recombinant receptors in heterologous systems and native receptors in rodent brain; signaling was examined by measuring GTP binding, β-arrestin recruitment, MAPK activation and neurotransmitter release. While micromolar concentrations of ketamine alone had weak agonist activity at mu opioid receptors, the combination of submicromolar concentrations of ketamine with endogenous opioid peptides produced robust synergistic responses with statistically significant increases in efficacies. All three opioid receptors (mu, delta, and kappa) showed synergism with submicromolar concentrations of ketamine and either Met-enkephalin, Leu-enkephalin, and/or dynorphin A17, albeit the extent of synergy was variable between receptors and peptides. S-ketamine exhibited higher modulatory effect compared to R-ketamine or racemic ketamine with nearly ~100% increase in efficacy. Importantly, the ketamine metabolite 6-hydroxynorketamine showed robust allosteric modulatory activity at mu opioid receptors; this metabolite is known to have analgesic and antidepressant activity but does not bind to glutamate receptors. Ketamine enhanced potency and efficacy of Met-enkephalin signaling both in mouse midbrain membranes and in rat ventral tegmental area neurons, as determined by electrophysiology recordings in brain slices. Taken together, these findings support the hypothesis that some of the therapeutic effects of ketamine and its metabolites are mediated by directly engaging the endogenous opioid system.

Significance Statement:

We found that ketamine and its major biologically-active metabolites function as potent allosteric modulators of mu, delta, and kappa opioid receptors, with submicromolar concentrations of these compounds synergizing with endogenous opioid peptides such as enkephalin and dynorphin. This allosteric activity may contribute to ketamine's therapeutic effectiveness for treating acute and chronic pain and as a fast-acting antidepressant drug.

Introduction:

Ketamine is a general anesthetic developed in the 1960s. The S-stereoisomer of ketamine was recently approved by the FDA to treat major depressive disorder (MDD); the R-isomer also has antidepressant activity in animal models and the racemic mixture is used clinically to treat MDD (Andrade, 2017; Jelen et al., 2021; Kritzer et al., 2022; Passie et al., 2021). For MDD, ketamine is as effective as electroconvulsive shock therapy, eliciting a clinical response in ~50% of patients within hours of the first dose, in contrast to conventional antidepressants which take weeks for therapeutic effect onset (Almohammed et al., 2022; Anand et al., 2023; Berman et al., 2000; Cowen and Browning, 2015; Machado-Vieira et al., 2009; Zarate et al., 2006). Ketamine is also a powerful analgesic for acute and chronic pain (Barrett et al., 2020; Niesters et al., 2014).

The mechanism of ketamine's anesthetic activity is antagonism of N-methyl-D-aspartate (NMDA) receptors (Jelen and Stone, 2021; Zorumski et al., 2016). Some studies reported that NMDA receptors contribute to ketamine's antidepressant and analgesic activities t(Ma et al., 2023; Xue et al., 2023). However, there are several issues. First, doses of ketamine that treat MDD and chronic pain are typically 0.15-0.5 mg/kg i.v., which is a fraction of the anesthetic dose of 1-2 mg/kg i.v. (Zanos et al., 2018). Second, the antidepressant and analgesic effects often last for days or weeks while anesthesia wears off within minutes when plasma levels drop below ~5 μM (Zanos et al., 2018). Third, the major ketamine metabolite 6-hydroxynorketamine (6-HNK) is a potent antidepressant and analgesic but does not bind to NMDA receptors (Yost et al., 2022; Zanos et al., 2016). Thus, other targets have been proposed to contribute to ketamine's effects; these targets include α-amino-3-hydroxy-5-methyl-4-isoxazole propionic acid (AMPA) receptors (Zanos et al., 2016), formation of D-Ser (Singh et al., 2016), and the opioid system (Gupta et al., 2011).

The endogenous opioid system consists of >20 opioid peptides that act through three opioid receptors: mu (MOR), delta (DOR), and kappa (KOR) (Gomes et al., 2020; Mansour et al., 1995). Individual opioid peptides have distinct potencies and show variable signaling bias through G protein- versus β-arrestin-mediated signaling at each type of opioid receptor (Fricker et al., 2020; Gomes et al., 2020). Activation of MOR produces analgesia and has antidepressant activity (Gassaway et al., 2014; Jelen et al., 2022; Pollan, 2021; Samuels et al., 2017). Compounds that target DOR and KOR also have analgesic and antidepressant-like effects in mice (Browne and Lucki, 2019; Dubois and Gendron, 2010; Gaveriaux-Ruff et al., 2011; Suzuki et al., 2001; van Haaren et al., 2000; Wulf et al., 2022).

Ketamine weakly binds and activates opioid receptors, with reported K_i or EC_{50} values in the 7-100 μM range (Bonaventura et al., 2021; Finck and Ngai, 1982; Hess et al., 2022; Hirota et al., 1999a; Hirota et al., 1999b; Hustveit et al., 1995; Smith et al., 1980). Some studies reported that opioid antagonists block the antidepressant effects of ketamine (Klein et al., 2020; Williams et al., 2019; Williams et al., 2018; Zhang et al., 2021) although this was not observed in another study (Marton et al., 2019). Similarly, studies reported that ketamine-induced analgesia in mice is blocked by opioid receptor antagonists (Fidecka, 1987; Lawrence and Livingston, 1981; Petrocchi et al., 2019) while other studies did not see reversal by opioid antagonists (Mikkelsen et al., 1999; Wiley and Downs, 1982). In 2011, our laboratory found that low nM concentrations of ketamine potentiate the action of morphine and fentanyl (Gupta et al., 2011). This led us to hypothesize that ketamine is a positive allosteric modulator (PAM) of MOR at submicromolar concentrations, which differs from its direct agonist activity at micromolar concentrations. There are examples of other PAMs that enhance orthosteric ligand signaling at low concentrations and function as direct

agonists at higher concentrations (Abdel-Magid, 2015; Burford et al., 2013; Doornbos et al., 2018; Kandasamy et al., 2021; Pryce et al., 2021).

If ketamine's activity as an opioid receptor PAM contributes to its antidepressant and analgesic effects, then ketamine should enhance signaling of endogenous opioid peptides, as it does for opioid drugs (Gupta et al., 2011). Here, we investigated the ability of ketamine and ketamine metabolites to function as PAMs enhancing opioid peptide-engaged MOR signaling. We focused on Met-enkephalin (Met-enk), the most abundant opioid peptide in brain. We also tested the activity of ketamine at DOR and KOR. Collectively, our studies support the hypothesis that ketamine and its major metabolites are potent allosteric modulators of MOR.

Materials and Methods:

Materials: [D-Ala^2, *N*-MePhe^4, Gly-ol]-enkephalin (DAMGO, cat. No. 1171/1), R-norketamine (cat. No. 5996/10), S-norketamine (cat. No. 6112/10), CTOP (cat. No. 1578/1), were from Bio-Techne Corporation (Minneapolis, MN). Leu-enk (cat. No. 024-21), Met-enk (cat. No. 024-35), and Dyn A17 (cat. No. 021-03) were from Phoenix Pharmaceuticals, Inc (Burlingame, CA). Morphine (cat. No. M8777), RS-ketamine (cat. No.K-2753), 2R,6R-hydroxynorketamine (cat. No. SML1873), 2S,6S- hydroxynorketamine (cat. No. SML1875), protease inhibitor cocktail (cat. No. P2714), phosphatase inhibitor cocktail (cat. No. P0044), GDP (cat. No. G7127), GTPγS (cat. No. G8634) and antibodies recognizing tubulin (cat. No. T8660, RRID:AB_477590) were from Millipore Sigma (St. Louis, MO). R-ketamine (cat. No. 26316), S-ketamine (cat. No. 26317), and RS-norketamine (cat. No.15787) were from Cayman Chemicals (Ann Arbor, MI). 2R,6R-hydroxynorketamine was also purchased from Cayman Chemicals (Ann Arbor, MI; cat. No. 19603) and Bio-Techne Corporation (Minneapolis, MN; cat. No. 6094) and 2S,6S-

hydroxynorketamine from Bio-Techne Corporation (Minneapolis, MN; cat. No. 6095) and since only 2R,6R-hydroxynorketamine and 2S,6S-hydroxynorketamine purchased from Millipore Sigma gave consistent results in all our assays the data presented here are with compounds from Millipore Sigma. [^{35}S]GTPγS (cat. No. NEG030H250UC) was from Perkin-Elmer (Shelton, CT). Antibodies to phospho-ERK1/2 (cat. No. 4370S, RRID:AB_2315112) and total ERK1/2 (cat. No. 4696S, RRID:AB_390780) were from Cell Signaling Technology (Danvers, MA). Rabbit IRDye 800 (cat. No. 926-32211, RRID:AB_621843) and mouse IRDye 680 (cat. No. 926-68070, RRID:AB_10956588) secondary antibodies were from LI-COR Biosciences (Lincoln, NE). F12 media (cat. No. 11765-054), MEM Alpha media (cat. No. 12571-063), streptomycin-penicillin (cat. No. 15140-122), hygromycin (cat. No. 10687010) were from Gibco/Thermo Fisher (Waltham, MA). Fetal bovine serum (FBS, cat. No. FBS-01) was from LDP, Inc (Towaco, NJ). Geneticin (G418, cat. No.G-418-10) was from GoldBio (St. Louis, MO). The PathHunter Chemiluminescence detection kit (cat. No. 93-0001) was from DiscoverX (Eurofins Corporation, Fremont, CA). GF/B filters (cat. No. FP-100) were from Brandel, Inc. (Gaithersburg, MD). Additional reagents for the electrophysiology study included bestatin (Thermofisher, cat. No. 78433), thiorphan (Cayman Chemicals, cat. No. 15600), 6,7-Dinitroquinoxaline-2,3-dione (DNQX) from Hello Bio (cat. No. HB0261), and D-Phe-Cys-Tyr-D-Trp-Arg-Thr-Pen-Thr-NH2 (CTAP) from Fisher Scientific (cat. No. AAJ66219MCR).

Animals: Adult (12 weeks old) male C57BL/6 mice (Jackson Laboratories, Ban Harbor, ME; RRID:IMSR_JAX:000664) weighing 20-25 g were sacrificed using CO_2 from compressed gas according to the protocol approved by the Icahn School of Medicine Institutional Animal Care and

Use Committee (LA11-00322), midbrain regions were extracted from individual mice by gross dissection and used to prepare membranes as described above.

Adult male Sprague-Dawley rats (Envigo, Indianapolis, IN; RRID:RGD_734476) weighing 250-300 g were used for whole cell electrophysiology recordings. Procedures were conducted in strict accordance with the recommendations of the National Institutes of Health (NIH) described in the Guide for the Care and Use of Laboratory Animals. Research protocols were approved by the Institutional Animal Care and Use Committee (University of California at San Francisco, CA), approval ID AN200119-00F.

Cell Culture: CHO cells (ATCC Cat# CCL-61, RRID:CVCL_0214) were grown in F12 media containing 10% (vol/vol) FBS and streptomycin-penicillin. CHO cells stably expressing Flag-tagged mouse MOR (*OPRM1*), mouse DOR (*OPRD1*), or rat KOR (*OPRK1*) were generated previously (Cvejic et al., 1996; Jordan and Devi, 1999; Trapaidze et al., 2000), and grown in F12 media containing 10% (vol/vol) FBS, streptomycin-penicillin, and 500 μg/mL geneticin. The plasmids for Flag-epitope tagged mouse mu and delta opioid receptors were a gift from Dr. M. von Zastrow, UCFS. The plasmid for untagged rat kappa opioid receptor was a gift from Dr. David Grandy, Oregon Health Sciences University and was tagged with a Flag epitope at the N-terminus as described in (Jordan and Devi, 1999). Saturation binding assays with [^{3}H]DAMGO show that CHO cells stably expressing Flag-tagged mouse MOR exhibit a Kd of 2±1nM and a Bmax of 517±9 fmol/mg protein, with [^{3}H]Deltorphin II show that Flag-tagged mouse DOR exhibit a Kd of 3±2 nM and a Bmax of 497±13 fmol/mg protein, with [^{3}H]U69,593 show that Flag-tagged rat kappa opioid receptor exhibits a Kd of 1±1nM and a Bmax of 322±10 fmol/mg protein. MOR UO5S cells expressing human MOR tagged with a ProLink/β-gal donor (PK) fragment at the C-

terminal region and β-arrestin tagged with a complementary β-gal activator (EA) fragment ($MOR^{\beta gal}$) were a gift from DiscoverX (Fremont, CA; cat. No. 93-0213C3). These cells were grown in MEM Alpha media containing 10% (vol/vol) FBS, streptomycin-penicillin, 500 μg/mL of geneticin, and 250 μg/mL of hygromycin. Saturation binding assays with [^{3}H]DAMGO show that the cells exhibit a Kd of 6±1nM and a Bmax of 690±50 fmol/mg protein.

Measurement of ERK1/2 phosphorylation: CHO cells expressing MOR (2×10^5 cells/well) were seeded into 24-well poly-D-lysine-coated plates (Corning, Kennebunk, ME; cat. No. 356414). Next day, cells were grown in growth media without FBS for 3 h followed by treatment with either vehicle, morphine, DAMGO, or Met-enk (0–10^{-6} M) in the absence or presence of 100 nM RS-ketamine for 5 min at 37 °C. RS-ketamine was added first followed by either morphine, DAMGO, or Met-enk. In a separate set of experiments, cells were treated with vehicle, RS-ketamine (0–10^{-6} M) in the absence or presence of 100 nM Met-enk for 5 min at 37 °C. RS-ketamine was added first followed by Met-enk.

Cells were lysed with 2% sodium dodecyl sulfate in 50 mM Tris-Cl, pH 6.8 containing protease and phosphatase inhibitor cocktails and aliquots of lysates were subjected to Western blot analysis as described (Gupta et al., 2011; Gupta et al., 2016) using antibodies to phosphoERK1/2 (1:1,000), to total ERK1/2 (1:1,000), and to tubulin (1:5000) as primary antibodies. Anti-rabbit IRDye 800 (1:10,000) and anti-mouse IRDye 680 (1:10,000) were used as secondary antibodies. Protein bands were visualized and densitized using the Odyssey infrared imaging system (LI-COR Biosciences; Lincoln, NE).

Membrane preparation: Membranes from CHO cells alone, from CHO cells expressing either MOR, DOR, or KOR, or from the midbrain of 4 individual wild-type C57Bl/6 mice were prepared as described previously (Gomes et al., 2016; Mack et al., 2022). Briefly, cells/midbrain tissue were homogenized in 25 volumes (1 g wet weight per 25 ml) of ice-cold 20 mM Tris-Cl buffer, pH 7.4, containing 250 mM sucrose, 2 mM EGTA, and 1 mM $MgCl_2$, followed by centrifugation at 27,000*g* for 15 minutes at 4°C. The pellet was resuspended in 25 ml of the same buffer, and the centrifugation step was repeated. The resulting membrane pellet was resuspended in 10 volumes (of original wet weight) of 2 mM Tris-Cl buffer, pH 7.4, containing 2 mM EGTA and 10% glycerol. The protein content of the homogenates was determined using the Pierce BCA Protein Assay reagent (Rockford, IL), after which homogenates were stored in aliquots at -80°C until use.

[^{35}S]GTPγS binding: [^{35}S]GTPγS binding assays were carried out as described previously (Gomes et al., 2020; Mack et al., 2022). In experiments examining if RS-ketamine exhibits signaling at MOR, membranes (20 μg protein) from CHO cells alone or from CHO cells expressing MOR were incubated for 1 hour at 30°C with different concentrations of RS-ketamine in the absence or presence of 1 μM final concentration CTOP (CTOP/assay buffer was added first to the tubes followed by RS-ketamine) in assay buffer A (50 mM Tris-Cl buffer, pH 7.4, containing 100 mM NaCl, 10 mM $MgCl_2$, 0.2 mM EGTA, and protease inhibitor cocktail) containing freshly prepared 30 μM GDP, and 0.1 nM [^{35}S]GTPγS. Nonspecific binding was determined in the presence of 10 μM cold GTPγS. Basal values represent values obtained in the presence of GDP and in the absence of ligand. In experiments examining the allosteric effects of different ketamines on opioid-mediated G-protein activity, membranes (20 μg protein) from cells expressing either MOR, DOR, or KOR, or from midbrain of each single mouse were incubated with opioids and/or ketamines;

ketamines (concentrations described in figure legends) were added first followed by different concentrations of opioids and assay carried out as described above. At the end of the incubation period, samples were filtered using a Brandel filtration system and GF/B filters. Filters were washed three times with 3 ml of ice-cold 50 mM Tris-Cl buffer, pH 7.4, and bound radioactivity was measured using a scintillation counter (MicroBeta TriLux; PerkinElmer).

β-arrestin recruitment: Cells expressing $MOR^{\beta gal}$ were plated in each well of either a 96-well white clear bottom plate (Corning, Kennebunk, ME; cat. No. 3903; 10,000 cells/well) or a 384-well white clear bottom plate (Thermo Scientific, Rochester, NY; cat. No. 142762; 2,500 cells/well) in 100 μL media. The next day, cells were rinsed with buffer A and treated with different concentrations of ketamines (concentrations described in figure legends) followed by opioids; for 60 min at 37 °C in buffer A. At the end of the incubation period, the bottoms of the plates were sealed with white vinyl sealing tape, and *β*-arrestin recruitment measured using the PathHunter Chemiluminescence detection kit, as described in the manufacturer's protocol (DiscoverX).

Slice preparation and ex vivo whole-cell electrophysiology: Rats were anesthetized with isoflurane and their brains removed. Horizontal brain slices (200 μm thick) containing the ventral tegmental area (VTA) were prepared using a vibratome (Campden Instruments). Slices were cut in ice-cold artificial CSF solution containing (in mM): 126 NaCl, 2.5 KCl, 1.2 $MgCl_2$, 1.4 NaH_2PO_4, 2.5 $CaCl_2$, 25 $NaHCO_3$, and 11 glucose saturated with 95% O_2 – 5% CO_2 and then allowed to recover at 33°C for at least 1 h. Individual slices were visualized under a Zeiss AxioExaminer D1 with

differential interference contrast, Dodt, and near-infrared optics using a monochrome Axiocam 506 (Zeiss).

Whole-cell patch-clamp recordings were made at 33°C using 2.5–5 MΩ pipettes containing (in mM) 128 KCl, 20 NaCl, 1 $MgCl_2$, 1 EGTA, 0.3 $CaCl_2$, 10 HEPES, 2 MgATP, and 0.3 Na_3GTP (pH 7.2, osmolarity adjusted to 275). Signals were amplified using an IPA amplifier with SutterPatch software (Sutter Instrument) filtered at 1 kHz and collected at 10 kHz. Voltage clamp recordings were made at $V_{holding}$ = -70 mV. Series resistance and input resistance were tracked throughout the experiment (0.1 Hz) with 4 mV, 200 ms hyperpolarizing steps. $GABA_A$ receptor-mediated inhibitory postsynaptic potentials were pharmacologically isolated with 6,7-dinitroquinoxaline-2,3(1H,4H)-dione (DNQX: 10 μM). Stimulating electrodes were placed 80–250 μm anterior or posterior to the soma of the recorded neuron. To measure drug effects on evoked inhibitory post synaptic currents (IPSCs), paired pulses (50-ms interval) were delivered once every 10 s. At least 7 min of baseline evoked IPSCs were collected in control aCSF or 10 nM ketamine. Met-enk was then added to the aCSF perfusion for 7 min. In a subset of experiments 500 nM CTAP was then added to the Met-enk solution for an additional 7-10 min.

The IPSC amplitude was calculated by comparing the peak PSC voltage to a 2 ms interval just before stimulation. All drugs were bath-applied.

Data Analysis: Each experiment was carried out 3 independent times with triplicates unless otherwise stated. Data were analyzed using GraphPad Prism 10 software. Each data set was fit in GraphPad Prism 10 using sigmoidal or bell-shaped concentration response models to determine which one fits best with confidence intervals of 95% for EC_{50} and $E_{max.}$ Statistical analysis was carried out in GraphPad Prism 10 using either Student's t-test, One-Way ANOVA with Tukey's

multiple comparison test (indicated as preferred tests in GraphPad Prism 10) or Two-Way ANOVA with Sidak's or Tukey's multiple comparison test GraphPad Prism 10 (indicated as preferred tests in GraphPad Prism 10) with $p<0.05$ considered to be significant. Since the studies in this manuscript are exploratory, the described p-values are descriptive.

Whole cell recording data were analyzed in IGOR (Wavemetrics). Drug effects were quantified by comparing the mean evoked IPSC amplitude during the 4 min of baseline just preceding drug application and the mean response amplitudes during minutes 4–7 of drug application. $p < 0.05$ was considered significant.

Results

Modulation of MOR-mediated ERK1/2 phosphorylation by RS-ketamine

We previously used ERK1/2 phosphorylation as a readout for MOR activation and found that a combination of morphine and RS-ketamine in a 1:1 ratio caused a greater response than either drug alone (Gupta et al., 2011). Here we extend this finding with a peptidic synthetic ligand, DAMGO, and an endogenous peptide, Met-enk. First, to confirm earlier findings, studies were carried out with morphine. As previously found, treatment with 100 nM RS-ketamine plus morphine produced a significant increase in ERK1/2 phosphorylation compared to cells treated with morphine alone (***$p>0.001$; Fig. 1A, Supplemental Fig. 1). The increase was especially dramatic at the lowest concentration of morphine tested (0.1 nM). Next, we examined the effect of 100 nM RS-ketamine on DAMGO, a classic synthetic peptidic agonist. The results revealed that for morphine RS-ketamine significantly enhanced signaling by DAMGO (***$p<0.001$; Fig. 1B, Supplemental Fig. 1).

The endogenous opioid peptide Met-enk also showed synergism with RS-ketamine (Fig. 1C, Supplemental Fig. 1), and the RS-ketamine-mediated increase was most pronounced at low concentrations of Met-enk. For example, 0.1 nM Met-enk alone produced a negligible response, but when combined with 100 nM RS-ketamine there was an 8-fold increase in signaling over basal (Fig. 1C). The E_{max} for all three opioids was higher in the presence of 100 nM RS-ketamine (Supplemental Table 1). The EC_{50} values for each opioid were dramatically lower in the presence of 100 nM RS-ketamine although statistical analyses failed to reach significance (Supplemental Table 1). It should be pointed out that RS-ketamine alone showed a small increase in phosophoERK1/2 levels but only at high concentrations (1 μM), whereas in the presence of 100 nM Met-Enk there was an enhancement of phosphoERK1/2 levels with submicromolar concentrations of RS-ketamine (Fig. 1D; Supplemental Table 1). Comparison of the effect of 100 nM RS-ketamine alone, or 100 nM Met-enk alone, with that of a combination of RS-ketamine and Met-enk clearly indicates that the combination of ligands produces a greater increase compared to either ligand alone (Fig. 1E). Moreover, because submicromolar concentrations of RS-ketamine alone have no effect, the increases seen with the combination of submicromolar RS-ketamine and Met-enk are much greater than additive changes. Together, these results confirm our earlier study and extend it by showing that submicromolar concentrations of RS-ketamine potently synergize with opioid peptides.

Modulation of MOR-mediated G-protein activity by RS-ketamine

Activation of opioid receptors can lead to activation of G-protein-dependent and β-arrestin-dependent pathways of signaling (Al-Hasani and Bruchas, 2011; McLennan et al., 2008; Zheng et al., 2008a; Zheng et al., 2008b). In order to directly examine the effect of RS-ketamine on G protein

signaling, increases in [^{35}S]GTPγS binding was measured in CHO cells expressing MOR and compared to CHO cells alone. In CHO cells alone (without MOR), RS-ketamine did not cause measurable signaling (Fig. 2A) whereas in cells with MOR a small increase in signal (~20% over basal) was observed at high concentrations (10 μM), and this was completely blocked by the MOR antagonist CTOP (Fig. 2B, Supplemental Table 2). These data fit with a previous study that found that ketamine alone had partial agonist activity at MOR, with an EC_{50} of ~9 and ~34 μM for the S- and R-stereoisomers, respectively (Bonaventura et al., 2021).

Next, the ability of RS-ketamine to enhance signaling by the classic MOR agonist DAMGO was examined. Because nanomolar concentrations of RS-ketamine do not increase signaling in the absence of opioid agonists (Fig. 2B), we examined the effects of these concentrations on [^{35}S]GTPγS binding mediated by DAMGO (Fig. 2C). RS-ketamine at a concentration as low as 1 nM was able to enhance maximal signaling by DAMGO with an increase in the potency (Fig. 2C, Supplemental Table 2). Next, the ability of RS-ketamine to synergize with the endogenous opioid peptide, Met-enk was examined (Fig. 2D, E). Met-enk responses in the absence or presence of different concentrations of RS-ketamine show a concentration-dependent enhancement of Met-enk efficacy (Fig. 2D, E; Supplemental Fig. 2D, E; Supplemental Table 2). For example, 1 nM RS-ketamine caused a ~64% increase and 100 nM RS-ketamine a ~78% increase in the [^{35}S]GTPγS binding mediated by 1 μM Met-enk (taken as 100%; Fig. 2E; Supplemental Fig. 2E; Supplemental Table 2). Morphine responses in the absence and presence of different concentrations of RS-ketamine also show that nanomolar concentrations of RS-ketamine increase the efficacy for morphine, with 100 nM RS-ketamine increasing the efficacy of signaling by 100 nM morphine by ~131% (Fig. 2F, G; Supplemental Fig. 2F, G; Supplemental Table 2). Taken together, these results

show that RS-ketamine enhances G protein signaling by MOR mediated by peptidic (DAMGO, Met-Enk) and non-peptidic (morphine) agonists.

Modulation of MOR-mediated β-arrestin recruitment by RS-ketamine

Next, we examined the effect of RS-ketamine on opioid peptide- or morphine-mediated β-arrestin recruitment using the enzyme-fragment complementation technology developed by DiscoverX. In their $MOR^{\beta gal}$ cell line, MOR is tagged at the C-terminus with a β-galactosidase fragment and β-arrestin is tagged with the enzyme acceptor fragment; activation of the receptor selectively recruits β-arrestin leading to β-galactosidase activity, providing a rapid, sensitive, and selective read-out of MOR activation (Gomes et al., 2020). In this assay, RS-ketamine elicits a weak signal (~17% above basal) at the maximum concentration tested, 10 μM (Fig. 2H; Supplemental Table 2). Because signaling by submicromolar concentrations of RS-ketamine was not different from basal signaling in this assay (Fig. 2H, Supplemental Fig. 2H; Supplemental Table 2), the effects of these concentrations on β-arrestin recruitment by Met-enk and morphine were examined (Figs. 2I-L; Supplemental Fig. 2I-L). The effect of various concentrations of RS-ketamine on Met-enk response curves revealed enhancement of the efficacy for β-arrestin recruitment at most of the concentrations tested (Supplemental Fig. 2J). For example, addition of 1 nM RS-ketamine caused ~78% increase in the E_{max} of Met-enk-mediated β-arrestin recruitment, while higher concentrations of RS-ketamine were less effective (Fig. 2J; Supplemental Fig. 2J; Supplemental Table 2). RS-ketamine effects on morphine-mediated β-arrestin recruitment were not as robust as that seen with Met-enk, and enhancement of RS-ketamine mediated signaling was dependent on the concentration of morphine used (Fig. 2K, L; Supplemental Fig. 2K, L; Supplemental Table 2). Also, morphine alone increased β-arrestin recruitment to a much lesser

extent than Met-enk with an E_{max} of ~40% over basal (Fig. 2L; Supplemental Fig. 2L; Supplemental Table 2). These results indicate that β-arrestin recruitment to MOR is greatly enhanced by the combination of ketamine with Met-enk, but not with morphine.

RS-ketamine modulation of Leu-Enkephalin- and Dynorphin A17-mediated G-protein signaling by MOR, DOR, and KOR.

In order to examine if potentiated signaling by RS-ketamine at CHO-MOR could also be seen with other endogenous opioid peptides, we examined signaling by Leu-enk and Dyn A17 each of which has previously been shown to activate MOR (Gomes et al., 2020). RS-ketamine increased the efficacy of Leu-Enk signaling (Fig. 3B) albeit to a lesser extent than Met-Enk (Fig. 3A; Supplemental Fig. 2, 3). For example, treatment with 1 nM RS-ketamine leads to a ~20% increase in signaling mediated by 1 μM Leu-enk as compared to a ~64% increase in signaling mediated by 1 μM Met-enk (Fig. 3A, B; Supplemental Fig. 2, 3; Supplemental Table 2, 3). Treatment with RS-ketamine also increased the efficacy of Dyn A17 signaling at MOR (Fig. 3C; Supplemental Fig. 3; Supplemental Table 3). In the case of [^{35}S]GTPγS binding mediated by 1 μM Dyn A17, the addition of 1 nM RS-ketamine caused a ~43% increase, and 100 nM RS-ketamine caused a ~66% increase in signaling (Fig. 3C; Supplemental Fig. 3; Supplemental Table 3). Together these results show that RS-ketamine increases the efficacy of these endogenous opioid peptides at MOR in the following order: Met-enk>Dyn A17>Leu-enk.

There is evidence that the analgesic and/or antidepressant effects of ketamine can be mediated in part through DOR and KOR (Pacheco et al., 2014; Wulf et al., 2022). Therefore, we examined synergism of RS-ketamine and opioid peptides in CHO cells stably expressing DOR or KOR using [^{35}S]GTPγS binding as a measure of receptor activation (Fig. 3; Supplemental Fig. 3). In general,

the EC_{50} values for the opioid peptides in the absence of RS-ketamine were similar to previously published results, although there were some differences that could be due to the different cell lines used (Gomes et al., 2020).

In CHO-DOR cells, submicromolar concentrations of RS-ketamine alone did not substantially influence [^{35}S]GTPγS binding (Supplemental Fig. 3E; Supplemental Table 4) but did enhance signaling by 1 μM Met-enk, Leu-enk, or Dyn A17 (Fig. 3D-F; Supplemental Fig. 3E-J). For 1 μM Met-enk, addition of 1 nM RS-ketamine caused a ~34% increase in signaling, and 100 nM RS-ketamine a ~50% increase in signaling (Fig. 3D; Supplemental Fig. 3E, F; Supplemental Table 4), while for 1 μM Leu-enk, 1 nM RS-ketamine caused ~20% increase and 100 nM RS-ketamine caused a ~28% increase in signaling (Fig. 3E; Supplemental Fig. 3G, H; Supplemental Table 4). For 1 μM Dyn A17, 1 nM RS-ketamine caused a ~22% increase and 100 nM RS-ketamine caused a ~28% increase in signaling (Fig. 3F; Supplemental Fig. 3I, J; Supplemental Table 4).

In CHO-KOR cells, submicromolar concentrations of RS-ketamine alone had a negligible effect on [^{35}S]GTPγS binding (Supplemental Fig. 4K; Supplemental Table 5). RS-ketamine at 1 nM enhanced signaling by Met-enk and Dyn A17 while there was no significant impact on Leu-enk signaling (Fig. 3G-I; Supplemental Fig. 3 K-P; Supplemental Table 5). RS-ketamine at 1 nM caused a ~26% increase and at 100 nM a ~40% increase in [^{35}S]GTPγS binding mediated by 1 μM Met-enk (Fig. 3G; Supplemental Fig. 3K, L; Supplemental Table 5). No such increases were seen for Leu-enk (Fig. 3H; Supplemental Fig. 3M, N; Supplemental Table 5). For 1 μM Dyn A17, the increase was ~20% with 1 nM and ~31% with 100 nM RS-ketamine (Fig. 3I; Supplemental Fig. 3O, P; Supplemental Table 5). Together, these results show that RS-ketamine can enhance opioid peptide-mediated signaling at MOR, DOR, and KOR (with the exception of Leu-enk at KOR), and are most robust with MOR.

Modulation of MOR mediated [^{35}S]GTPγS binding and β-arrestin recruitment by ketamine enantiomers

The response curves with the racemic mixture, RS-ketamine, were compared to those for the individual stereoisomers in the [^{35}S]GTPγS binding assay. Both R- and S-ketamine produced a small increase above basal signaling in the [^{35}S]GTPγS binding assay at μM concentration, but not at submicromolar concentrations (Supplemental Fig. 4A; Supplemental Table 6). Met-enk concentration response curves in the absence and presence of different concentrations of R- or S-ketamine show that both isomers enhanced Met-enk responses (Fig. 4A, B; Supplemental Figs. 4B-E; Supplemental Table 6). The enhancement was more robust with S-ketamine compared to R-ketamine (Fig. 4A, B; Supplemental Fig. 4B-E; Supplemental Table 6). Addition of 1 nM S-ketamine caused a ~186% increase whereas 1 nM R-ketamine a ~72% increase in [^{35}S]GTPγS binding mediated by 1 μM Met-enk (Fig. 4A, B; Supplemental Table 6).

In the β-arrestin recruitment assay in the absence of opioid peptide, the profile of S-ketamine is similar to that of RS-ketamine with a small signal at the maximum tested concentration (10 μM), while R-ketamine produced a negligible response (Supplemental Fig. 4F; Supplemental Table 6). Met-enk response curves in the absence and presence of different concentrations of R- or S-ketamine show that R-ketamine had no effect on β-arrestin recruitment (Fig. 4C; Supplemental Fig. 4G-H) while S-ketamine caused a marked enhancement of Met-enk responses with peak enhancement seen with 1 nM S-ketamine (Fig. 4D; Supplemental Fig. 4I-J; Supplemental Table 6). Taken together, these results suggest that S-ketamine is more effective than R-ketamine in the enhancement of G protein activity and β-arrestin recruitment at MOR.

Modulation of MOR activity by ketamine metabolites

The ketamine metabolite 6-hydroxynorketamine (6-HNK) is active as an analgesic and antidepressant but does not bind to NMDA receptors (Zanos et al., 2016), therefore a key question is whether it interacts with opioid receptors. We tested stereoisomers of 6-HNK and also the intermediate metabolite norketamine (NK) in the [^{35}S]GTPγS binding and β-arrestin recruitment assays with MOR. In both assays, without Met-enk the ketamine metabolites produce negligible effects at submicromolar concentrations (Supplemental Fig. 5; Supplemental Table 7).

In the [^{35}S]GTPγS binding assay, Met-enk signaling was concentration-dependently enhanced by various ketamine metabolites (Fig 5A-D; Supplemental Fig. 5B-E). The NK isomers enhanced the efficacy for Met-enk to different extents; 1 nM R-NK increased the efficiency of Met-enk signaling by ~23% and S-NK increased the efficiency by ~71% (Fig. 5C; Supplemental Fig. 5; Supplemental Table 7). Met-enk efficacy was increased by the NK compounds in the following order: S-NK>RS-NK>R-NK and a small decrease in EC_{50} was observed with R-NK (Fig. 5C; Supplemental Fig. 5G-L; Supplemental Table 7). With HNKs we find that both isomers enhanced the efficacy of Met-Enk signaling to a similar extent; 10 nM RR-HNK increased the efficacy by ~40% and 10 nM SS-HNK increased the efficacy by ~47% (Fig. 5D; Supplemental Fig. 5; Supplemental Table 7).

In the β-arrestin recruitment assay, Met-enk concentration response curves in the absence and presence of different concentrations of the ketamine metabolites showed enhancement of Met-enk-mediated β-arrestin recruitment, with the enhancement being more robust for RS-NK, S-NK and RR-HNK compared to R-NK and SS-HNK (Fig. 5E-I; Supplemental Fig. 5). Submicromolar concentrations of ketamine metabolites increase the efficacy for Met-enk to varying extents (Fig. 5E-I; Supplemental Fig. 5; Supplemental Table 7). For example, 1 nM RS-NK enhanced Met-Enk

efficacy by ~71%, R-NK by ~20% and S-NK by ~110% (Figs. 5E-G, Supplemental Fig. 5; Supplemental Table 7). While ketamine metabolites showed minimal β-arrestin recruitment when tested alone at submicromolar concentrations, when tested at micromolar levels some metabolites produced a small response (Supplemental Fig. 5). When combined with Met-Enk, both HNK isomers enhanced the efficacy of Met-Enk, with 1 nM RR-HNK increasing the efficacy by ~65% and 1 nM SS-HNK increasing the efficacy by ~24% (Fig. 5H, I; Supplemental Figs. 5O-Q; Supplemental Table 7). Taken together, the finding that ketamine stereoisomers and metabolites are all able to enhance the efficacy of Met-enk supports the idea that opioid receptors contribute to the therapeutic activity of ketamine and its major metabolites as analgesics and antidepressants.

RS-ketamine modulates MOR activity in brain.

The assays described above used opioid receptors heterologously expressed in various cell lines to measure [^{35}S]GTPγS binding, β-arrestin recruitment and MAPK phosphorylation. We also used the TRUPATH biosensor assay (Olsen et al., 2020) to detect modulation of Met-enk responses by RS-ketamine; however, this assay did not yield reproducible results. Because all of the assays above were with cell lines heterologously expressing opioid receptors and/or in engineered systems, it is important to test whether ketamine enhances opioid peptide-mediated signaling with native receptors in brain. We first used midbrain membranes from wild-type mice and examined the effect of RS-ketamine on DAMGO-mediated [^{35}S]GTPγS binding. Both 1 and 100 nM RS-ketamine increased the potency and efficacy of DAMGO signaling (Fig. 6A). The EC_{50} of DAMGO was reduced from 3 nM to 0.2 nM by 100 nM RS-ketamine, and the E_{max} was increased by 52% (Fig. 6A).

Next, MOR agonist induced inhibition of GABA release onto VTA neurons, an action of MOR that is strongly associated with the *in vivo* rewarding effects of opioids, was examined. For this, *ex vivo* whole cell recordings were carried out in acutely prepared rat brain slices to test whether ketamine modifies Met-enk responses at MOR in the VTA. Representative traces from recordings without ketamine show responses to saturating concentrations of Met-enk that are completely reversed by the MOR selective antagonist CTAP (500 nM), indicating the response is fully mediated by MOR (Fig. 6B, left panel). In a second example neuron, the combination of 1 μM Met-enk and 10 nM RS-ketamine produced a greater response than 10 μM Met-enk alone (Fig. 6B, right panel). This augmented response was also fully reversed by CTAP (Fig. 6B, right panel). Concentration response curves for Met-enk in the absence or presence of 10 nM RS-ketamine show that RS-ketamine increased both the potency and E_{max} of Met-enk at this synaptic site (Fig. 6C). Specifically, the EC_{50} for Met-enk was shifted 10-fold by ketamine (Fig 6C). The maximal inhibition was also increased: calculated as % of baseline IPSC amplitude, ~44% of the IPSC persisted with Met-enk alone but only ~23% remained in the presence of 10 nM ketamine. Together, these results indicate that the PAM effect of RS-ketamine characterized in [^{35}S]GTPγS binding and β-arrestin recruitment assays can also occur at endogenously expressed MORs in brain.

Discussion

Major findings of the present study are that ketamine and its metabolites synergize with endogenous opioid peptides to increase opioid receptor-mediated signaling but do not directly activate opioid receptors at 100 nM or lower concentrations. These results build on our previous finding that treatment of cells expressing MOR with a combination of ketamine and morphine led

to a 2-3-fold increase in ERK1/2 phosphorylation relative to either drug alone (Gupta et al., 2011). By extending this finding to endogenous opioid peptides, we provide a potential mechanism for the analgesic and antidepressant actions reported for ketamine. This ketamine interaction is not limited to MOR; it was also observed with DOR and KOR, albeit with different efficacies. Our finding that stereoisomers of ketamine and its major metabolites share this effect is important because all of these compounds are known to have analgesic and antidepressant activity (Zanos et al., 2018). Our finding that ketamine augments Met-enk's actions at MOR in mouse brain membranes and rat brain slices extends the results to endogenous receptors. Collectively, these studies advance our understanding of the physiological actions of ketamine that likely account for some of its therapeutic effects.

Previously, opioid peptides and drugs were found to exhibit differential signaling at opioid receptors (Civciristov et al., 2019; Gomes et al., 2020; Ho et al., 2018; Raehal et al., 2011; Stoeber et al., 2018; Thompson et al., 2016). This was also found in the present study comparing the synergism between ketamine and three different classes of opioids: an opiate (morphine), a synthetic peptide (DAMGO), and native opioid peptides (Met-enk, Leu-enk, and DynA17). The magnitude of the synergism was most dramatic with Met-enk, especially with low concentrations of ketamine and Met-enk. Our finding that three different opioid peptides showed different efficacies with ketamine also fits with previous studies which found signaling differences between peptides (Gomes et al., 2020; Thompson et al., 2016). The term 'bias' is often used to describe differential signaling seen with agonists and positive allosteric modulators (Kandasamy et al., 2021; Livingston and Traynor, 2018; Ramos-Gonzalez et al., 2023; Slosky et al., 2021). An example of this was observed in the present study; S-ketamine was synergistic with Met-enk in both G protein activity and β-arrestin recruitment assays, while R-ketamine significantly enhanced

only G protein activity and not β-arrestin recruitment activity of Met-enk. The subtle differences in the way S- and R-ketamine affect the opioid system may contribute to their analgesic and antidepressant activities, which are similar but not identical (Bonaventura et al., 2021; Jelen et al., 2021).

The present results are consistent with the proposal that ketamine is a PAM for opioid receptors. PAMs can enhance binding affinity by modulating k_{on} and k_{off} rates of the orthosteric agonist; they can enhance the efficacy of the orthosteric agonist; and they can prevent receptor downregulation triggered by sustained exposure to orthosteric agonists (Valant et al., 2012). Although k_{on} and k_{off} rates were not measured in the present study, the observation of a significant change in EC_{50} under some conditions is consistent with these rates being altered by ketamine. Direct evidence of an altered signaling efficacy was observed for most combinations of ketamine and opioid peptides, and because ketamine alone at submicromolar concentrations had no effect on signaling in the absence of opioids, it can be considered an opioid receptor PAM. However, due to its weak effects as a direct agonist at micromolar concentrations, technically ketamine should be considered a combined agonist/PAM.

The potent activity of ketamine as an opioid receptor PAM may explain previous controversial data. Several studies reported that micromolar concentrations of ketamine affect opioid receptor activity, but relatively low concentrations of ketamine are required for behavioral effects (Adzic et al., 2023; Browne et al., 2018; Browne et al., 2020; Browne and Lucki, 2019; Levinstein and Michaelides, 2024; Wulf et al., 2022; Zhang et al., 2021; Zhou et al., 2023). Evidence that the opioid system is involved in mediating ketamine's therapeutic effects came from studies testing the effect of opioid antagonists such as naloxone or naltrexone. Some studies reported that antagonists blocked the analgesic effects of ketamine (Fidecka, 1987; Lawrence and Livingston,

1981; Petrocchi et al., 2019) although other studies did not see reversal by the opioid antagonists (Mikkelsen et al., 1999; Wiley and Downs, 1982; Yost et al., 2022). Similarly, some clinical studies reported that naltrexone blocked the antidepressant effect of ketamine (Klein et al., 2020; Williams et al., 2019; Williams et al., 2018; Zhang et al., 2021), although this effect was not observed in another study (Marton et al., 2019). Naltrexone blocked the antidepressant action of ketamine in mice, and the authors concluded that the "opioid system is necessary...for antidepressive actions of ketamine in rodents" (Klein et al., 2020). However, because morphine did not provide comparable antidepressant activity to ketamine, the authors stated that the opioid system was "not sufficient" for ketamine's antidepressant action (Klein et al., 2020). This apparent paradox can be explained by ketamine functioning as an opioid receptor PAM rather than a direct agonist. Morphine is an orthosteric agonist that activates all MORs, regardless of whether endogenous peptides are present. In contrast, PAMs amplify endogenous signals, only driving a response when the orthosteric ligand is present. Thus, the biological effects of PAMs are usually distinct from those of orthosteric receptor agonists (Livingston and Traynor, 2018).

Studies examining ketamine's analgesic effects in mice are consistent with an action as an opioid receptor PAM (Petrocchi et al., 2019). Specifically, Petrocchi et al. demonstrated that a nonselective opioid receptor antagonist (naloxone) as well as selective MOR and DOR antagonists blocked ketamine-induced peripheral antinociception (Petrocchi et al., 2019). Importantly, they found that bestatin significantly potentiated ketamine-induced peripheral antinociception (Petrocchi et al., 2019). Bestatin inhibits a key enzyme involved in opioid peptide degradation and prolongs the half-life of extracellular opioid peptides (Chaillet et al., 1983). Thus, the synergism between bestatin and ketamine is consistent with a role for ketamine as a PAM of peptide-engaged opioid receptors.

Our finding that stereoisomers of ketamine and its major metabolites (norketamine and 6-hydroxynorketamine) show opioid receptor PAM activity is important for two reasons. First, each of these compounds have analgesic and antidepressant activity (Zanos et al., 2016; Zanos et al., 2018). While ketamine and norketamine act as non-competitive NMDA receptor antagonists, 6-hydroxynorketamine does not (Zanos et al., 2016; Zanos et al., 2018). This is strong evidence that NMDA activity cannot fully account for the analgesic and antidepressant effects. Second, the activity of ketamine metabolites can potentially explain why antidepressant and analgesic effects last considerably longer than the elimination half-life of ketamine, which is typically 2-3 hours (Niesters et al., 2014; Orhurhu et al., 2019; Zanos et al., 2018). Norketamine has a longer half-life, approximately 12 hours, and 6-hydroxynorketamine also has a long elimination half-life (Zanos et al., 2018). Ketamine metabolites are detectable in plasma >24 hours after administration and may be present at nM levels in brain or other tissues for days due to their hydrophobicity and/or binding to tissue proteins (Zanos et al., 2018). The antidepressive and analgesic concentrations of ketamine typically produce peak plasma levels of ~1 μM (Zanos et al., 2018), which is orders of magnitude higher than the ~1 nM levels of ketamine and metabolites that were found in the present study to synergize with opioid peptides. It takes approximately 10 half-lives for levels to drop 3 orders of magnitude from 1 μM to 1 nM, assuming linearity. Thus, the biological activity of the metabolites together with their ultra-high potency as opioid receptor PAMs are consistent with the days-long therapeutic effects. Other mechanisms may also contribute, such as the reported upregulation of opioid peptides and receptors in rat brain following ketamine treatment (Jiang et al., 2024).

In summary, we found a potential mechanism for the antidepressant and analgesic effects of ketamine. By acting as PAMs at opioid receptors, ketamine and its metabolites amplify the activity of endogenous opioid peptides. Because this activity only affects opioid receptors that are

stimulated by the nearby release of endogenous opioid peptides, this is a distinct target from conventional opioid agonists. PAMs of opioid receptors are being developed for clinical use due to their potential to have fewer side effects than orthosteric opioid agonists (Kandasamy et al., 2021; Livingston et al., 2018; Livingston and Traynor, 2018). It remains to be determined if the allosteric binding site targeted by these other PAMs is where ketamine binds, or if there are multiple allosteric sites on these receptors. Because low nanomolar concentrations of ketamine do not drive opioid receptor signaling in the absence of orthosteric agonists, but much higher micromolar concentrations show weak agonist activity in our studies, it is possible that there are multiple binding sites on the opioid receptors. A recent molecular modeling study predicted that MOR binds 6-hydroxynorketamine in the orthosteric pocket, but experimentally the metabolite had only modest effects on GTPγS binding and appeared to function as an inverse agonist (Joseph et al., 2021). Further studies are needed to directly examine binding of ketamine and metabolites to opioid receptors.

Acknowledgments:

We thank Daniela Guerrero Mulix for help in carrying out Western blots and β-arrestin recruitment assays and Dr. Aya Osman for critical reading of the manuscript.

Data Availability Statement:

The authors declare that all the data supporting the findings of this study are available within the paper and its Supplemental Data.

Author Contributions:

Participated in research design: IG, EBM, LDF, LAD

Conducted experiments: IG, AG, EBM

Performed data analysis: IG, EBM

Contributed to manuscript writing: IG, EBM, LDF, LAD

Footnotes:

This research was funded by National Institute of Drug Abuse DA058681 and DA008863 grants to LAD and DA058681 and AA026609 to EBM.

Figure Legends:

Figure 1. RS-ketamine enhances MOR-mediated ERK1/2 phosphorylation. CHO cells expressing MOR were treated for 5 min at 37°C with either vehicle alone (basal) or with 10^{-10} - 10^{-6} M morphine (**A**), DAMGO (**B**), or Met-enkephalin (Met-enk; **C**) in the absence or presence of 100 nM RS-ketamine (RS-ket) or with RS-ketamine (10^{-10} - 10^{-6} M) in the absence or presence of 100 nM Met-enk (**D**). Cell lysates were subjected to Western blot analysis as described in Methods. Representative blots are shown in the figure (also see Supplemental Fig.1). Data (**A-D**) represents Mean±SD n=3; ***p<0.001 for treatment effect; Two-Way ANOVA with Sidak's multiple comparison test (Statistical Analysis in Supplemental Table 8). (**E**) Comparison of phosphoERK1/2 levels obtained under basal conditions, with 100 nM RS-ketamine, 100 nM Met-enk and a combination of the two. Basal values were taken as 100%. Each dot represents the mean of an individual experiment. Data represents Mean±SD. n.s. = not significant, *p<0.05, **p<0.01

One-Way ANOVA with Tukey's multiple comparison test (Statistical Analysis in Supplemental Table 8).

Figure 2. RS-ketamine modulates MOR-mediated signaling. (**A, B**) CHO cells (**A**) or CHO cells expressing Flag-MOR (CHO-MOR; **B**) were subjected to a [^{35}S]GTPγS binding assay with 0 - 10 μM RS-ketamine in the absence or presence of 1 μM CTOP as described in Methods. (**C**) CHO-MOR cells were subjected to a [^{35}S]GTPγS binding assay with 0 - 10 μM DAMGO in the absence or presence of 1 or 100 nM RS-ketamine (RS-ket) as described in Methods. Data was normalized by taking basal values in the absence of any drug as 0% and the response with 10 μM DAMGO as 100%. (**D, F**) CHO-MOR cells were subjected to a [^{35}S]GTPγS binding assay with 0 – 100 nM or 1 μM RS-ketamine in the absence or presence of 1 or 100 nM of either Met-enkephalin (ME; **D**) or morphine (Morp; **F**) as described in Methods. (**E, G**) CHO-MOR cells were subjected to a [^{35}S]GTPγS binding assay with 0 - 1 μM Met-enkephalin (**E**) or 0 - 100 nM morphine (**G**) in the absence or presence of 1 nM or 100 nM RS-ketamine (RS-ket) as described in Methods. Data was normalized by taking basal values in the absence of any drug as 0% and the response with 1 μM Met-enkephalin (**E**) or 100 nM morphine (**G**) as 100%. (**H**) Cells expressing MOR$^{\beta gal}$ were treated with 0 - 10 μM RS-ketamine and β-arrestin recruitment measured as described in Methods. Data represents Mean±SD, n=3. (**I, K**) Cells expressing MOR$^{\beta gal}$ were treated with 0 - 100 nM RS-ketamine in the absence or presence of 1 or 100 nM of either Met-enkephalin (ME; **I**) or morphine (Morp, **K**) and β-arrestin recruitment measured as described in Methods. (**J, L**) Cells expressing MOR$^{\beta gal}$ were treated with different concentrations of either 0 - 10 μM Met-enkephalin (**J**) or 0 - 3 μM morphine (**L**) in the absence or presence of 1 nM or 100 nM RS-ketamine (RS-ket) and β-arrestin recruitment measured as described in Methods. Data was normalized by taking

basal values in the absence of any drug as 0% and the response with 10 μM Met-enk or 3 μM morphine as 100%. Data represents Mean±SD, n=3; ***p<0.001 for treatment effect; Two-Way ANOVA with Sidak's (**B, K**) or Tukey's (**C-G, I, J, L**) multiple comparison tests (Statistical Analysis in Supplemental Table 8). Original data for figure shown in Supplemental Figure 2.

Figure 3. Comparison of the effects of RS-ketamine on Met-enkephalin-, Leu-enkephalin-, and dynorphin A17-mediated G-protein activity at MOR, DOR, KOR. CHO cells stably expressing Flag-MOR (**A - C**), Flag-DOR (**D - F**) or Flag-KOR (**G - I**) were subjected to a [^{35}S]GTPγS binding assay with different concentrations 0 - 1 μM Met-enkephalin (**A, D, G**), 0 - 1 μM Leu-enkephalin (**B, E, H**) or 0 - 1 μM Dynorphin A17 (**C, F, I**) in the absence or presence of 1 nM or 100 nM RS-ketamine (RS-ket) as described in Methods. Data was normalized by taking basal values in the absence of any drug as 0% and the response at 1 μM of either Met-enkephalin (**A, D, G**), Leu-enkephalin (**B, E, H**) or Dynorphin A17 (**C, F, I**) as 100%. Data represents Mean±SD n=3; n.s. = not significant; **p<0.01; ***p<0.001 for treatment effect; Two-Way ANOVA with Tukey's (**A, B, E-I**) or Sidak's (**C, D**) multiple comparison tests (Statistical Analysis in Supplemental Table 8). Original data for figure shown in Supplemental Figure 2 and 3.

Figure 4. Effects of ketamine enantiomers (R-ketamine and S-ketamine) on signaling mediated by Met-enkephalin at MOR. CHO-MOR cells were treated with 0 - 1 μM Met-enkephalin in the absence or presence of 1 nM or 100 nM of either R-ketamine (R-ket; **A**) or S-ketamine (S-ket; **B**) and [^{35}S]GTPγS binding measured as described in Methods. Data was normalized by taking basal values in the absence of any drug as 0% and the response with 1 μM Met-enkephalin as 100%. Cells expressing MOR$^{\beta gal}$ were treated with 0 - 1 μM Met-enkephalin (**C, D**) in the absence or presence of 1 nM or 100 nM of either R-ketamine (R-ket; **C**) or S-

ketamine (S-ket; **D**) and β-arrestin recruitment measured as described in Methods. Data was normalized by taking basal values in the absence of any drug as 0% and the response with 1 μM Met-enkephalin as 100%. Data represents Mean±SD, n=3. n.s. = not significant, ***p<0.001 for treatment effect; Two-Way ANOVA with Sidak's (**A**) or Tukey's (**B-D**) multiple comparison tests (Statistical Analysis in Supplemental Table 8). Original data for figure shown in Supplemental Figure 4.

Figure 5. Effects of ketamine metabolites on signaling mediated by Met-enkephalin at MOR. CHO-MOR cells were treated with 0 - 1 μM Met-enkephalin in the absence or presence of 1 nM or 100 nM of RS-norketamine (RS-NK; **A**) and [^{35}S]GTPγS binding measured as described in Methods. Data was normalized by taking basal values in the absence of any drug as 0% and the response with 1 μM Met-enkephalin as 100%. A comparison of the effect of 1 nM RS-NK, R-norketamine (R-NK) or S-norketamine (S-NK) on 100 nM Met-enkephalin (Met-enk)-mediated G-protein activity (**B**); basal values in the absence of any ligand were taken as 100%. CHO-MOR cells were treated with 0 - 1 μM Met-enkephalin in the absence or presence of 1 nM of RS-, R-, or S-norketamine (**C**) or in the absence or presence of 10 nM RR- or SS-hydroxynorketamine (RR-HNK or SS-HNK) (**D**) and [^{35}S]GTPγS binding measured as described in Methods. Data was normalized by taking basal values in the absence of any drug as 0% and the response with 1 μM Met-enkephalin as 100%. Cells expressing MOR$^{\beta gal}$ were treated with 0 - 1 μM Met-enkephalin in the absence or presence of 1 nM or 100 nM of either RS-norketamine (RS-NK; **E**), R-norketamine (R-NK; **F**), S-norketamine (S-NK; **G**), RR-hydroxynorketamine (RR-HNK; **H**) or SS-hydroxynorketamine (SS-HNK; **I**) and β-arrestin recruitment measured as described in Methods. Data was normalized by taking basal values in the absence of any drug as 0% and the

response with 1 μM Met-enkephalin as 100%. Data represents Mean±SD n=3. n.s. = not significant, *p<0.05, **p<0.01, ***p<0.001; One-Way ANOVA (**B**) or Two-Way ANOVA with Tukey's multiple comparison test (**A, C-I**) (Statistical Analysis in Supplemental Table 8). Original data for figure shown in Supplemental Figure 5.

Figure 6. RS-ketamine modulates MOR activity in brain. (**A**) Midbrain membranes from individual wild-type C57BL/6 mice were treated with 0 - 10 μM DAMGO in the absence or presence of 1 nM or 100 nM of RS-ketamine (RS-ket) and [^{35}S]GTPγS binding measured as described in Methods. Data was normalized by taking basal values in the absence of any drug as 0% and the response with 10 μM DAMGO as 100%. Data are Mean ±SD n= 4 animals each in triplicate. (**B, C**) Whole cell electrophysiology recordings of electrically evoked inhibitory postsynaptic currents (IPSCs) were made in ventral tegmental area (VTA) neurons. (**B**) Example traces from two different neurons, with 10 μM Met-enkephalin (ME) in artificial cerebrospinal fluid (aCSF) (left), and 1 μM Met-enk(ME)+10 nM RS-ketamine (ket) in aCSF (right) in the absence or presence of 500 nM CTAP. (**C**) Concentration-response curves for Met-enkephalin induced inhibition of electrically evoked IPSCs in the absence and presence of 10 nM RS-ketamine (RS-ket). ***p<0.001 for treatment effect, Two-Way ANOVA with Tukey's (**A**) or Sidak's (**C**) multiple comparison test (Statistical Analysis in Supplemental Table 8). For insets *p<0.05, **p<0.01 and ***p<0.001 One-Way ANOVA Tukey's multiple comparison test (**A**) or Student's t-test (**C**). Original data for (**A**) is in in Supplemental Figure 3Q.

References

Abdel-Magid AF (2015) Allosteric modulators: an emerging concept in drug discovery. *ACS Med Chem Lett* **6**(2): 104-107.

Adzic M, Lukic I, Mitic M, Glavonic E, Dragicevic N and Ivkovic S (2023) Contribution of the opioid system to depression and to the therapeutic effects of classical antidepressants and ketamine. *Life Sci* **326**: 121803.

Al-Hasani R and Bruchas MR (2011) Molecular mechanisms of opioid receptor-dependent signaling and behavior. *Anesthesiology* **115**(6): 1363-1381.

Almohammed OA, Alsalem AA, Almangour AA, Alotaibi LH, Al Yami MS and Lai L (2022) Antidepressants and health-related quality of life (HRQoL) for patients with depression: Analysis of the medical expenditure panel survey from the United States. *PLoS One* **17**(4): e0265928.

Anand A, Mathew SJ, Sanacora G, Murrough JW, Goes FS, Altinay M, Aloysi AS, Asghar-Ali AA, Barnett BS, Chang LC, Collins KA, Costi S, Iqbal S, Jha MK, Krishnan K, Malone DA, Nikayin S, Nissen SE, Ostroff RB, Reti IM, Wilkinson ST, Wolski K and Hu B (2023) Ketamine versus ECT for Nonpsychotic Treatment-Resistant Major Depression. *N Engl J Med* **388**(25): 2315-2325.

Andrade C (2017) Ketamine for Depression, 3: Does Chirality Matter? *J Clin Psychiatry* **78**(6): e674-e677.

Barrett W, Buxhoeveden M and Dhillon S (2020) Ketamine: a versatile tool for anesthesia and analgesia. *Curr Opin Anaesthesiol* **33**(5): 633-638.

Berman RM, Cappiello A, Anand A, Oren DA, Heninger GR, Charney DS and Krystal JH (2000) Antidepressant effects of ketamine in depressed patients. *Biol Psychiatry* **47**(4): 351-354.

Bonaventura J, Lam S, Carlton M, Boehm MA, Gomez JL, Solis O, Sanchez-Soto M, Morris PJ, Fredriksson I, Thomas CJ, Sibley DR, Shaham Y, Zarate CA, Jr. and Michaelides M (2021) Pharmacological and behavioral divergence of ketamine enantiomers: implications for abuse liability. *Mol Psychiatry* **26**(11): 6704-6722.

Browne CA, Falcon E, Robinson SA, Berton O and Lucki I (2018) Reversal of Stress-Induced Social Interaction Deficits by Buprenorphine. *Int J Neuropsychopharmacol* **21**(2): 164-174.

Browne CA, Jacobson ML and Lucki I (2020) Novel Targets to Treat Depression: Opioid-Based Therapeutics. *Harv Rev Psychiatry* **28**(1): 40-59.

Browne CA and Lucki I (2019) Targeting opioid dysregulation in depression for the development of novel therapeutics. *Pharmacol Ther* **201**: 51-76.

Burford NT, Clark MJ, Wehrman TS, Gerritz SW, Banks M, O'Connell J, Traynor JR and Alt A (2013) Discovery of positive allosteric modulators and silent allosteric modulators of the mu-opioid receptor. *Proc Natl Acad Sci U S A* **110**(26): 10830-10835.

Chaillet P, Marcais-Collado H, Costentin J, Yi CC, De La Baume S and Schwartz JC (1983) Inhibition of enkephalin metabolism by, and antinociceptive activity of, bestatin, an aminopeptidase inhibitor. *Eur J Pharmacol* **86**(3-4): 329-336.

Civciristov S, Huang C, Liu B, Marquez EA, Gondin AB, Schittenhelm RB, Ellisdon AM, Canals M and Halls ML (2019) Ligand-dependent spatiotemporal signaling profiles of the mu-opioid receptor are controlled by distinct protein-interaction networks. *J Biol Chem* **294**(44): 16198-16213.

Cowen PJ and Browning M (2015) What has serotonin to do with depression? *World Psychiatry* **14**(2): 158-160.

Cvejic S, Trapaidze N, Cyr C and Devi LA (1996) Thr353, located within the COOH-terminal tail of the delta opiate receptor, is involved in receptor down-regulation. *J Biol Chem* **271**(8): 4073-4076.

Doornbos MLJ, Vermond SC, Lavreysen H, Tresadern G, AP IJ and Heitman LH (2018) Impact of allosteric modulation: Exploring the binding kinetics of glutamate and other orthosteric ligands of the metabotropic glutamate receptor 2. *Biochem Pharmacol* **155**: 356-365.

Dubois D and Gendron L (2010) Delta opioid receptor-mediated analgesia is not altered in preprotachykinin A knockout mice. *Eur J Neurosci* **32**(11): 1921-1929.

Fidecka S (1987) Interactions of ketamine, naloxone and morphine in the rat. *Pol J Pharmacol Pharm* **39**(1): 33-40.

Finck AD and Ngai SH (1982) Opiate receptor mediation of ketamine analgesia. *Anesthesiology* **56**(4): 291-297.

Fricker LD, Margolis EB, Gomes I and Devi LA (2020) Five Decades of Research on Opioid Peptides: Current Knowledge and Unanswered Questions. *Mol Pharmacol* **98**(2): 96-108.

Gassaway MM, Rives ML, Kruegel AC, Javitch JA and Sames D (2014) The atypical antidepressant and neurorestorative agent tianeptine is a mu-opioid receptor agonist. *Transl Psychiatry* **4**: e411.

Gaveriaux-Ruff C, Nozaki C, Nadal X, Hever XC, Weibel R, Matifas A, Reiss D, Filliol D, Nassar MA, Wood JN, Maldonado R and Kieffer BL (2011) Genetic ablation of delta opioid receptors in nociceptive sensory neurons increases chronic pain and abolishes opioid analgesia. *Pain* **152**(6): 1238-1248.

Gomes I, Bobeck EN, Margolis EB, Gupta A, Sierra S, Fakira AK, Fujita W, Muller TD, Muller A, Tschop MH, Kleinau G, Fricker LD and Devi LA (2016) Identification of GPR83 as the receptor for the neuroendocrine peptide PEN. *Sci Signal* **9**(425): ra43.

Gomes I, Sierra S, Lueptow L, Gupta A, Gouty S, Margolis EB, Cox BM and Devi LA (2020) Biased signaling by endogenous opioid peptides. *Proc Natl Acad Sci U S A* **117**(21): 11820-11828.

Gupta A, Devi LA and Gomes I (2011) Potentiation of mu-opioid receptor-mediated signaling by ketamine. *J Neurochem* **119**(2): 294-302.

Gupta A, Gomes I, Bobeck EN, Fakira AK, Massaro NP, Sharma I, Cave A, Hamm HE, Parello J and Devi LA (2016) Collybolide is a novel biased agonist of kappa-opioid receptors with potent antipruritic activity. *Proc Natl Acad Sci U S A* **113**(21): 6041-6046.

Hess EM, Riggs LM, Michaelides M and Gould TD (2022) Mechanisms of ketamine and its metabolites as antidepressants. *Biochem Pharmacol* **197**: 114892.

Hirota K, Okawa H, Appadu BL, Grandy DK, Devi LA and Lambert DG (1999a) Stereoselective interaction of ketamine with recombinant mu, kappa, and delta opioid receptors expressed in Chinese hamster ovary cells. *Anesthesiology* **90**(1): 174-182.

Hirota K, Sikand KS and Lambert DG (1999b) Interaction of ketamine with mu2 opioid receptors in SH-SY5Y human neuroblastoma cells. *J Anesth* **13**(2): 107-109.

Ho JH, Stahl EL, Schmid CL, Scarry SM, Aube J and Bohn LM (2018) G protein signaling-biased agonism at the kappa-opioid receptor is maintained in striatal neurons. *Sci Signal* **11**(542).

Hustveit O, Maurset A and Oye I (1995) Interaction of the chiral forms of ketamine with opioid, phencyclidine, sigma and muscarinic receptors. *Pharmacol Toxicol* **77**(6): 355-359.

Jelen LA and Stone JM (2021) Ketamine for depression. *Int Rev Psychiatry* **33**(3): 207-228.

Jelen LA, Stone JM, Young AH and Mehta MA (2022) The opioid system in depression. *Neurosci Biobehav Rev* **140**: 104800.

Jelen LA, Young AH and Stone JM (2021) Ketamine: A tale of two enantiomers. *J Psychopharmacol* **35**(2): 109-123.

Jiang C, DiLeone RJ, Pittenger C and Duman RS (2024) The endogenous opioid system in the medial prefrontal cortex mediates ketamine's antidepressant-like actions. *Transl Psychiatry* **14**(1): 90.

Jordan BA and Devi LA (1999) G-protein-coupled receptor heterodimerization modulates receptor function. *Nature* **399**(6737): 697-700.

Joseph TT, Bu W, Lin W, Zoubak L, Yeliseev A, Liu R, Eckenhoff RG and Brannigan G (2021) Ketamine Metabolite (2R,6R)-Hydroxynorketamine Interacts with mu and kappa Opioid Receptors. *ACS Chem Neurosci* **12**(9): 1487-1497.

Kandasamy R, Hillhouse TM, Livingston KE, Kochan KE, Meurice C, Eans SO, Li MH, White AD, Roques BP, McLaughlin JP, Ingram SL, Burford NT, Alt A and Traynor JR (2021) Positive allosteric modulation of the mu-opioid receptor produces analgesia with reduced side effects. *Proc Natl Acad Sci U S A* **118**(16).

Klein ME, Chandra J, Sheriff S and Malinow R (2020) Opioid system is necessary but not sufficient for antidepressive actions of ketamine in rodents. *Proc Natl Acad Sci U S A* **117**(5): 2656-2662.

Kritzer MD, Mischel NA, Young JR, Lai CS, Masand PS, Szabo ST and Mathew SJ (2022) Ketamine for treatment of mood disorders and suicidality: A narrative review of recent progress. *Ann Clin Psychiatry* **34**(1): 33-43.

Lawrence D and Livingston A (1981) Opiate-like analgesic activity in general anaesthetics. *Br J Pharmacol* **73**(2): 435-442.

Levinstein MR and Michaelides M (2024) Exploring the role of mu opioid receptors in the therapeutic potential and abuse liability of (S)-ketamine. *Neuropsychopharmacology* **49**(1): 315-316.

Livingston KE, Stanczyk MA, Burford NT, Alt A, Canals M and Traynor JR (2018) Pharmacologic Evidence for a Putative Conserved Allosteric Site on Opioid Receptors. *Mol Pharmacol* **93**(2): 157-167.

Livingston KE and Traynor JR (2018) Allostery at opioid receptors: modulation with small molecule ligands. *Br J Pharmacol* **175**(14): 2846-2856.

Ma S, Chen M, Jiang Y, Xiang X, Wang S, Wu Z, Li S, Cui Y, Wang J, Zhu Y, Zhang Y, Ma H, Duan S, Li H, Yang Y, Lingle CJ and Hu H (2023) Sustained antidepressant effect of ketamine through NMDAR trapping in the LHb. *Nature* **622**(7984): 802-809.

Machado-Vieira R, Salvadore G, Diazgranados N and Zarate CA, Jr. (2009) Ketamine and the next generation of antidepressants with a rapid onset of action. *Pharmacol Ther* **123**(2): 143-150.

Mack SM, Gomes I, Fakira AK, Duarte ML, Gupta A, Fricker L and Devi LA (2022) GPR83 engages endogenous peptides from two distinct precursors to elicit differential signaling. *Mol Pharmacol*.

Mansour A, Hoversten MT, Taylor LP, Watson SJ and Akil H (1995) The cloned mu, delta and kappa receptors and their endogenous ligands: evidence for two opioid peptide recognition cores. *Brain Res* **700**(1-2): 89-98.

Marton T, Barnes DE, Wallace A and Woolley JD (2019) Concurrent Use of Buprenorphine, Methadone, or Naltrexone Does Not Inhibit Ketamine's Antidepressant Activity. *Biol Psychiatry* **85**(12): e75-e76.

McLennan GP, Kiss A, Miyatake M, Belcheva MM, Chambers KT, Pozek JJ, Mohabbat Y, Moyer RA, Bohn LM and Coscia CJ (2008) Kappa opioids promote the proliferation of astrocytes via Gbetagamma and beta-arrestin 2-dependent MAPK-mediated pathways. *J Neurochem* **107**(6): 1753-1765.

Mikkelsen S, Ilkjaer S, Brennum J, Borgbjerg FM and Dahl JB (1999) The effect of naloxone on ketamine-induced effects on hyperalgesia and ketamine-induced side effects in humans. *Anesthesiology* **90**(6): 1539-1545.

Niesters M, Martini C and Dahan A (2014) Ketamine for chronic pain: risks and benefits. *Br J Clin Pharmacol* **77**(2): 357-367.

Olsen RHJ, DiBerto JF, English JG, Glaudin AM, Krumm BE, Slocum ST, Che T, Gavin AC, McCorvy JD, Roth BL and Strachan RT (2020) TRUPATH, an open-source biosensor platform for interrogating the GPCR transducerome. *Nat Chem Biol* **16**(8): 841-849.

Orhurhu V, Orhurhu MS, Bhatia A and Cohen SP (2019) Ketamine Infusions for Chronic Pain: A Systematic Review and Meta-analysis of Randomized Controlled Trials. *Anesth Analg* **129**(1): 241-254.

Pacheco DdF, Romero TR and Duarte ID (2014) Central antinociception induced by ketamine is mediated by endogenous opioids and mu- and delta-opioid receptors. *Brain Res* **1562**: 69-75.

Passie T, Adams HA, Logemann F, Brandt SD, Wiese B and Karst M (2021) Comparative effects of (S)-ketamine and racemic (R/S)-ketamine on psychopathology, state of consciousness

and neurocognitive performance in healthy volunteers. *Eur Neuropsychopharmacol* **44**: 92-104.

Petrocchi JA, de Almeida DL, Paiva-Lima P, Queiroz-Junior C, Caliari MV, Duarte IDG and Lima Romero TR (2019) Peripheral antinociception induced by ketamine is mediated by the endogenous opioid system. *Eur J Pharmacol* **865**: 172808.

Pollan M (2021) *This is your mind on plants*. Random House.

Pryce KD, Kang HJ, Sakloth F, Liu Y, Khan S, Toth K, Kapoor A, Nicolais A, Che T, Qin L, Bertherat F, Kaniskan HU, Jin J, Cameron MD, Roth BL, Zachariou V and Filizola M (2021) A promising chemical series of positive allosteric modulators of the mu-opioid receptor that enhance the antinociceptive efficacy of opioids but not their adverse effects. *Neuropharmacology* **195**: 108673.

Raehal KM, Schmid CL, Groer CE and Bohn LM (2011) Functional selectivity at the mu-opioid receptor: implications for understanding opioid analgesia and tolerance. *Pharmacol Rev* **63**(4): 1001-1019.

Ramos-Gonzalez N, Paul B and Majumdar S (2023) IUPHAR themed review: Opioid efficacy, bias, and selectivity. *Pharmacol Res* **197**: 106961.

Samuels BA, Nautiyal KM, Kruegel AC, Levinstein MR, Magalong VM, Gassaway MM, Grinnell SG, Han J, Ansonoff MA, Pintar JE, Javitch JA, Sames D and Hen R (2017) The Behavioral Effects of the Antidepressant Tianeptine Require the Mu-Opioid Receptor. *Neuropsychopharmacology* **42**(10): 2052-2063.

Singh NS, Rutkowska E, Plazinska A, Khadeer M, Moaddel R, Jozwiak K, Bernier M and Wainer IW (2016) Ketamine Metabolites Enantioselectively Decrease Intracellular D-Serine Concentrations in PC-12 Cells. *PLoS One* **11**(4): e0149499.

Slosky LM, Caron MG and Barak LS (2021) Biased Allosteric Modulators: New Frontiers in GPCR Drug Discovery. *Trends Pharmacol Sci* **42**(4): 283-299.

Smith DJ, Pekoe GM, Martin LL and Coalgate B (1980) The interaction of ketamine with the opiate receptor. *Life Sci* **26**(10): 789-795.

Stoeber M, Jullie D, Lobingier BT, Laeremans T, Steyaert J, Schiller PW, Manglik A and von Zastrow M (2018) A Genetically Encoded Biosensor Reveals Location Bias of Opioid Drug Action. *Neuron* **98**(5): 963-976 e965.

Suzuki Y, Goto K, Shiizaki K, Omiya Y, Ishige A, Komatsu Y and Kamei J (2001) Antinociceptive effect of U-50488H, a kappa-opioid agonist, in streptozotocin-induced diabetic mice. *J Pharm Pharmacol* **53**(4): 521-526.

Thompson GL, Lane JR, Coudrat T, Sexton PM, Christopoulos A and Canals M (2016) Systematic analysis of factors influencing observations of biased agonism at the mu-opioid receptor. *Biochem Pharmacol* **113**: 70-87.

Trapaidze N, Gomes I, Cvejic S, Bansinath M and Devi LA (2000) Opioid receptor endocytosis and activation of MAP kinase pathway. *Brain Res Mol Brain Res* **76**(2): 220-228.

Valant C, Felder CC, Sexton PM and Christopoulos A (2012) Probe dependence in the allosteric modulation of a G protein-coupled receptor: implications for detection and validation of allosteric ligand effects. *Mol Pharmacol* **81**(1): 41-52.

van Haaren F, Scott S and Tucker LB (2000) kappa-opioid receptor-mediated analgesia: hotplate temperature and sex differences. *Eur J Pharmacol* **408**(2): 153-159.

Wiley JN and Downs DA (1982) Lack of antagonism by naloxone of the analgesic and locomotor stimulant actions of ketamine. *Life Sci* **31**(11): 1071-1075.

Williams NR, Heifets BD, Bentzley BS, Blasey C, Sudheimer KD, Hawkins J, Lyons DM and Schatzberg AF (2019) Attenuation of antidepressant and antisuicidal effects of ketamine by opioid receptor antagonism. *Mol Psychiatry* **24**(12): 1779-1786.

Williams NR, Heifets BD, Blasey C, Sudheimer K, Pannu J, Pankow H, Hawkins J, Birnbaum J, Lyons DM, Rodriguez CI and Schatzberg AF (2018) Attenuation of Antidepressant Effects of Ketamine by Opioid Receptor Antagonism. *Am J Psychiatry* **175**(12): 1205-1215.

Wulf HA, Browne CA, Zarate CA and Lucki I (2022) Mediation of the behavioral effects of ketamine and (2R,6R)-hydroxynorketamine in mice by kappa opioid receptors. *Psychopharmacology (Berl)* **239**(7): 2309-2316.

Xue SG, He JG, Lu LL, Song SJ, Chen MM, Wang F and Chen JG (2023) Enhanced TARP-gamma8-PSD-95 coupling in excitatory neurons contributes to the rapid antidepressant-like action of ketamine in male mice. *Nat Commun* **14**(1): 7971.

Yost JG, Wulf HA, Browne CA and Lucki I (2022) Antinociceptive and Analgesic Effects of (2R,6R)-Hydroxynorketamine. *J Pharmacol Exp Ther* **382**(3): 256-265.

Zanos P, Moaddel R, Morris PJ, Georgiou P, Fischell J, Elmer GI, Alkondon M, Yuan P, Pribut HJ, Singh NS, Dossou KS, Fang Y, Huang XP, Mayo CL, Wainer IW, Albuquerque EX, Thompson SM, Thomas CJ, Zarate CA, Jr. and Gould TD (2016) NMDAR inhibition-independent antidepressant actions of ketamine metabolites. *Nature* **533**(7604): 481-486.

Zanos P, Moaddel R, Morris PJ, Riggs LM, Highland JN, Georgiou P, Pereira EFR, Albuquerque EX, Thomas CJ, Zarate CA, Jr. and Gould TD (2018) Ketamine and Ketamine Metabolite Pharmacology: Insights into Therapeutic Mechanisms. *Pharmacol Rev* **70**(3): 621-660.

Zarate CA, Jr., Singh JB, Carlson PJ, Brutsche NE, Ameli R, Luckenbaugh DA, Charney DS and Manji HK (2006) A randomized trial of an N-methyl-D-aspartate antagonist in treatment-resistant major depression. *Arch Gen Psychiatry* **63**(8): 856-864.

Zhang F, Hillhouse TM, Anderson PM, Koppenhaver PO, Kegen TN, Manicka SG, Lane JT, Pottanat E, Van Fossen M, Rice R and Porter JH (2021) Opioid receptor system contributes to the acute and sustained antidepressant-like effects, but not the hyperactivity motor effects of ketamine in mice. *Pharmacol Biochem Behav* **208**: 173228.

Zheng H, Chu J, Qiu Y, Loh HH and Law PY (2008a) Agonist-selective signaling is determined by the receptor location within the membrane domains. *Proc Natl Acad Sci U S A* **105**(27): 9421-9426.

Zheng H, Loh HH and Law PY (2008b) Beta-arrestin-dependent mu-opioid receptor-activated extracellular signal-regulated kinases (ERKs) Translocate to Nucleus in Contrast to G protein-dependent ERK activation. *Mol Pharmacol* **73**(1): 178-190.

Zhou JS, Peng GF, Liang WD, Chen Z, Liu YY, Wang BY, Guo ML, Deng YL, Ye JM, Zhong ML and Wang LF (2023) Recent advances in the study of anesthesia-and analgesia-related mechanisms of S-ketamine. *Front Pharmacol* **14**: 1228895.

Zorumski CF, Izumi Y and Mennerick S (2016) Ketamine: NMDA Receptors and Beyond. *J Neurosci* **36**(44): 11158-11164.

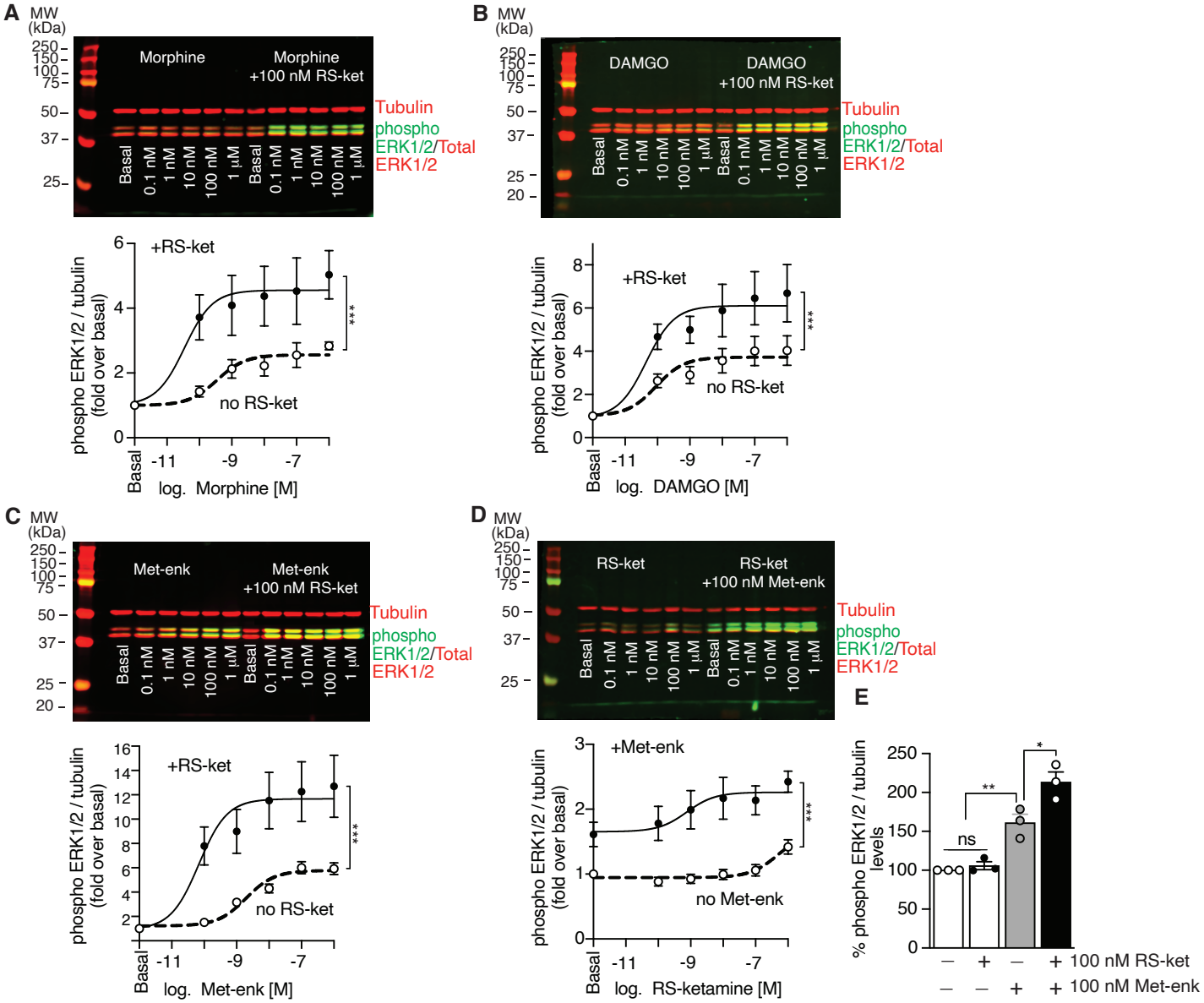
A
MW (kDa)
250
150
100
75
50
37
25
Morphine
Morphine +100 nM RS-ket
Basal
0.1 nM
1 nM
10 nM
100 nM
1 µM
Tubulin
phospho ERK1/2/Total ERK1/2
+RS-ket
no RS-ket
phospho ERK1/2 / tubulin (fold over basal)
log. Morphine [M]
B
DAMGO
DAMGO +100 nM RS-ket
log. DAMGO [M]
C
Met-enk
Met-enk +100 nM RS-ket
log. Met-enk [M]
D
RS-ket
RS-ket +100 nM Met-enk
+Met-enk
no Met-enk
log. RS-ketamine [M]
E
% phospho ERK1/2 / tubulin levels
ns
100 nM RS-ket
100 nM Met-enk

Fig.1

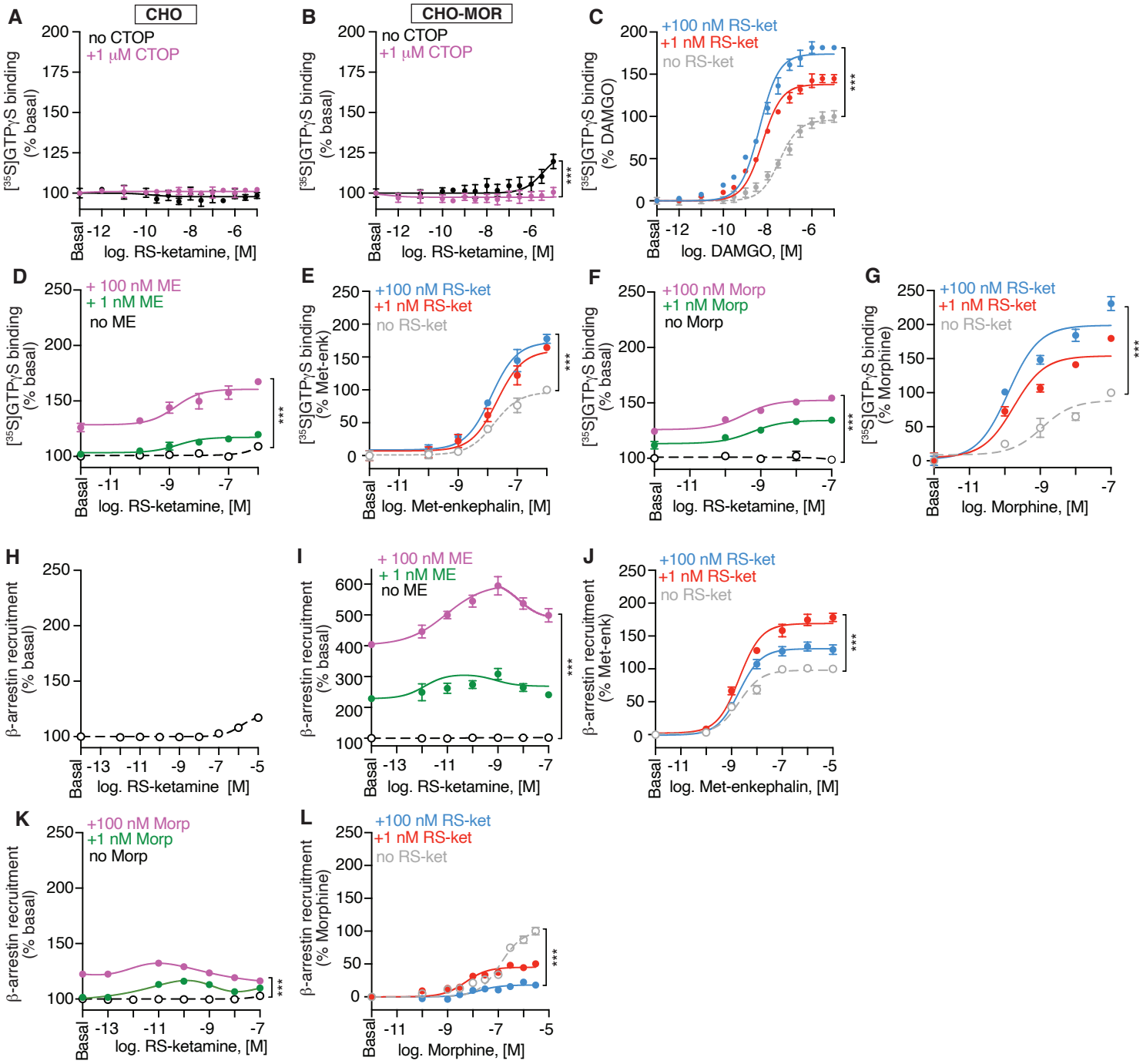
A
CHO
no CTOP
+1 μM CTOP
[35S]GTPγS binding (% basal)
log. RS-ketamine, [M]
B
CHO-MOR
no CTOP
+1 μM CTOP
[35S]GTPγS binding (% basal)
log. RS-ketamine, [M]
C
+100 nM RS-ket
+1 nM RS-ket
no RS-ket
[35S]GTPγS binding (% DAMGO)
log. DAMGO, [M]
D
+ 100 nM ME
+ 1 nM ME
no ME
[35S]GTPγS binding (% basal)
log. RS-ketamine, [M]
E
+100 nM RS-ket
+1 nM RS-ket
no RS-ket
[35S]GTPγS binding (% Met-enk)
log. Met-enkephalin, [M]
F
+100 nM Morp
+1 nM Morp
no Morp
[35S]GTPγS binding (% basal)
log. RS-ketamine, [M]
G
+100 nM RS-ket
+1 nM RS-ket
no RS-ket
[35S]GTPγS binding (% Morphine)
log. Morphine, [M]
H
β-arrestin recruitment (% basal)
log. RS-ketamine [M]
I
+ 100 nM ME
+ 1 nM ME
no ME
β-arrestin recruitment (% basal)
log. RS-ketamine, [M]
J
+100 nM RS-ket
+1 nM RS-ket
no RS-ket
β-arrestin recruitment (% Met-enk)
log. Met-enkephalin, [M]
K
+100 nM Morp
+1 nM Morp
no Morp
β-arrestin recruitment (% basal)
log. RS-ketamine, [M]
L
+100 nM RS-ket
+1 nM RS-ket
no RS-ket
β-arrestin recruitment (% Morphine)
log. Morphine, [M]

Fig. 2

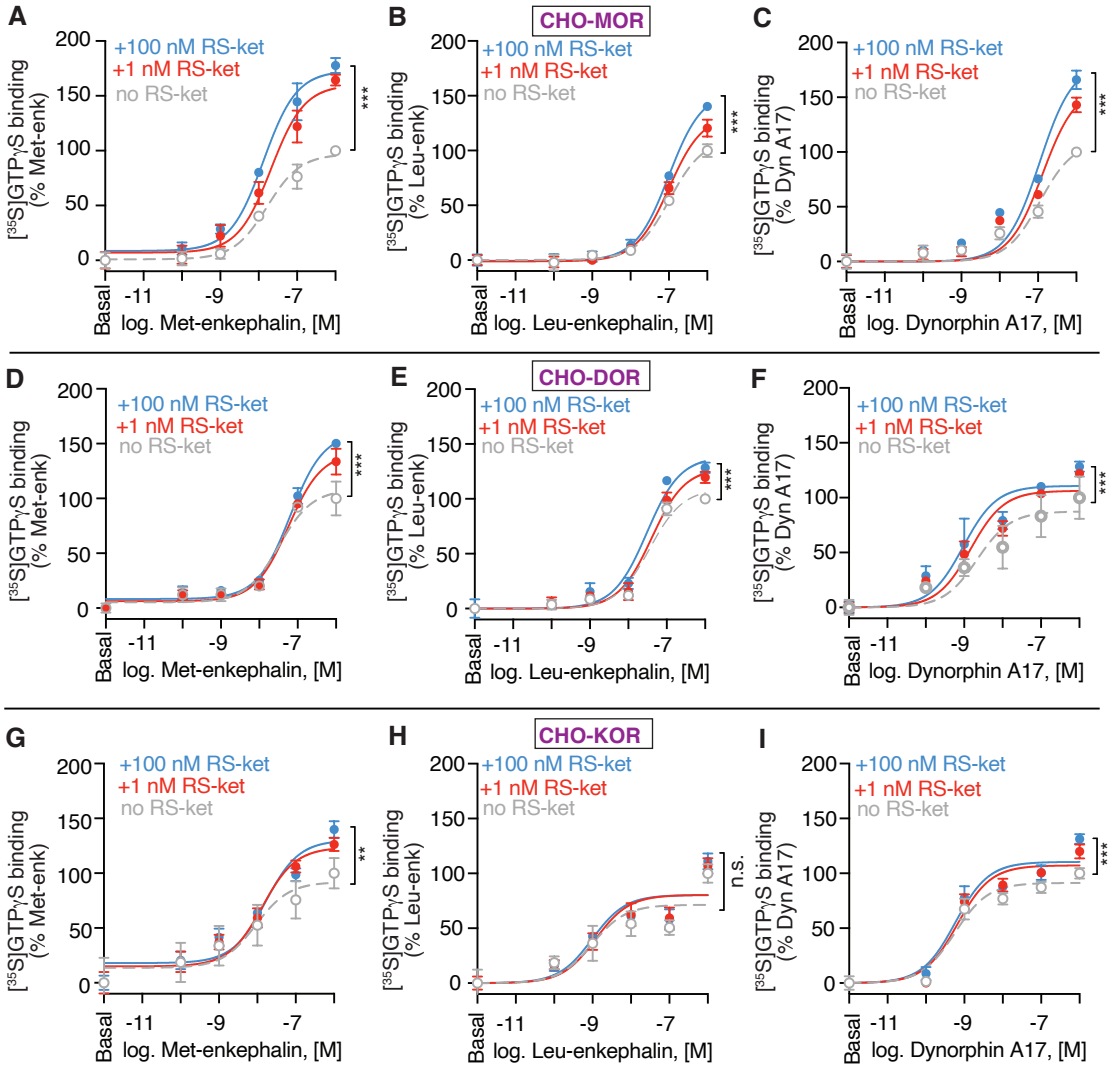
A
B
CHO-MOR
C
D
E
CHO-DOR
F
G
H
CHO-KOR
I
+100 nM RS-ket
+1 nM RS-ket
no RS-ket
[35S]GTPγS binding (% Met-enk)
[35S]GTPγS binding (% Leu-enk)
[35S]GTPγS binding (% Dyn A17)
log. Met-enkephalin, [M]
log. Leu-enkephalin, [M]
log. Dynorphin A17, [M]
Basal
***
**
n.s.

Fig. 3

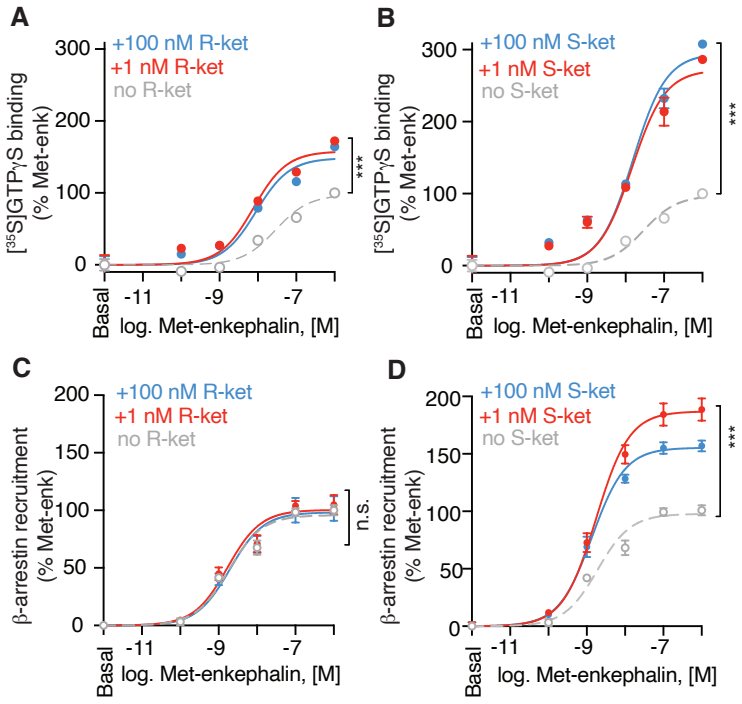
A
+100 nM R-ket
+1 nM R-ket
no R-ket
[35S]GTPγS binding (% Met-enk)
300
200
100
0
***
Basal
-11
-9
-7
log. Met-enkephalin, [M]
B
+100 nM S-ket
+1 nM S-ket
no S-ket
[35S]GTPγS binding (% Met-enk)
300
200
100
0
***
Basal
-11
-9
-7
log. Met-enkephalin, [M]
C
+100 nM R-ket
+1 nM R-ket
no R-ket
β-arrestin recruitment (% Met-enk)
200
150
100
50
0
n.s.
Basal
-11
-9
-7
log. Met-enkephalin, [M]
D
+100 nM S-ket
+1 nM S-ket
no S-ket
β-arrestin recruitment (% Met-enk)
200
150
100
50
0
***
Basal
-11
-9
-7
log. Met-enkephalin, [M]

Fig. 4

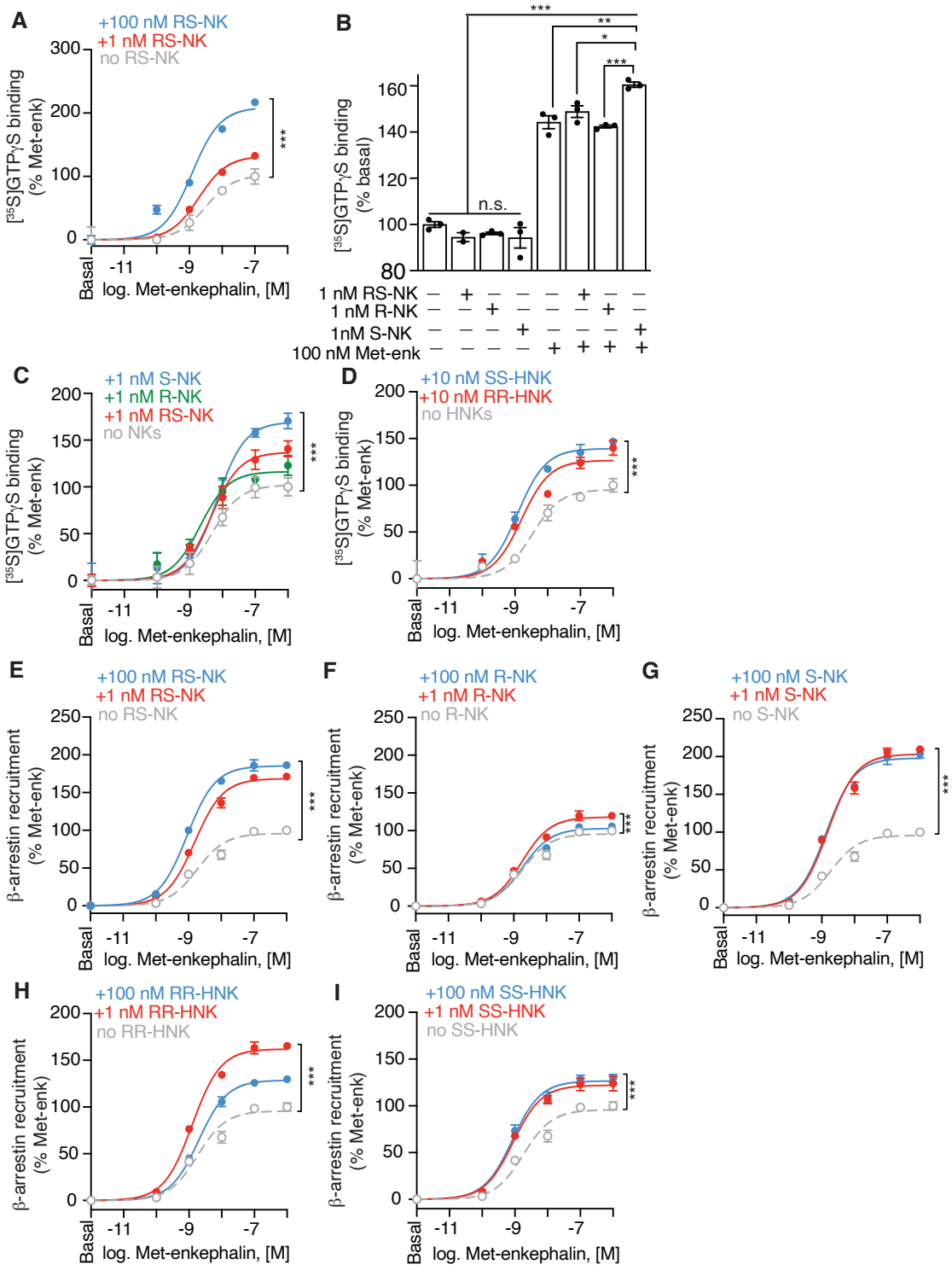
A
+100 nM RS-NK
+1 nM RS-NK
no RS-NK
[35S]GTPγS binding (% Met-enk)
log. Met-enkephalin, [M]
B
[35S]GTPγS binding (% basal)
n.s.
1 nM RS-NK
1 nM R-NK
1nM S-NK
100 nM Met-enk
C
+1 nM S-NK
+1 nM R-NK
+1 nM RS-NK
no NKs
D
+10 nM SS-HNK
+10 nM RR-HNK
no HNKs
E
+100 nM RS-NK
+1 nM RS-NK
no RS-NK
β-arrestin recruitment (% Met-enk)
F
+100 nM R-NK
+1 nM R-NK
no R-NK
G
+100 nM S-NK
+1 nM S-NK
no S-NK
H
+100 nM RR-HNK
+1 nM RR-HNK
no RR-HNK
I
+100 nM SS-HNK
+1 nM SS-HNK
no SS-HNK

Fig. 5

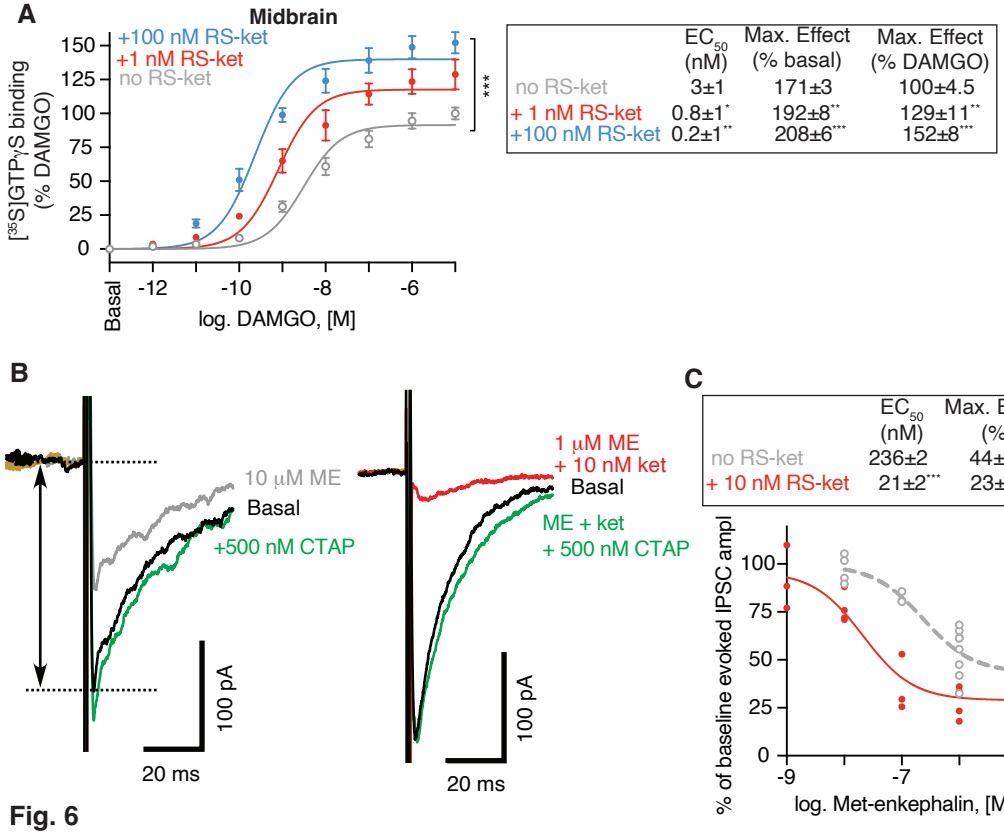
A
Midbrain
+100 nM RS-ket
+1 nM RS-ket
no RS-ket
[35S]GTPγS binding (% DAMGO)
150
125
100
75
50
25
0
Basal
-12
-10
-8
-6
log. DAMGO, [M]
***
EC50 (nM)
Max. Effect (% basal)
Max. Effect (% DAMGO)
no RS-ket 3±1 171±3 100±4.5
+ 1 nM RS-ket 0.8±1* 192±8** 129±11**
+100 nM RS-ket 0.2±1** 208±6*** 152±8***
B
10 μM ME
Basal
+500 nM CTAP
100 pA
20 ms
1 μM ME
+ 10 nM ket
Basal
ME + ket
+ 500 nM CTAP
100 pA
20 ms
C
EC50 (nM)
Max. Effect (%)
no RS-ket 236±2 44±8
+ 10 nM RS-ket 21±2*** 23±16*
% of baseline evoked IPSC ampl
100
75
50
25
0
-9
-7
-5
log. Met-enkephalin, [M]
***

Fig. 6

MOLPHARM-AR-2024-000947

Ketamine and major ketamine metabolites function as allosteric modulators of opioid receptors

Ivone Gomes[1], Achla Gupta[1], Elyssa B. Margolis[2], Lloyd D. Fricker[3], Lakshmi A. Devi[1,4,5,@]

Supplemental Figures

Supplemental Figure 1. Effect of RS-ketamine on phosphorylation of ERK1/2 in CHO-MOR cells. Representative blots for CHO cells expressing MOR (CHO-MOR) treated with different concentrations (10^{-10} - 10^{-6} M) of either morphine (**A**), DAMGO (**B**), or Met-enkephalin (Met-enk; **C**) in the absence or presence of 100 nM RS-ketamine (RS-ket) or with different concentrations (10^{-10} - 10^{-6} M) of RS-ketamine (RS-ket) in the absence or presence of 100 nM Met-enkephalin (Met-enk; **D**). Basal represents signal obtained in the absence of any ligand treatment. Blots were probed with antibodies to phospho ERK1/2, total ERK1/2 and tubulin as described in Methods.

Supplemental Figure 2. RS-ketamine modulates MOR-mediated signaling. CHO cells (**A**) or CHO cells expressing Flag-MOR (**B**) were subjected to a [^{35}S]GTPγS binding assay with RS-ketamine (0 - 1 mM) in the absence or presence of 1 μM CTOP as described in Methods. CHO-MOR cells were subjected to a [^{35}S]GTPγS binding assay with DAMGO (0 - 10 μM) in the absence or presence of 1 or 100 nM RS-ketamine (RS-ket) as described in Methods (**C**). CHO-MOR cells were treated with 0 - 1 μM of RS-ketamine in the absence or presence of 100 pM - 1 μM of Met-enkephalin (ME; **D**) or 100 pM - 100 nM of morphine (Morp; **F**) and [^{35}S]GTPγS binding measured as described in Methods. CHO-MOR cells were treated with 0 - 1 μM Met-enkephalin (**E**) or 0 – 100 nM morphine (**G**) in the absence or presence of 100 pM - 100 nM or 1 μM RS-ketamine (RS-ket), and [^{35}S]GTPγS binding measured as described in Methods. Cells expressing MOR$^{\beta gal}$ were treated with 0 - 10 μM of either RS-ketamine (RS-ket), R-ketamine (R-ket) or S-

ketamine (S-ket) and β-arrestin recruitment measured as described in Methods (**H**). Cells expressing $MOR^{\beta gal}$ were treated with 0 - 100 nM of RS-ketamine in the absence or presence of 100 pM - 1 μM Met-enkephalin (ME; **I**) or morphine (Morp; **K**) and β-arrestin recruitment measured as described in Methods. Cells expressing $MOR^{\beta gal}$ were treated with 0 - 10 μM Met-enkephalin (**J**) or 0 - 3 μM morphine (**L**) in the absence or presence of 1 pM - 100 nM RS-ketamine (RS-ket) and β-arrestin recruitment measured as described in Methods. Data represents Mean±SD.

Supplemental Figure 3. Effects of RS-ketamine on opioid peptide-mediated G-protein activity at MOR, DOR, and KOR. CHO-MOR cells were treated with 0 - 1 μM RS-ketamine in the absence or presence of 100 pM-1 μM Leu-enkephalin (Leu-enk; **A**) or Dynorphin A17 (Dyn A17; **C**) and [^{35}S]GTPγS binding measured as described in Methods. CHO-MOR cells were treated with either 0 - 1 μM Leu-enkephalin (**B**) or Dynorphin A17 (**D**) in the absence or presence of 100 pM - 1 μM RS-ketamine (RS-ket) and [^{35}S]GTPγS binding measured as described in Methods. CHO cells stably expressing Flag-DOR (CHO-DOR) were treated with 0 - 1 μM RS-ketamine in the absence or presence of either 100 pM - 1 μM Met-enkephalin (Met-enk; **E**), Leu-enk (Leu-enk; **G**) or Dynorphin A17 (Dyn A17; **I**) and [^{35}S]GTPγS binding measured as described in Methods. CHO-DOR cells were treated with either 0 - 1 μM Met-enkephalin (**F**), Leu-enkephalin (**H**) or Dynorphin A17 (**J**) in the absence or presence of 100 pM - 1 μM RS-ketamine (RS-ket) and [^{35}S]GTPγS binding measured as described in Methods. CHO cells stably expressing Flag-KOR (CHO-KOR) were treated with 0 - 1 μM RS-ketamine in the absence or presence of either 100 pM - 1 μM Met-enkephalin (Met-enk; **K**), Leu-enkephalin (Leu-enk; **M**) or Dynorphin A17 (Dyn A17; **O**) and [^{35}S]GTPγS binding measured as described in Methods. CHO-KOR cells were treated with

either 0 - 1 μM Met-enkephalin (**L**), Leu-enkephalin (**N**) or Dynorphin A17 (**P**) in the absence or presence of 100 pM - 1 μM RS-ketamine (RS-ket) and [^{35}S]GTPγS binding measured as described in Methods. Midbrain membranes from individual mice (n=4 mice) were treated with either 0 - 10 μM DAMGO (**Q**) in the absence of presence of 1 or 100 nM RS-ket and [^{35}S]GTPγS binding measured as described in Methods. Data represents Mean±SD.

Supplemental Figure 4. Effects of ketamine enantiomers (R-ketamine and S-ketamine) on G-protein activity and β-arrestin recruitment mediated by Met-enkephalin at MOR. CHO-MOR cells were treated with 0 - 1 μM of either RS-ketamine (RS-ket), R-ketamine (R-ket), or S-ketamine (S-ket) and [^{35}S]GTPγS binding measured as described in Methods (**A)**. CHO-MOR cells were treated with either 0 - 1 μM R-ketamine in the absence or presence of 100 pM-1 μM Met-enkephalin (Met-enk; **B**), or with 0 - 1 μM Met-enkephalin in the absence or presence of 100 pM - 1 μM R-ketamine (R-ket; **C**) and [^{35}S]GTPγS binding measured as described in Methods. CHO-MOR were treated with either 0 - 1 μM S-ketamine in the absence or presence of 100 pM - 1 μM Met-enkephalin (Met-enk; **D**), or with 0 - 1 μM Met-enkephalin in the absence or presence of 100 pM - 1 μM S-ketamine (S-ket; **E**) and [^{35}S]GTPγS binding measured as described in Methods. Cells expressing MOR$^{\beta gal}$ were treated with 0 - 10 μM of either RS-ketamine (RS-ket), R-ketamine (R-ket) or S-ketamine (S-ket) and β-arrestin recruitment measured as described in Methods (**F**). Cells expressing MOR$^{\beta gal}$ were treated with either 0 - 100 nM R-ketamine in the absence or presence of 100 pM - 1 μM Met-enkephalin (Met-enk; **G**), or with 0 - 1 μM Met-enkephalin in the absence or presence of 100 pM - 100 nM R-ketamine (R-ket; **H**) and β-arrestin recruitment measured as described in Methods. Cells expressing MOR$^{\beta gal}$ were treated with either 0 - 100 nM S-ketamine in the absence or presence of 100 pM - 1 μM Met-enkephalin (Met-enk; **I**), or with 0

- 1 μM Met-enkephalin in the absence or presence of 100 pM - 100 nM S-ketamine (S-ket; **J**) and β-arrestin recruitment measured as described in Methods. Data represents Mean±SD.

Supplemental Figure 5. Effects of ketamine metabolites on G-protein activity and β-arrestin recruitment mediated by Met-enkephalin at MOR.

CHO-MOR cells were treated with either 0 - 1 μM RS-norketamine (RS-NK) in the absence or presence of 100 pM-100 nM Met-enkephalin (Met-enk; **A**), or with 0 - 100 nM Met-enkephalin in the absence or presence of 100 pM - 1 μM RS-norketamine (RS-NK; **B**) and [^{35}S]GTPγS binding measured as described in Methods. CHO-MOR cells were treated with 0 - 100 nM Met-enkephalin in the absence or presence of either 1 nM RS-norketamine (RS-NK), R- or S-norketamine (R- or S-NK; **C**) and [^{35}S]GTPγS binding measured as described in Methods. CHO-MOR cells were treated with 0 - 1 μM RR-hydroxynorketamine (RR-HNK; **D**) or SS-hydroxynorketamine (SS-HNK; **E**) in the absence or presence of 10 nM Met-enkephalin (Met-enk) and [^{35}S]GTPγS binding measured as described in Methods. CHO-MOR cells were treated with 0 - 100 nM Met-enkephalin in the absence or presence of either 10 nM RR-hydroxynorketamine (RR-HNK), or SS-hydroxynorketamine (SS-HNK) and [^{35}S]GTPγS binding measured as described in Methods (**F**). Cells expressing MOR$^{\beta gal}$ were treated 0 - 10 μM of either RS-norketamine (RS-NK), R- or S-norketamine (R-NK or S-NK) and β-arrestin recruitment measured as described in Methods (**G**). Cells expressing MOR$^{\beta gal}$ were treated with either 0 - 100 nM RS-norketamine (RS-NK) in the absence or presence of 100 pM - 1 μM Met-enkephalin (Met-enk; **H**), or with 0 - 1 μM Met-enkephalin in the absence or presence of 100 pM - 100 nM RS-norketamine (RS-NK; **I**) and β-arrestin recruitment measured as described in Methods. Cells expressing MOR$^{\beta gal}$ were treated with either 0 - 100 nM R-norketamine (R-NK) in the absence or presence of 100 pM - 1 μM Met-

enkephalin (Met-enk; **J**), or with 0 - 1 μM Met-enkephalin in the absence or presence of 100 pM – 100 nM R-norketamine (R-NK; **K**) and β-arrestin recruitment measured as described in Methods. Cells expressing $MOR^{\beta gal}$ were treated with either 0 - 100 nM S-norketamine (S-NK) in the absence or presence of 100 pM – 1 μM Met-enkephalin (Met-enk; **L**), or with 0 - 1 μM Met-enkephalin in the absence or presence of 100 pM - 100 nM S-norketamine (S-NK; **M**) and β-arrestin recruitment measured as described in Methods. Cells expressing $MOR^{\beta gal}$ were treated with 0 - 10 μM of either RR- or SS-hydroxynorketamine (RR-HNK or SS-HNK) and β-arrestin recruitment measured as described in Methods (**N**). Cells expressing $MOR^{\beta gal}$ were treated with either 0 - 100 nM RR-hydroxynorketamine (RR-HNK) in the absence or presence of 100 pM - 1 μM Met-enkephalin (Met-enk; **O**), or with 0 - 1 μM Met-enkephalin in the absence or presence of 100 pM - 100 nM RR- hydroxynorketamine (RR-HNK; **P**) and β-arrestin recruitment measured as described in Methods. Cells expressing $MOR^{\beta gal}$ were treated with either 0 - 100 nM SS-hydroxynorketamine (SS-HNK) in the absence or presence of 100 pM - 1 μM Met-enkephalin (Met-enk; **Q**), or with 0 - 1 μM Met-enkephalin in the absence or presence of 100 pM - 100 nM SS-hydroxynorketamine (SS-HNK; **R**) and β-arrestin recruitment measured as described in Methods. Data represents Mean±SD.

MOLPHARM-AR-2024-000947

Ketamine and major ketamine metabolites function as allosteric modulators of opioid receptors

Ivone Gomes[1], Achla Gupta[1], Elyssa B. Margolis[2], Lloyd D. Fricker[3], Lakshmi A. Devi[1,4,5,@]

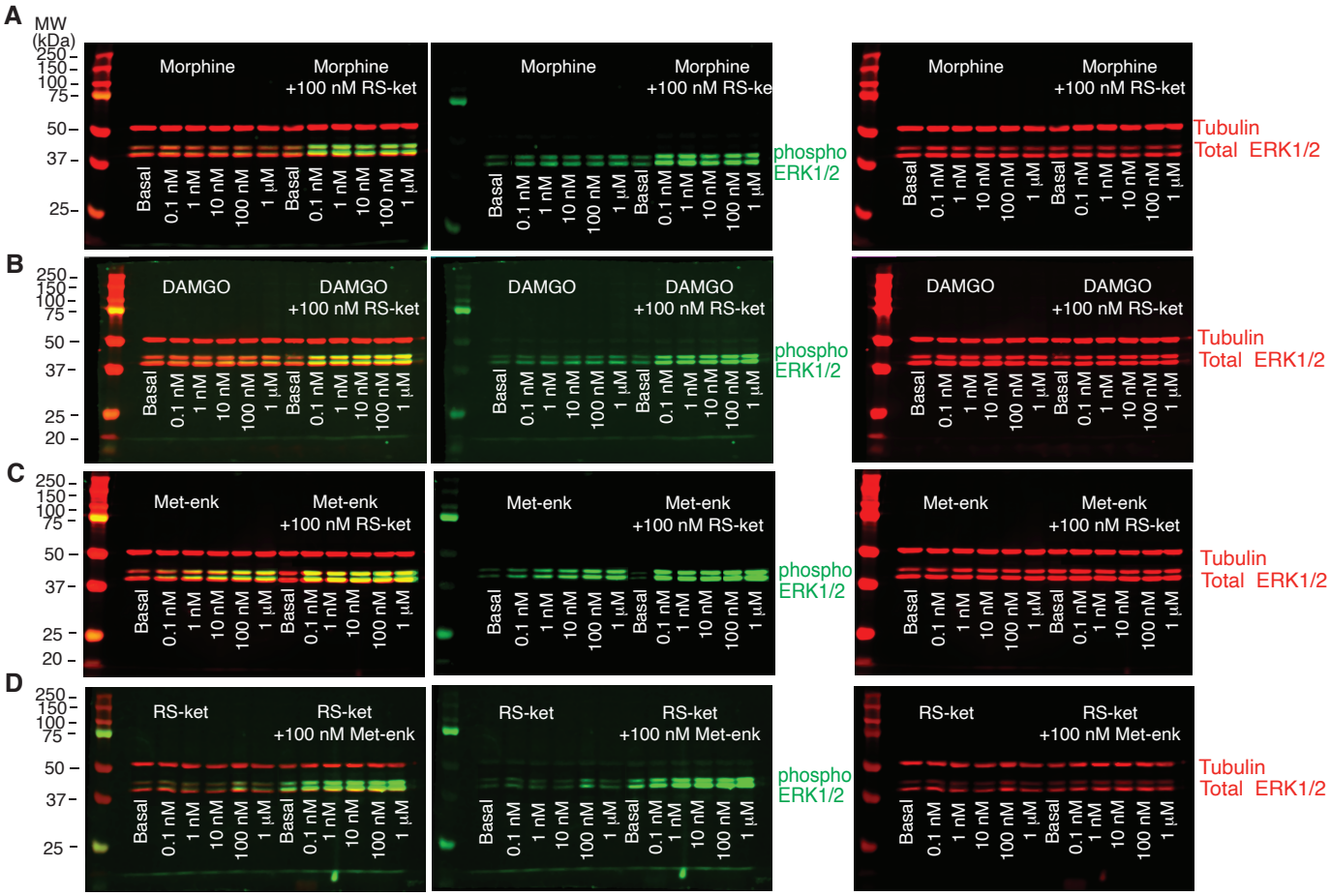

Supl. Fig 1

MOLPHARM-AR-2024-000947

Ketamine and major ketamine metabolites function as allosteric modulators of opioid receptors

Ivone Gomes[1], Achla Gupta[1], Elyssa B. Margolis[2], Lloyd D. Fricker[3], Lakshmi A. Devi[1,4,5,@]

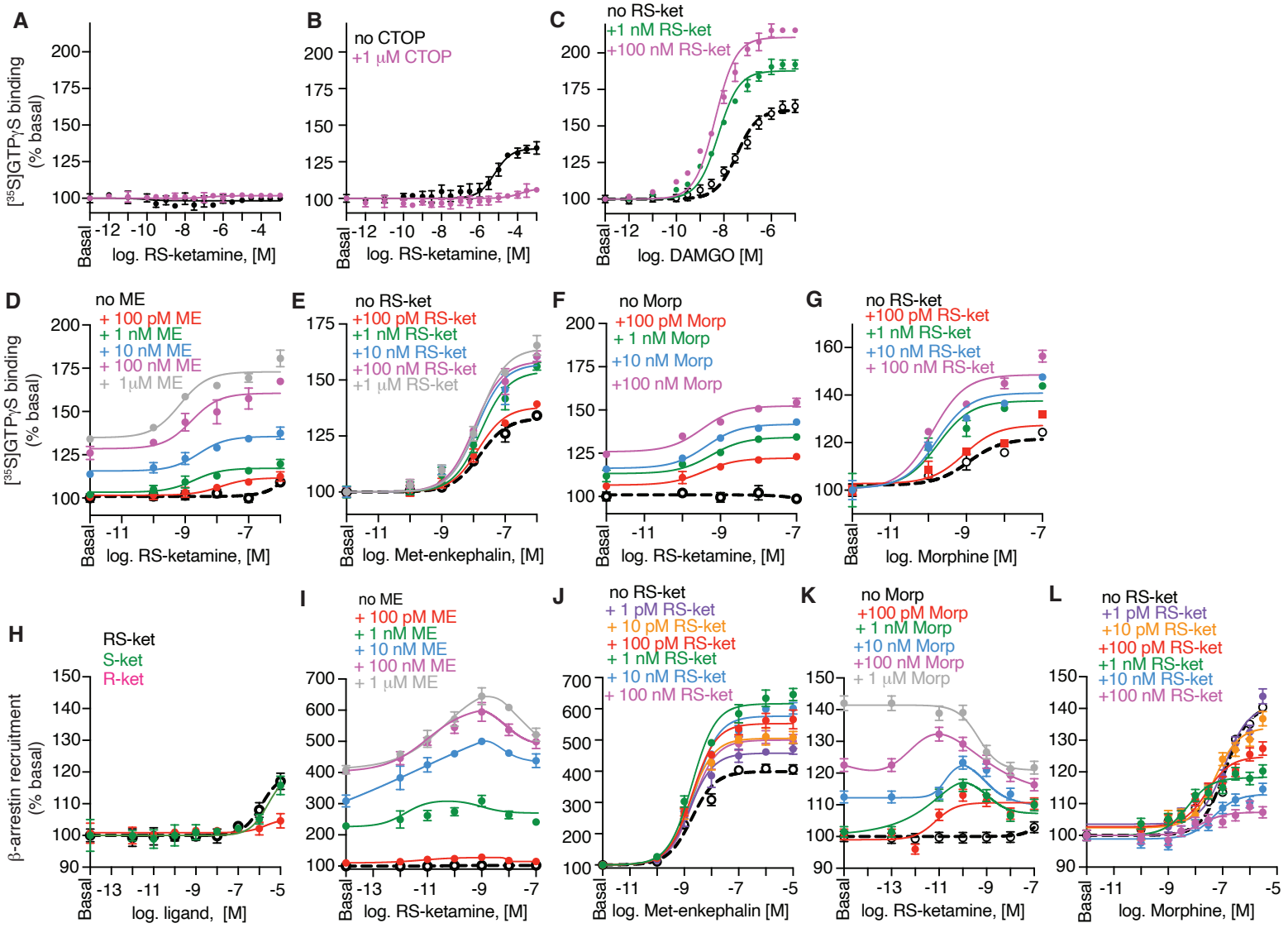

Supl. Fig. 2

MOLPHARM-AR-2024-000947

Ketamine and major ketamine metabolites function as allosteric modulators of opioid receptors

Ivone Gomes[1], Achla Gupta[1], Elyssa B. Margolis[2], Lloyd D. Fricker[3], Lakshmi A. Devi[1,4,5,@]

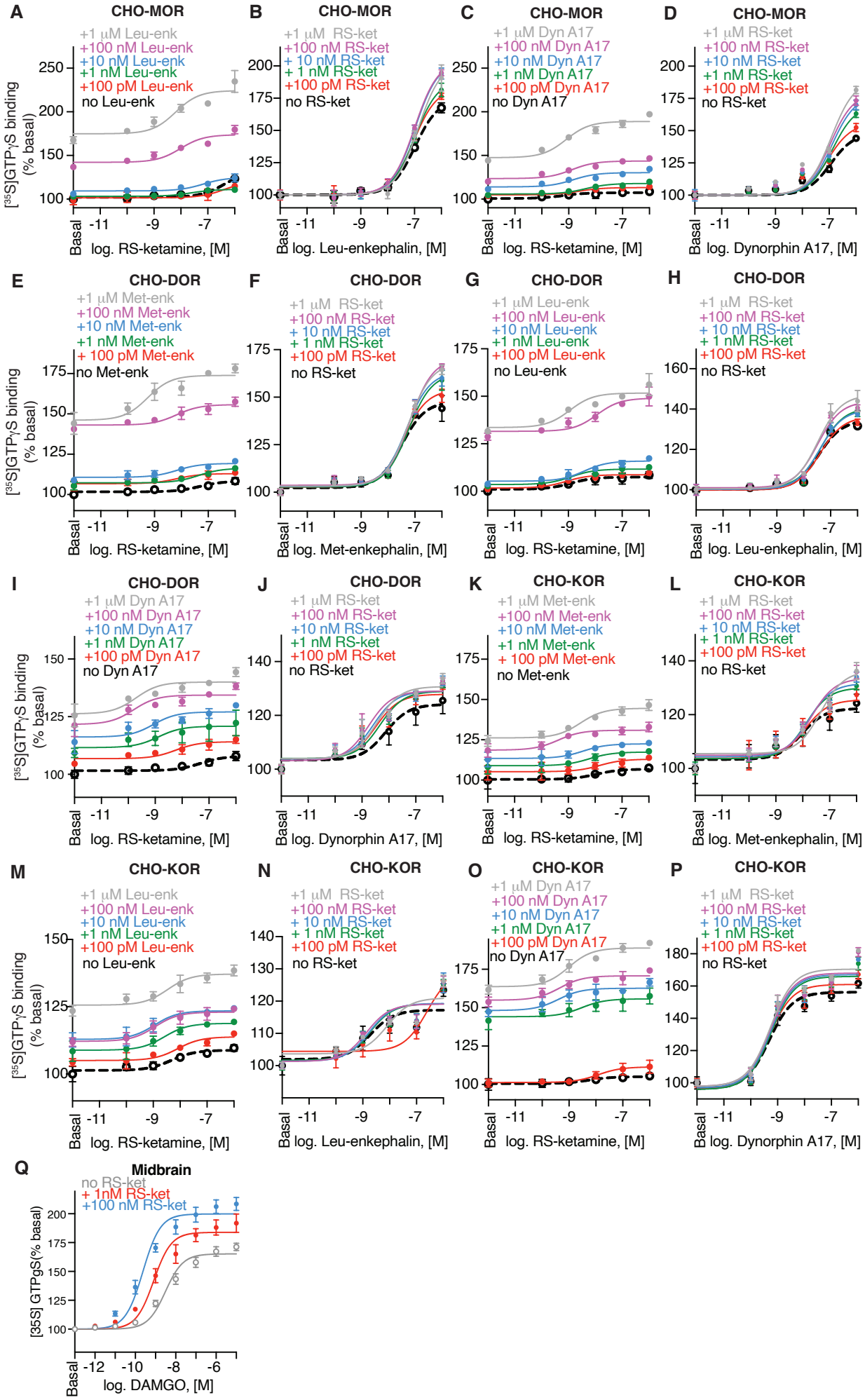

Supl. Fig. 3

MOLPHARM-AR-2024-000947

Ketamine and major ketamine metabolites function as allosteric modulators of opioid receptors

Ivone Gomes[1], Achla Gupta[1], Elyssa B. Margolis[2], Lloyd D. Fricker[3], Lakshmi A. Devi[1,4,5,@]

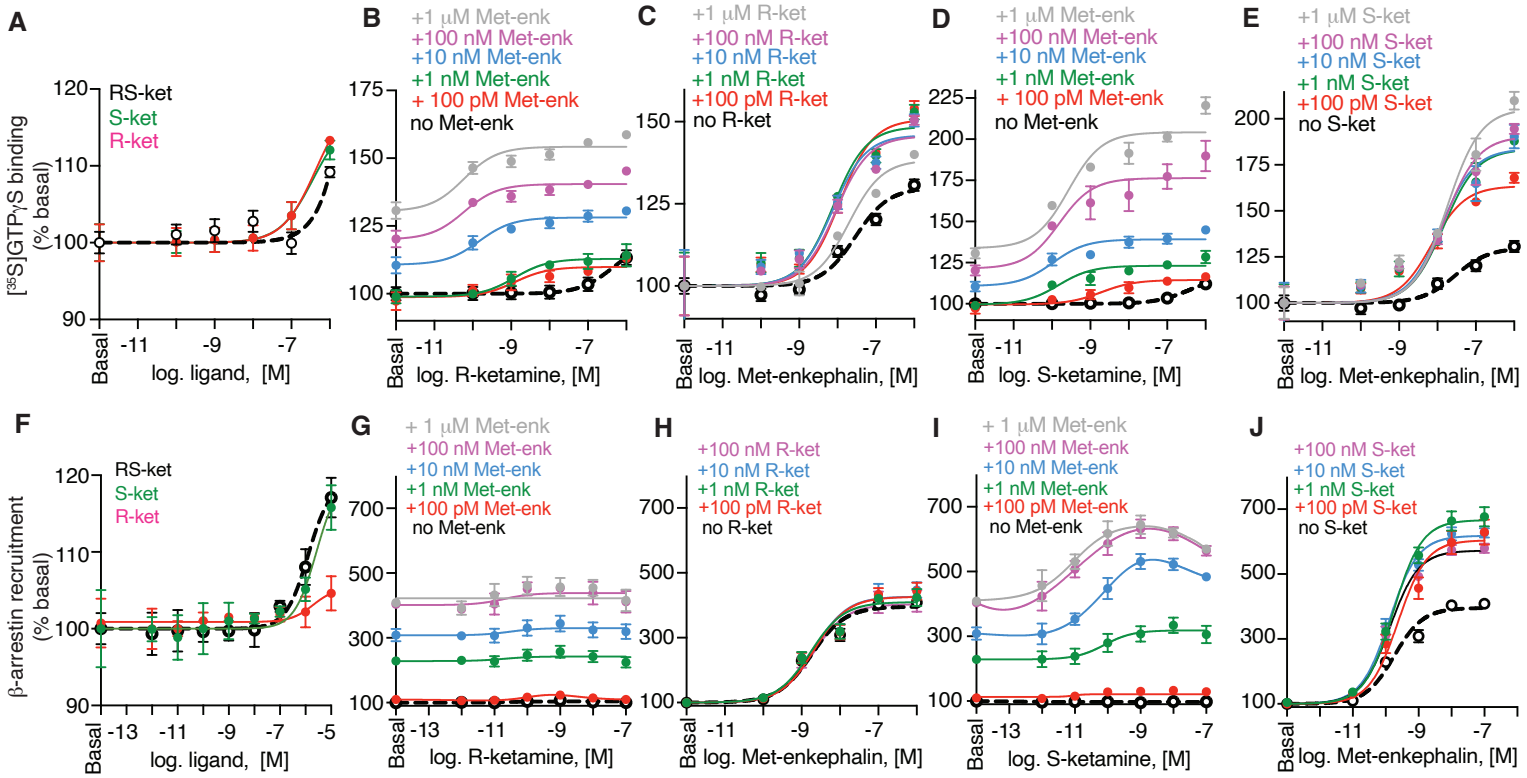

Supl. Fig. 4

MOLPHARM-AR-2024-000947

Ketamine and major ketamine metabolites function as allosteric modulators of opioid receptors

Ivone Gomes[1], Achla Gupta[1], Elyssa B. Margolis[2], Lloyd D. Fricker[3], Lakshmi A. Devi[1,4,5,@]

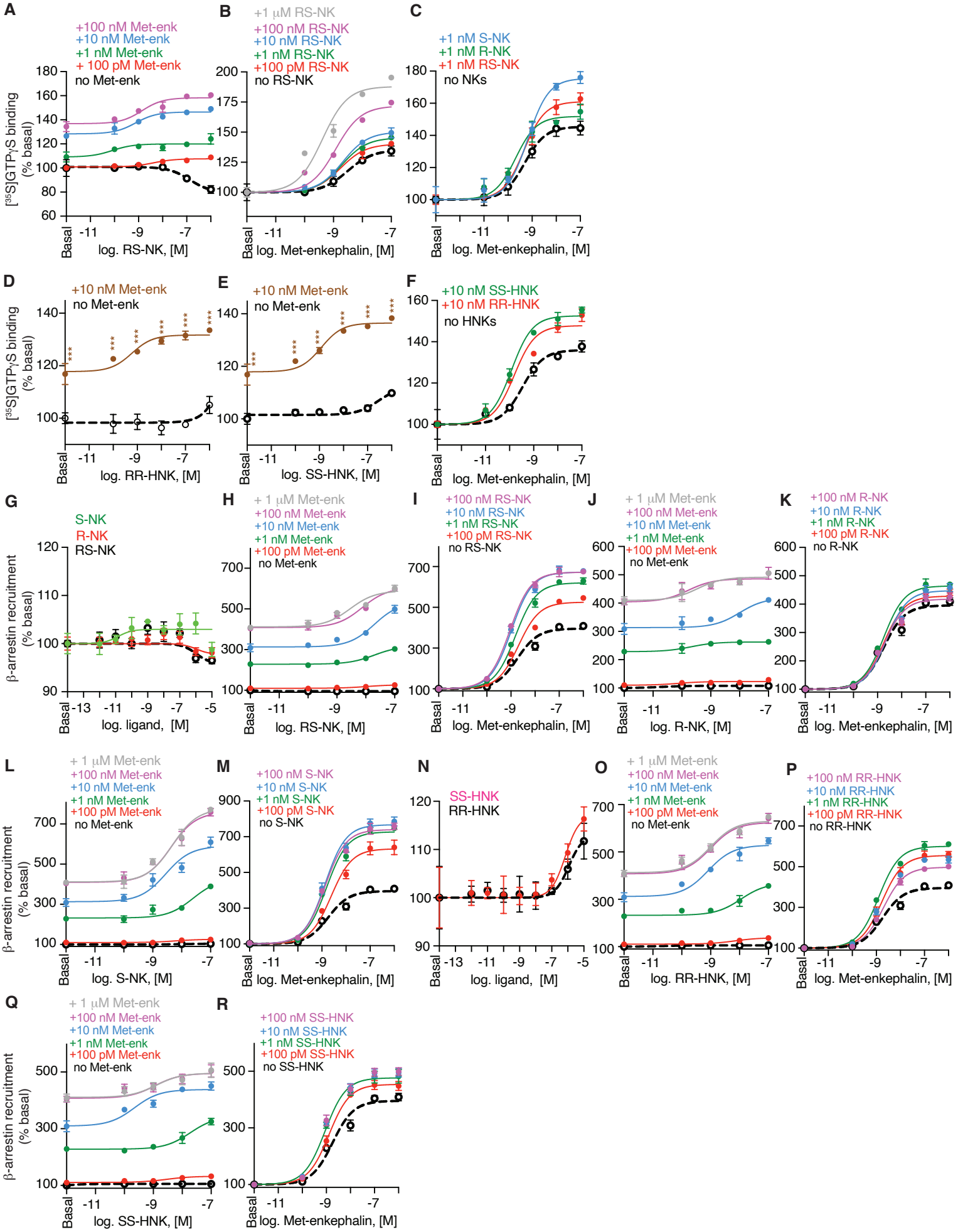

Supl. Fig. 5

MOLPHARM-AR-2024-000947

Ketamine and major ketamine metabolites function as allosteric modulators of opioid receptors

Ivone Gomes[1], Achla Gupta[1], Elyssa B. Margolis[2], Lloyd D. Fricker[3], Lakshmi A. Devi[1,4,5,@]

Supplemental Table 1. Analysis of phosphoERK1/2 levels at MOR in the presence of RS-ketamine

Ligand	phosphoERK1/2 / tubulin levels (fold over basal)	
	EC_{50} [nM]	E_{max} at 1 μM
Morphine	0.4±2	2.84±0.12
+ 100 nM RS-ketamine	0.03±2	5.03±0.74**
DAMGO	0.09±2	4.03±0.69
+ 100 nM RS-ketamine	0.04±2	6.68±1.33*
Met-enkephalin	1.96±1	5.93±0.49
+ 100 nM RS-ketamine	0.07±2	12.70±2.55*
RS-ketamine	> 1,000	1.42±0.11
+100 nM Met-enkephalin	0.8±3***	2.42±0.16***

Analysis of data for phosphorylation of ERK1/2 at MOR by morphine, DAMGO, Met-enkephalin (0-1 μM) in the absence and presence of 100 nM RS-ketamine or for RS-ketamine (0-1 μM) in the absence or presence of 100 Met-enkephalin shown in Fig.1. and Supplemental Fig 1. Data was fitted to sigmoidal dose equations in Prism 10.0. Data is Mean±SD of 3 independent experiments.*p<0.05;**0.01;***p<0.001, t-test.

Supplemental Table 2. Analysis of effect of RS-ketamine on DAMGO-, Met-enkephalin- or morphine-mediated signaling at MOR

Data from Fig.	Ligand	[^{35}S]GTPγS binding		Data from Fig.	Ligand	[^{35}S]GTPγS binding			
		EC_{50} [nM]	Peak Response (% basal)			EC_{50} [nM]	Peak Response (% basal)	Normalized to DAMGO response	% change in normalized response
Supl Fig. 2A (CHO cells)	RS-ketamine (0-1 mM)	n.a.	100±2[a]						
	+ 1 μM CTOP	n.a.	102±2[a]						
Fig. 2A (CHO cells)	RS-ketamine (0-10 μM)	n.a.	99±2[b]						
	+ 1 μM CTOP	n.a.	102±1[b]						
Supl Fig. 2B (CHO-MOR cells)	RS-ketamine (0-1 mM)	6,400± 1,000	134±4[a]						
	+ 1 μM CTOP	n.a.	106±1[a,***]						
Fig. 2B (CHO-MOR cells)	RS-ketamine (0-10 μM)	>1,000	120±4[b]	**Fig. 2C Supl Fig. 2C (CHO-MOR cells)**	DAMGO (0-10 μM)	35±1	164±4[b]	100±7	
	+ 1 μM CTOP	n.a.	101±3[b,**]		+1 nM RS-ketamine	6±1[***]	192±3[b,***]	145±5[***]	45±3
					+100 nM RS-ketamine	4±1[***]	215±2[b,***]	182±3[***]	82±3
		EC_{50} [nM]	Peak Response (% basal)			EC_{50} [nM]	Peak Response (% basal)	Normalized to Met-enk response	% change in normalized response
Fig. 2D; Supl Fig. 2D	RS-ketamine (0-1 μM)	>1,000	109±1[c]	**Supl Fig. 2E; Fig. 2E, 3A**	Met-enk (0-1 μM)	16±1	134±1[c]	100±4	
	+ 100 pM Met-enk	13±2[***]	112±3[c]		+100 pM RS-ketamine	14±1	139±1[c]	115±3	15±3
	+ 1 nM Met-enk	2±2[***]	120±3[c,**]		+1 nM RS-ketamine	17±1	156±2[c,***]	164±5[***]	64±4
	+10 nM Met-enk	3±2[***]	138±4[c,***]		+10 nM RS-ketamine	13±1[*]	161±1[c,***]	177±3[***]	77±3
	+100 nM Met-enk	2±2[***]	167±1[c,***]		+100 nM RS-ketamine	11±1[***]	161±2[c,***]	178±7[***]	78±5
	+ 1 μM Met-enk	0.7±1[***]	181±5[c,***]		+ 1 μM RS-ketamine	14±1	165±4[c,***]	192±13[***]	92±8
		EC_{50} [nM]	Peak Response (% basal)			EC_{50} [nM]	Peak Response (% basal)	Normalized to Morphine response	% change in normalized response
Fig. 2F; Supl Fig. 2F	RS-ketamine (0-100 nM)	>1,000	99±2[d]	**Supl Fig. 2G; Fig. 2G**	Morphine (0-100 nM)	1±2	124±1[d]	100±3	
	+ 100 pM Morphine	0.4±2[***]	123±1[d,***]		+100 pM RS-ketamine	0.9±2	132±1[d,***]	131±2[***]	31±2
	+ 1 nM Morphine	0.6±1[***]	134±2[d,***]		+1 nM RS-ketamine	0.2±1	144±1[d,***]	180±2[***]	80±2
	+10 nM Morphine	0.4±1[***]	143±2[d,***]		+10 nM RS-ketamine	0.2±1	148±1[d,***]	195±4[***]	95±3
	+100 nM Morphine	0.3±1[***]	154±2[d,***]		+100 nM RS-ketamine	0.1±1	156±3[d,***]	231±10[***]	131±6
Data from Fig.	**Ligand**	**β-arrestin recruitment**		**Data from Fig.**	**Ligand**	**β-arrestin recruitment**			
		EC_{50} [nM]	Peak Response (% basal)						
Supl Fig. 2H; Fig. 2H	RS-ketamine (0-10 μM)	>1,000	117±3[b]						

	R-ketamine (0-10 μM)	>1,000	105±2[b,**]						
	S-ketamine (0-10 μM)	>1,000	116±3[b]						
		EC_{50} [nM]	Peak Response (% basal)			EC_{50} [nM]	Peak Response (% basal)	Normalized to Met-enk response	% change in normalized response
Supl Fig. 2I; Fig. 2I	RS-ketamine (0-100 nM)	>1000	102±2[d]	**Supl Fig. 2J; Fig. 2J**	Met-enk (0-10 μM)	2±1	409±13[c]	100±4.9	
	+ 100 pM Met-enk	0.004±4; 2±3[***]	128±2[e]		+1 pM RS-ketamine	2±1	471±17[b,*]	121±6[**]	21±3
	+ 1 nM Met-enk	0.01±2; 4±2[***]	309±18[e,***]		+10 pM RS-ketamine	2±1	511±27[c,***]	134±6[***]	34±4
	+10 nM Met-enk	0.002±2; 6±2[***]	500±10[e,***]		+100 pM RS-ketamine	2±1	566±30[b,***]	152±10[***]	52±6
	+100 nM Met-enk	0.008±1; 6±3[***]	595±30[e,***]		+1 nM RS-ketamine	2±1	646±19[b,***]	178±6[***]	78±4
	+ 1 μM Met-enk	0.01±1; 31±2[***]	645±27[e,***]		+10 nM RS-ketamine	3±1	602±18[b,***]	164±6[***]	64±4
					+100 nM RS-ketamine	2±1	510±21[c,***]	129±7[***]	29±4
		EC_{50} [nM]	Peak Response (% basal)			EC_{50} [nM]	Peak Response (% basal)	Normalized to Morphine response	% change in normalized response
Supl Fig. 2K; Fig. 2K	RS-ketamine (0-100 nM)	>1,000	103±2[d]	**Supl Fig. 2L; Fig. 2L**	Morphine (0-3 μM)	125±1	140±2[i]	100±5.7	
	+ 100 pM Morphine	0.007±2[***]	113±2[f,*]		+1 pM RS-ketamine	120± 1[***]	144±2[i]	108±6	8±5
	+ 1 nM Morphine	0.003±2; 0.8±3[***]	116±2[f,**]		+10 pM RS-ketamine	53±1[***]	137±2[i]	91±6	-8.9±5
	+10 nM Morphine	0.02±1; 1±2[***]	123±2[f,***]		+100 pM RS-ketamine	27±1[***]	127±2[i,***]	68±5[***]	-32±5
	+100 nM Morphine	0.002±18; 1±2[***]	132±2[g,***]		+1 nM RS-ketamine	5±1[***]	120±2[i,***]	50±5[***]	-50±4
	+ 1 μM Morphine	0.4±1[***]	142±2[h,***]		+10 nM RS-ketamine	46±1[***]	115±2[i,***]	36±5[***]	-64±4
					+100 nM RS-ketamine	17±2[***]	109±2[c,***]	18±4[***]	-82±4

Analysis of data for [^{35}S]GTPγS binding at MOR by (i) RS-ketamine (0-10 μM or 1 mM) in the absence or presence of 1 μM CTOP; (ii) RS-ketamine (0-1 μM) in the absence or presence of Met-enkephalin (Met-enk; 100 pM - 1 μM) or Met-enk (0-1 μM)) in the absence or presence of RS-ketamine (100 pM - 1 μM), (iii) RS-ketamine (0-100 nM) in the absence or presence of morphine (100 pM - 100 nM) or morphine (0-100 nM) in the absence or presence of RS-ketamine (100 pM - 100 nM). Analysis of data for β-arrestin recruitment at MOR by (i) RS-ketamine, R-ketamine or S-ketamine (0-10 μM), (ii) RS-ketamine (0-100 nM) in the absence or presence of either Met-enkephalin (Met-enk) or morphine (100 pM - 1 μM), (iii) Met-enk (0- 10 μM) or morphine (0-3 μM) in the absence or presence of RS-ketamine (1 pM-100 nM). Data was fitted using either bell-shaped or sigmoidal dose response curves in Prism 10.0. Data is Mean±SD of 3 independent experiments. *p<0.05;**0.01;***p<0.001, t-test or One-Way ANOVA. [a]Peak response at 1 mM; [b]Peak response at 10 μM; [c]Peak response at 1 μM; [d]Peak response at 100 nM; [e]Peak response at 1 nM; [f]Peak response at 100 pM; [g]Peak response at 10 pM; ; [h]Peak response at 0.1 pM; [i]Peak response at 3 μM. n.a.= not applicable.

Supplemental Table 3. Analysis of effect of RS-ketamine on Leu-enkephalin- or Dynorphin A17-mediated [^{35}S]GTPγS binding at MOR

Data from Fig.	Ligand	[^{35}S]GTPγS binding		Data from Fig.	Ligand	[^{35}S]GTPγS binding			
		EC_{50} [nM]	Peak Response (% basal)			EC_{50} [nM]	Peak Response (% basal)	Normalized to Leu-enk response	% change in normalized response
Supl Fig. 3A	RS-ketamine (0-1 μM)	>1,000	123±4[a]	**Supl Fig. 3B; Fig. 3B**	Leu-enk (0-1 μM)	104±1	168±4[a]	100±6	
	+ 100 pM Leu-enk	390±5[***]	115±1[a]		+100 pM RS-ketamine	93±1[***]	177±2[a,*]	113±4	13±4
	+ 1 nM Leu-enk	25±3[***]	111±2[a,*]		+1 nM RS-ketamine	104±1	181±5[a,**]	120±8[**]	20±6
	+10 nM Leu-enk	67±2[***]	124±5[a]		+10 nM RS-ketamine	106±1	194±4[a,***]	139±6[***]	39±5
	+100 nM Leu-enk	10±2[***]	180±5[a,***]		+100 nM RS-ketamine	101±1*	195±2[a,***]	140±4[***]	40±4
	+ 1 μM Leu-enk	6±2[***]	235±12[a,***]		+ 1 μM RS-ketamine	137±1[***]	191±10[a,**]	134±15[**]	34±9
		EC_{50} [nM]	Peak Response (% basal)			EC_{50} [nM]	Peak Response (% basal)	Normalized to Dyn A17 response	% change in normalized response
Supl Fig. 3C	RS-ketamine (0-1 μM)	>1,000	109±1[a]	**Supl Fig. 3D; Fig. 3C**	Dyn A17 (0-1 μM)	112±1	144±1[a]	100±1	
	+ 100 pM Dyn A17	2±2[***]	114±2[a,*]		+100 pM RS-ketamine	91±1[***]	152±3[a,*]	119±7[*]	19±4
	+ 1 nM Dyn A17	4±2[***]	120±1[a,***]		+1 nM RS-ketamine	132±1[***]	163±3[a,***]	143±7[***]	43±4
	+10 nM Dyn A17	1±2[***]	135±1[a,***]		+10 nM RS-ketamine	126±1[***]	170±4[a,***]	158±9[***]	58±5
	+100 nM Dyn A17	1±2[***]	147±2[a,***]		+100 nM RS-ketamine	111±1	173±4[a,***]	166±8[***]	66±5
	+ 1 μM Dyn A17	0.8±2[***]	197±3[a,***]		+ 1 μM RS-ketamine	120±1[***]	181±3[a,***]	185±7[***]	85±4

Analysis of data for [^{35}S]GTPγS binding at MOR by (i) RS-ketamine (0-1 μM) in the absence or presence of either Leu-enkephalin (Leu-enk; 100 pM – 1 μM) or Dynorphin A17 (Dyn A17; 100 pM - 1 μM), (ii) Leu-enk (0-1 μM) or Dyn A17 (0-1 μM) in the absence or presence of RS-ketamine (100 pM-1 μM). Data was fitted using sigmoidal dose response curves in Prism 10.0. Data is Mean±SD of 3 independent experiments. *p<0.05;**0.01;***p<0.001, One-Way ANOVA. [a]Peak response at 1 μM.

Supplemental Table 4. Analysis of effect of RS-ketamine on Met-enkephalin-, Leu-enkephalin-, or Dynorphin A17-mediated [^{35}S]GTPγS binding at DOR

Data from Fig.	Ligand	[^{35}S]GTPγS binding		Data from Fig.	Ligand	[^{35}S]GTPγS binding			
		EC_{50} [nM]	Peak Response (% basal)			EC_{50} [nM]	Peak Response (% basal)	Normalized to Met-enk response	% change in normalized response
Supl Fig. 3E	RS-ketamine (0-1 μM)	>1,000	108±2[a]	**Supl Fig. 3F; Fig. 3D**	Met-enk (0-1 μM)	28±1	144±7[a]	100±15	
	+ 100 pM Met-enk	7±3[***]	114±1[a, **]		+100 pM RS-ketamine	38±1[***]	151±3[a]	115±8	15±10
	+ 1 nM Met-enk	8±2[***]	116±1[a, **]		+1 nM RS-ketamine	48±1[***]	159±5[a,**]	134±12[**]	34±11
	+10 nM Met-enk	7±2[***]	121±1[a, ***]		+10 nM RS-ketamine	40±1[***]	160±4[a, **]	136±10[**]	36±10
	+100 nM Met-enk	7±2[***]	158±3[a, ***]		+100 nM RS-ketamine	52±1[***]	166±1[a, ***]	150±3[***]	50±9
	+ 1 μM Met-enk	0.6±2[***]	178±3[a, ***]		+ 1 μM RS-ketamine	47±1[***]	164±2[a, ***]	146±6[***]	46±10
		EC_{50} [nM]	Peak Response (% basal)			EC_{50} [nM]	Peak Response (% basal)	Normalized to Leu-enk response	% change in normalized response
Supl Fig. 3G	RS-ketamine (0-1 μM)	>1,000	109±2[a]	**Supl Fig. 3H; Fig. 3E**	Leu-enk (0-1 μM)	37±1	132±1[a]	100±3	
	+ 100 pM Leu-enk	0.8±2[***]	110±1[a]		+100 pM RS-ketamine	41±1[**]	133±2[a]	106±5	6±3
	+ 1 nM Leu-enk	1±2[***]	113±2[a]		+1 nM RS-ketamine	43±1[***]	138±2[a,***]	120±5[*]	20±3
	+10 nM Leu-enk	4±2[***]	117±1[a,*]		+10 nM RS-ketamine	40±1[*]	137±1[a,**]	118±1	18±2
	+100 nM Leu-enk	12±2[***]	150±5[a, ***]		+100 nM RS-ketamine	33±1[**]	141±2[a, ***]	128±5[**]	28±3
	+ 1 μM Leu-enk	1±2[***]	156±6[a, ***]		+ 1 μM RS-ketamine	34±1[*]	144±5[a, ***]	139±17[***]	39±10
		EC_{50} [nM]	Peak Response (% basal)			EC_{50} [nM]	Peak Response (% basal)	Normalized to Dyn A17 response	% change in normalized response
Supl Fig. 3I	RS-ketamine (0-1 μM)	>1,000	108±2[a]	**Supl Fig. 3J; Fig. 3F**	Dyn A17 (0-1 μM)	2±2	126±5[a]	100±19	
	+ 100 pM Dyn A17	6±2[***]	115±2[a]		+100 pM RS-ketamine	1±1	131±1[a]	120±4[*]	20±11
	+ 1 nM Dyn A17	1±4[***]	122±6[a, ***]		+1 nM RS-ketamine	5±1	131±1[a]	122±4	22±11
	+10 nM Dyn A17	0.9±2[***]	130±1[a, ***]		+10 nM RS-ketamine	1±1	133±2[a, *]	128±7[*]	28±12
	+100 nM Dyn A17	0.2±2[***]	138±1[a, ***]		+100 nM RS-ketamine	0.9±1	133±1[a, *]	128±5[*]	28±11
	+ 1 μM Dyn A17	0.2±2[***]	144±2[a, ***]		+ 1 μM RS-ketamine	1±1	134±2[a, *]	132±7[*]	32±12

Analysis of data for [^{35}S]GTPγS binding at DOR by (i) RS-ketamine (0-1 μM) in the absence or presence of either Met-enkephalin (Met-enk; 100 pM - 1 μM), Leu-enkephalin (Leu-enk; 100 pM – 1 μM) or Dynorphin A17 (Dyn A17; 100 pM - 1 μM), or (ii) Met-enk (0-1 μM), Leu-enk (0-1 μM) or Dyn A17 (0-1 μM) in the absence or presence of RS-ketamine (100 pM-1 μM). Data was fitted using sigmoidal dose response curves in Prism 10.0. Data is Mean±SD of 3 independent experiments. *p<0.05;**0.01;***p<0.001, One-Way ANOVA. [a]Peak response at 1 μM.

Supplemental Table 5. Analysis of effect of RS-ketamine on Met-enkephalin-, Leu-enkephalin-, or Dynorphin A17-mediated [^{35}S]GTPγS binding at KOR

Data from Fig.	Ligand	[^{35}S]GTPγS binding		Data from Fig.	Ligand	[^{35}S]GTPγS binding			
		EC_{50} [nM]	Peak Response (% basal)			EC_{50} [nM]	Peak Response (% basal)	Normalized to Met-enk response	% change in normalized response
Supl Fig. 3K	RS-ketamine (0-1 μM)	>1,000	108±2[a]	**Supl Fig. 3L; Fig. 3G**	Met-enk (0-1 μM)	3±2	124±3[a]	100±14	
	+ 100 pM Met-enk	15±3[***]	114±1[a, *]		+100 pM RS-ketamine	4±2	127±2[a]	113±9	13±9
	+ 1 nM Met-enk	6±3[***]	118±2[a, ***]		+1 nM RS-ketamine	7±1	131±1[a, **]	126±6[*]	26±9
	+10 nM Met-enk	4±3[***]	123±2[a, ***]		+10 nM RS-ketamine	7+1	134±2[a, ***]	140±8[**]	40±9
	+100 nM Met-enk	0.4±2[***]	133±3[a, ***]		+100 nM RS-ketamine	7±2	136±2[a, ***]	140±8[**]	40±9
	+ 1 μM Met-enk	3±2[***]	147±3[a, ***]		+ 1 μM RS-ketamine	12±2[**]	136±3[a, **]	149±13[**]	49±11
		EC_{50} [nM]	Peak Response (% basal)			EC_{50} [nM]	Peak Response (% basal)	Normalized to Leu-enk response	% change in normalized response
Supl Fig. 3M	RS-ketamine (0-1 μM)	>1,000	110±1[a]	**Supl Fig. 3N; Fig. 3H**	Leu-enk (0-1 μM)	1±2	123±2[a]	100±8	
	+ 100 pM Leu-enk	8±2[***]	115±1[a, ***]		+100 pM RS-ketamine	5±2	125±2[a]	105±8	5±7
	+ 1 nM Leu-enk	3±2[***]	119±1[a, ***]		+1 nM RS-ketamine	1±2	125±2[a]	107±7	7±6
	+10 nM Leu-enk	1±2[***]	124±1[a, ***]		+10 nM RS-ketamine	2±2	126±3[a]	110±13	10±9
	+100 nM Leu-enk	1±2[***]	124±1[a, ***]		+100 nM RS-ketamine	1±2	126±2[a]	111±7	11±6
	+ 1 μM Leu-enk	3±2[***]	138±2[a, ***]		+ 1 μM RS-ketamine	1±2	126±2[a]	112±8	12±7
		EC_{50} [nM]	Peak Response (% basal)			EC_{50} [nM]	Peak Response (% basal)	Normalized to Dyn A17 response	% change in normalized response
Supl Fig. 3O	RS-ketamine (0-1 μM)	>1,000	106±2[a]	**Supl Fig. 3P; Fig. 3I**	Dyn A17 (0-1 μM)	0.6±1	162±3[a]	100±5	
	+ 100 pM Dyn A17	12±2[***]	112±4[a]		+100 pM RS-ketamine	0.6±1	167±3[a]	109±5	9±4
	+ 1 nM Dyn A17	3±3[***]	158±5[a, ***]		+1 nM RS-ketamine	0.7±1	174±4[a, **]	120±6[**]	20±5
	+10 nM Dyn A17	0.4±2[***]	167±2[a, ***]		+10 nM RS-ketamine	0.6±1	176±1[a, ***]	124±2[***]	24±3
	+100 nM Dyn A17	0.4±2[***]	174±2[a, ***]		+100 nM RS-ketamine	0.6±1	181±3[a, ***]	131±4[***]	31±4
	+ 1 μM Dyn A17	1±2[***]	192±1[a, ***]		+ 1 μM RS-ketamine	0.6±1	182±1[a, ***]	133±1[***]	33±3

Analysis of data for [^{35}S]GTPγS binding at KOR by (i) RS-ketamine (0-1 μM) in the absence or presence of either Met-enkephalin (Met-enk; 100 pM - 1 μM), Leu-enkephalin (Leu-enk; 100 pM – 1 μM) or Dynorphin A17 (Dyn A17; 100 pM - 1 μM), (ii) Met-enk (0-1 μM), Leu-enk (0-1 μM) or Dyn A17 (0-1 μM) in the absence or presence of RS-ketamine (100 pM-1 μM). Data was fitted using sigmoidal dose response curves in Prism 10.0. Data is Mean±SD of 3 independent experiments. *p<0.05;**0.01;***p<0.001, One-Way ANOVA. [a]Peak response at 1 μM.

Supplemental Table 6. Analysis of effect of R- and S-ketamine on Met-enkephalin-mediated signaling at MOR

Data from Fig.	Ligand	[^{35}S]GTPγS binding		Data from Fig.	Ligand	[^{35}S]GTPγS binding			
		EC_{50} [nM]	Peak Response (% basal)			EC_{50} [nM]	Peak Response (% basal)	Normalized to Met-enk response	% change in normalized response
Supl Fig. 4A	RS-ketamine (0-1 μM)	>1,000	109±1[a]						
	R-ketamine (0-1 μM)	>1,000	113±1[a]						
	S-ketamine (0-1 μM)	>1,000	112±3[a]						
		EC_{50} [nM]	Peak Response (% basal)			EC_{50} [nM]	Peak Response (% basal)	Normalized to Met-enk response	% change in normalized response
Supl Fig. 4B	R-ketamine (0-1 μM)	>1,000	113±3[a]	**Supl Fig. 4C; Fig. 4A**	Met-enk (0-1 μM)	19±1	131±2[a]	100±6	
	+ 100 pM Met-enk	1±2[***]	113±1[a]		+ 100 pM R-ketamine	11±1[***]	154±1[a, ***]	176±4[***]	76±4
	+ 1 nM Met-enk	1±2[***]	114±4[a]		+ 1 nM R-ketamine	8±1[***]	153±1[a, ***]	172±4[***]	72±4
	+10 nM Met-enk	0.1±1[***]	131±1[a, ***]		+10 nM R-ketamine	7±2[***]	150±1[a, ***]	164±4[***]	64±4
	+100 nM Met-enk	0.06±2[***]	145±2[a, ***]		+100 nM R-ketamine	9±1[***]	150±1[a, ***]	164±3[***]	64±4
	+ 1 μM Met-enk	0.06±2[***]	159±1[a, ***]		+ 1 μM R-ketamine	20±1	140±1[a, ***]	130±1[***]	30±3
		EC_{50} [nM]	Peak Response (% basal)			EC_{50} [nM]	Peak Response (% basal)	Normalized to Met-enk response	% change in normalized response
Supl Fig. 4D; Fig. 5C	S-ketamine (0-1 μM)	>1,000	112±5[a]	**Supl Fig. 4E; Fig. 4B**	Met-enk (0-1 μM)	19±1	131±2[a]	100±6	
	+ 100 pM Met-enk	2±2[***]	116±1[a]		+ 100 pM S-ketamine	7±1[***]	168±2[a, ***]	221±5[***]	121±4
	+ 1 nM Met-enk	0.1±2[***]	128±4[a, **]		+ 1 nM S-ketamine	15±1[**]	188±1[a, ***]	286±3[***]	186±4
	+10 nM Met-enk	0.1±2[***]	145±2[a, ***]		+10 nM S-ketamine	13±1[***]	190±4[a, ***]	294±12[***]	194±8
	+100 nM Met-enk	0.2±2[***]	190±9[a, ***]		+100 nM S-ketamine	16±1[*]	194±2[a, ***]	308±5[***]	208±5
	+ 1 μM Met-enk	0.3±2[***]	221±5[a, ***]		+ 1 μM S-ketamine	18±1	210±3[a, ***]	358±9[***]	258±6
Data from Fig.	**Ligand**	**β-arrestin recruitment**		**Data from Fig.**	**Ligand**	**β-arrestin recruitment**			
		EC_{50} [nM]	Peak Response (% basal)						
Supl Fig. 4F	RS-ketamine (0-10 μM)	>1,000	117±3[b]						
	R-ketamine (0-10 μM)	>1,000	105±2[b, **]						
	S-ketamine (0-10 μM)	>1,000	116±3[b]						
		EC_{50} [nM]	Peak Response (% basal)			EC_{50} [nM]	Peak Response (% basal)	Normalized to Met-enk response	% change in normalized response
Supl Fig. 4G	R-ketamine (0-100 nM)	n.a.	101±7[c]	**Supl Fig. 4H; Fig. 4C**	Met-enk (0-1 μM)	2±1	409±13[a]	100±4	

	+ 100 pM Met-enk	n.a.	110±8[c]		+ 100 pM R-ketamine	2±1	443±26[a]	111±9	11±5
	+ 1 nM Met-enk	0.02±9	225±16[c, ***]		+ 1 nM R-ketamine	2±1	424±26[a]	105±9	5±5
	+10 nM Met-enk	0.03±10	319±23[c, ***]		+10 nM R-ketamine	2±1	447±24[a]	112±8	12±5
	+100 nM Met-enk	0.02±4	411±33[c, ***]		+100 nM R-ketamine	2±1	414±33[a]	102±11	2±6
	+ 1 μM Met-enk	0.01±4	416±33[c, ***]						
		EC_{50} [nM]	Peak Response (% basal)			EC_{50} [nM]	Peak Response (% basal)	Normalized to Met-enk response	% change in normalized response
Supl Fig. 4I	S-ketamine (0-100 nM)	n.a.	98±10[c]	**Supl Fig. 4J; Fig. 4D**	Met-enk (0-1 μM)	2±1	409±13[a]	100±4	
	+ 100 pM Met-enk	0.02±2	129±3[c]		+ 100 pM S-ketamine	2±1	629±39[a, ***]	171±12[***]	71±7
	+ 1 nM Met-enk	0.08±2	306±26[c, ***]		+ 1 nM S-ketamine	2±1	677±30[a, ***]	187±10[***]	87±6
	+10 nM Met-enk	0.06±1; 75±14	531±23[d, ***]		+10 nM S-ketamine	1±1	627±14[a, ***]	171±5[***]	71±3
	+100 nM Met-enk	0.01±1; 52±9	632±28[d, ***]		+100 nM S-ketamine	1±1	580±14[a, ***]	155±5[***]	55±3
	+ 1 μM Met-enk	0.01±1; 24±3	645±29[d, ***]						

Analysis of data for [^{35}S]GTPγS binding at MOR by (i) RS-ketamine, R-ketamine or S-ketamine (0-1 μM), (ii) R-ketamine or S-ketamine (0-1 μM) in the absence or presence of Met-enkephalin (Met-enk; 100 pM - 1 μM), (iii) Met-enk (0-1 μM) in the absence or presence of R-ketamine or S-ketamine (100 pM-1 μM). Analysis of data for β-arrestin recruitment at MOR by (i) RS-ketamine, R-ketamine or S-ketamine (0-10 μM), (ii) R-ketamine or S-ketamine (0-100 nM) in the absence or presence of Met-enkephalin (Met-enk; 100 pM - 1 μM), (iii) Met-enk (0 - 1 μM) in the absence or presence of either R-ketamine or S-ketamine (100 pM-100 nM). Data was fitted using either bell-shaped or sigmoidal dose response curves in Prism 10.0. Data is Mean±SD of 3 independent experiments. *p<0.05;**0.01;***p<0.001, One-Way ANOVA. [a]Peak response at 1 μM; [b]Peak response at 10 μM; [c]Peak response at 100 nM, [d]Peak response at 1 nM.

Supplemental Table 7. Analysis of effect ketamine metabolites on Met-enkephalin-mediated signaling at MOR

Data from Fig.	Ligand	[^{35}S]GTPγS binding		Data from Fig.	Ligand	[^{35}S]GTPγS binding			
		EC_{50} [nM]	Peak Response (% basal)			EC_{50} [nM]	Peak Response (% basal)	Normalized to Met-enk response	% change in normalized response
Supl Fig. 5A	RS-NK (0-1 μM)	>1000	82±3[a]	**Supl Fig. 5B; Fig. 5A**	Met-enk (0-100 nM)	3±1	134±4[b]	100±12	
	+ 100 pM Met-enk	4±2[***]	109±2[a, ***]		+ 100 pM RS-NK	2±1	140±2[b, *]	118±5[*]	18±7
	+ 1 nM Met-enk	0.08±2[***]	124±4[a, ***]		+ 1 nM RS-NK	2±1	146±1[b, ***]	132±2[***]	32±7
	+10 nM Met-enk	0.8±2[***]	149±1[a, ***]		+10 nM RS-NK	2±1	149±4[b, ***]	144±12[***]	44±10
	+100 nM Met-enk	1±2[***]	161±1[a, ***]		+100 nM RS-NK	1±1	175±1[b, ***]	217±1[***]	117±7
					+ 1 μM RS-NK	0.4±1[*]	195±1[b, ***]	278±2[***]	178±7
		EC_{50} [nM]	Peak Response (% basal)			EC_{50} [nM]	Peak Response (% basal)	Normalized to Met-enk response	% change in normalized response
Fig. 5B	1 nM RS-NK	n.a.	95±3	**Supl Fig. 5C; Fig. 5C**	Met-enk (0-1 μM)	5±1	145±4[a]	100±10	
	1 nM R-NK	n.a.	96±1		+1 nM RS-NK	5±1	163±4[a, **]	141±8[**]	41±7
	+1 nM S-NK	n.a.	94±8		+1 nM R-NK	2±1[*]	155±5[a]	123±10[*]	23±8
					+1 nM S-NK	7±1	176±4[a, ***]	171±8[***]	71±7
		EC_{50} [nM]	Peak Response (% basal)			EC_{50} [nM]	Peak Response (% basal)	Normalized to Met-enk response	% change in normalized response
Supl Fig. 5D, E	RR-HNK (0-1 μM)	>1,000	105±3[a]	**Supl Fig. 5F; Fig. 5D**	Met-enk (0-1 μM)	3±1	138±3[a]	100±7	
	+10 nM Met-enk	0.6±2[***]	134±1[a, ***]		+10 nM RR-HNK	2±1	153±3[a, ***]	140±8[***]	40±6
	SS-HNK (0-1 μM)	>1,000	110±1[a]		+10 nM-SS-HNK	1±1	155±1[a, ***]	147±4[***]	47±4
	+10 nM Met-enk	1±1[***]	138±1[a,***]						
Data from Fig.	**Ligand**	**β-arrestin recruitment**		**Data from Fig.**	**Ligand**	**β-arrestin recruitment**			
		EC_{50} [nM]	Peak Response (% basal)			EC_{50} [nM]	Peak Response (% basal)	Normalized to Met-enk response	% change in normalized response
Supl Fig. 5G	RS-NK (0-10 μM)	>1,000	97±1[c]						
	R-NK (0-10 μM)	>1,000	98±2[c]						
	S-NK (0-10 μM)	>1,000	99±3[c]						
		EC_{50} [nM]	Peak Response (% basal)			EC_{50} [nM]	Peak Response (% basal)	Normalized to Met-enk response	% change in normalized response
Supl Fig. 5H	RS-NK (0-100 nM)	>1000	96±4[b]	**Supl Fig. 5I; Fig. 5E**	Met-enk (0-1 μM)	2±1	409±13[a]	100±4	
	+ 100 pM Met-enk	11±4[***]	126±3[b, *]		+ 100 pM RS-NK	2±1	546±12[a, ***]	144±4[***]	44±3
	+ 1 nM Met-enk	20±1[***]	303±9[b, ***]		+ 1 nM RS-NK	2±1	629±16[a, ***]	171±5[***]	71±3
	+10 nM Met-enk	20±1[***]	498±19[b, ***]		+10 nM RS-NK	1±1	679±12[a, ***]	187±4[***]	87±3
	+100 nM Met-enk	8±1[***]	597±4[b, ***]		+100 nM RS-NK	0.9±1	675±13[a, ***]	186±4[***]	86±3
	+ 1 μM Met-enk	3±1[***]	602±15[b, ***]						

		EC_{50} [nM]	Peak Response (% basal)			EC_{50} [nM]	Peak Response (% basal)	Normalized to Met-enk response	% change in normalized response
Supl Fig. 5J	R-NK (0-100 nM)	>1,000	108±0.7[b]	**Supl Fig. 5K; Fig. 5F**	Met-enk (0-1 μM)	2±1	409±13[a]	100±4	
	+ 100 pM Met-enk	0.08±5 ***	129±1[b, *]		+ 100 pM R-NK	2±1	442±11[a, *]	111±4*	11±2
	+ 1 nM Met-enk	0.2±2 ***	263±2[b, ***]		+ 1 nM R-NK	2±1	470±3[a, ***]	120±1***	20±1
	+10 nM Met-enk	10±2 ***	411±3[b, ***]		+10 nM R-NK	2±1	459±14[a, **]	116±5**	16±3
	+100 nM Met-enk	0.2±2 ***	506±21[b, ***]		+100 nM R-NK	2±1	426±14[a]	105±5	5±3
	+ 1 μM Met-enk	0.3±2 ***	506±3[b, ***]						
		EC_{50} [nM]	Peak Response (% basal)			EC_{50} [nM]	Peak Response (% basal)	Normalized to Met-enk response	% change in normalized response
Supl Fig. 5L	S-NK (0-100 nM)	n.a.	103±7[b]	**Supl Fig. 5M; Fig. 5G**	Met-enk (0-1 μM)	2±1	409±13[a]	100±4	
	+ 100 pM Met-enk	6±5	125±2[b]		+ 100 pM S-NK	2±1	620±39[a, ***]	168±13***	68±7
	+ 1 nM Met-enk	13±1	389±11[b, ***]		+ 1 nM S-NK	2±1	747±3[a, ***]	210±1***	110±1
	+10 nM Met-enk	3±1	609±25[b, ***]		+10 nM S-NK	1±1	764±25[a, ***]	215±8***	115±5
	+100 nM Met-enk	4±1	759±19[b, ***]		+100 nM S-NK	1±1	729±17[a, ***]	204±6***	104±4
	+ 1 μM Met-enk	5±1	772±3[b, ***]						
		EC_{50} [nM]	Peak Response (% basal)			EC_{50} [nM]	Peak Response (% basal)	Normalized to Met-enk response	% change in normalized response
Supl Fig. N	RR-HNK (0-10 μM)	>1,000	112±4[c]						
	SS-HNK (0-10 μM)	>1,000	116±3[c]						
		EC_{50} [nM]	Peak Response (% basal)			EC_{50} [nM]	Peak Response (% basal)	Normalized to Met-enk response	% change in normalized response
Supl Fig. 5O	RR-HNK (0-100 nM)	>1,000	106±3[b]	**Supl Fig. 5P; Fig. 5H**	Met-enk (0-1 μM)	2±1	409±13[a]	100±4	
	+ 100 pM Met-enk	7±3***	136±7[b, *]		+ 100 pM RR-HNK	2±1	560±14[a, ***]	149±5***	49±3
	+ 1 nM Met-enk	11±1***	356±7[b, ***]		+ 1 nM RR-HNK	1±1	611±7[a, ***]	165±2***	65±2
	+10 nM Met-enk	0.8±1***	547±13[b, ***]		+10 nM RR-HNK	2±1	535±16[a, ***]	141±5***	41±3
	+100 nM Met-enk	1±1***	642±21[b, ***]		+100 nM RR-HNK	2±1	501±6[a, ***]	130±2***	30±2
	+ 1 μM Met-enk	1±1***	649±8[b, ***]						
		EC_{50} [nM]	Peak Response (% basal)			EC_{50} [nM]	Peak Response (% basal)	Normalized to Met-enk response	% change in normalized response
Supl Fig. 5Q	SS-HNK (0-100 nM)	>1,000	105±3[b]	**Supl Fig. 5R; Fig. 5I**	Met-enk (0-1 μM)	2±1	409±13[a]	100±4	
	+ 100 pM Met-enk	3±3***	132±3[b, **]		+ 100 pM SS-HNK	1±1	448±16[a, *]	113±5*	13±3
	+ 1 nM Met-enk	12±1***	325±11[b, ***]		+ 1 nM SS-HNK	0.9±1	482±24[a, ***]	124±8***	24±5
	+10 nM Met-enk	0.2±2***	451±15[b, ***]		+10 nM SS-HNK	0.9±1	495±16[a, ***]	128±5***	28±3
	+100 nM Met-enk	1±2***	504±22[b, ***]		+100 nM SS-HNK	0.8±1	499±14[a,***]	129±4***	29±3
	+ 1 μM Met-enk	1±2***	506±25[b, ***]						

Analysis of data for [^{35}S]GTPγS binding at MOR by (i) RS-norketamine (RS-NK; 0 - 1 μM) in the absence or presence of Met-enkephalin (Met-enk; 100 pM - 100 nM), (ii) Met-enk (0 - 100 nM) in the absence or presence of RS-NK (100 pM - 1 μM), (iii) 1 nM RS-NK, R-norketamine (R-NK), or S-norketamine (S-NK), (iv) Met-enk (0 - 1 μM) in the absence or presence of 1 nM RS-NK, R-NK or S-NK, (v) RR-hydroxynorketamine (RR-HNK) or SS-hydroxynorketamine (SS-HNK) (0 - 1 μM) in the absence or presence of Met-enk (10 nM, (vi) Met-enk (0 - 1 μM) in the absence or presence of 10 nM for RR- or SS-HNK. Analysis of data for β-arrestin recruitment at MOR by (i) RS-NK, R-NK, S-NK, RR-HNK, or SS-HNK (0 - 10 μM), (ii) RS-NK, R-NK, S-NK, RR-HNK or S,S-HNK (0 - 100 nM) in the absence or presence of Met-enkephalin (100 pM - 1 μM), (iii) Met-enkephalin (0 - 1 μM) in the absence or presence of either RS-NK, R-NK, S-NK, RR-HNK, or SS-HNK (100 pM - 100 nM). Data was fitted using either bell-shaped or sigmoidal dose response curves in Prism 10.0. Data is Mean±SD of 3 independent experiments. *p<0.05;**0.01;***p<0.001, t-test or One-Way ANOVA. [a]Peak response at 1 μM; [b]Peak response at 100 nM; [c]Peak response at 10 μM. n.a.=not applicable.

Supplemental Table 8. Description of statistical analysis for different figures. Morp, morphine; Met-enk, met-enkephalin; RS-ket, RS-ketamine; R-ket, R-ketamine; S-ket, S-ketamine; RS-NK, RS-norketamine; R-NK, R-norketamine; S-NK, S-norketamine; DFn, degrees of freedom (DF) in the numerator; DFd, degrees of freedom (DF) in the denominator; MCT, multiple comparison test

Fig.	One-way ANOVA		Two-way ANOVA		
	Test	**p-value**	**Test**	**p-value**	**F (DFn, DFd)**
1A			Interaction Dose Treatment **Sidak's MCT** *Morp v/s Morp+100 nM RS ket* Basal 0.1nM Morp 1nM Morp 10nM Morp 100nM Morp 1 μM Morp	p=0.0213 p<0.0001 p<0.0001 p>0.9999 p=0.0005 p=0.0026 p=0.001 p=0.0024 p=0.0008	F(5,24)= 3.281 F(5,24)= 18.64 F(1,24)= 80.32 DF=24 DF=24 DF=24 DF=24 DF=24 DF=24
1B			Interaction Dose Treatment **Sidak's MCT** *DAMGO v/s DAMGO+100 nM RS ket* Basal 0.1nM DAMGO 1nM DAMGO 10nM DAMGO 100nM DAMGO 1 μM DAMGO	p=0.0652 p<0.0001 p<0.0001 p>0.9999 p=0.019 p=0.0157 p=0.0063 p=0.0038 p=0.0017	F(5,24)= 2.421 F(5,24)= 26.74 F(1,24)= 57.25 DF=24 DF=24 DF=24 DF=24 DF=24 DF=24
1C			Interaction Dose Treatment **Sidak's MCT** *Met-enk v/s Met-enk+100 nM RS ket* Basal 0.1nM Met-enk 1nM Met-enk 10nM Met-enk 100nM Met-enk 1 μM Met-enk	p=0.002 p<0.0001 p<0.0001 p>0.9999 p<0.0001 p=0.0002 p<0.0001 p<0.0001 p<0.0001	F(5,24)= 5.329 F(5,24)= 29.89 F(1,24)= 128.9 DF=24 DF=24 DF=24 DF=24 DF=24 DF=24
1D			Interaction Dose Treatment **Sidak's MCT** *RS-ket v/s RS-ket+100 nM Met-enk* Basal 0.1nM RS-ket 1nM RS-ket 10nM RS-ket 100nM RS-ket 1μM RS-ket	p=0.1644 p<0.0001 p<0.0001 p=0.0028 p<0.0001 p<0.0001 p<0.0001 p<0.0001 p<0.0001	F(5,24)= 1.737 F(5,24)= 8.967 F(1,24)= 248.6 DF=24 DF=24 DF=24 DF=24 DF=24 DF=24
1E	**One-way ANOVA** Treatment **Tukey's MCP** Basal v/s 100nM RS-ket Basal v/s 100nM Met-enk Basal v/s RS-ket+Met-enk 100nM RS-ket v/s 100nM Met-enk 100nM RS-ket v/s RS-ket+Met-enk 100nM Met-enk v/s RS-ket+Met-enk	 p<0.0001; F(3,8)=36.66 p=0.9632; DF=8 p=0.0052; DF=8 p<0.0001; DF=8 p=0.0094; DF=8 p=0.0001; DF=8 p=0.0125; DF=8			
2B			Interaction Dose Treatment **Sidak's MCT** *RS-ket v/s + 1μM CTOP*	P=0.0014 p<0.0001 p<0.0001 p>0.9999	F(13,56)= 3.157 F(13,56)= 5.844 F(1,56)= 80.07 DF=56

			Basal	p=0.9998	DF=56
			1pM RS-ket	p>0.9999	DF=56
			10pM RS-ket	p=0.7217	DF=56
			100pM RS-ket	p=0.2115	DF=56
			300pM RS-ket	p=0.9253	DF=56
			1nM RS-ket	p=0.5300	DF=56
			3nM RS-ket	p=0.0591	DF=56
			10nM RS-ket	p=0.4399	DF=56
			30nM RS-ket	p=0.2546	DF=56
			100nM RS-ket	p=0.1392	DF=56
			300nM RS-ket	p=0.0931	DF=56
			1μM RS-ket	p=0.0005	DF=56
			3μM RS-ket	p<0.0001	DF=56
			10μM RS-ket		
Fig.	**One-way ANOVA**		**Two-way ANOVA**		
	Test	**p-value**	**Test**	**p-value**	**F (DFn, DFd)**
2C			Interaction	p<0.0001	F(26,84)= 45.40
			Dose	p<0.0001	F(13,84)= 1268
			Treatment	p<0.0001	F(2,84)= 1325
			Tukey's MCT		
			Basal		
			v/s +1nM RS-ket	p>0.9999	DF=84
			v/s +100nM RS-ket	p>0.9999	DF=84
			+1nM RS-ket	p>0.9999	DF=84
			v/s+100nM RS-ket		
			1pM DAMGO	0.8977	DF=84
			v/s +1nM RS-ket	0.5339	DF=84
			v/s +100nM RS-ket	0.8044	DF=84
			+1nM RS-ket		
			v/s+100nM RS-ket	0.4404	DF=84
			10pM DAMGO	0.1893	DF=84
			v/s +1nM RS-ket	0.8554	DF=84
			v/s +100nM RS-ket		
			+1nM RS-ket	0.0651	DF=84
			v/s+100nM RS-ket	p<0.0001	DF=84
			100pM DAMGO	0.0830	DF=84
			v/s +1nM RS-ket		
			v/s +100nM RS-ket	p=0.0185	DF=84
			+1nM RS-ket	p<0.0001	DF=84
			v/s+100nM RS-ket	p=0.0080	DF=84
			300pM DAMGO		
			v/s +1nM RS-ket	p<0.0001	DF=84
			v/s +100nM RS-ket	p<0.0001	DF=84
			+1nM RS-ket	p=0.0003	DF=84
			v/s+100nM RS-ket		
			1nM DAMGO	p<0.0001	DF=84
			v/s +1nM RS-ket	p<0.0001	DF=84
			v/s +100nM RS-ket	p<0.0001	DF=84
			+1nM RS-ket		
			v/s+100nM RS-ket	p<0.0001	DF=168
			3nM DAMGO	p<0.0001	DF=168
			v/s +1nM RS-ket	p<0.0001	DF=168
			v/s +100nM RS-ket		
			+1nM RS-ket	p<0.0001	DF=84
			v/s+100nM RS-ket	p<0.0001	DF=84
			10nM *DAMGO*	p<0.0001	DF=84
			v/s +1nM RS-ket		
			v/s +100nM RS-ket	p<0.0001	DF=84
			+1nM RS-ket	p<0.0001	DF=84
			v/s+100nM RS-ket	p<0.0001	DF=84
			30nM DAMGO		
			v/s +1nM RS-ket	p<0.0001	DF=84
			v/s +100nM RS-ket	p<0.0001	DF=84
			+1nM RS-ket	p<0.0001	DF=84
			v/s+100nM RS-ket		
			100nM DAMGO	p<0.0001	DF=84
			v/s +1nM RS-ket	p<0.0001	DF=84
			v/s +100nM RS-ket	p<0.0001	DF=84
			+1nM RS-ket		
			v/s+100nM RS-ket	p<0.0001	DF=84
			300nM DAMGO	p<0.0001	DF=84
			v/s +1nM RS-ket	p<0.0001	DF=84
			v/s +100nM RS-ket		
			+1nM RS-ket	p<0.0001	DF=84
			v/s+100nM RS-ket	p<0.0001	DF=84
			1μM DAMGO	p<0.0001	DF=84
			v/s +1nM RS-ket		

			v/s +100nM RS-ket +1nM RS-ket v/s+100nM RS-ket *3μM DAMGO* v/s +1nM RS-ket v/s +100nM RS-ket +1nM RS-ket v/s+100nM RS-ket *10μM DAMGO* v/s +1nM RS-ket v/s +100nM RS-ket +1nM RS-ket v/s+100nM RS-ket		
2D			Interaction Dose Treatment **Tukey's MCT** *Basal* v/s +1nM Met-enk v/s +100nM Met-enk +1nM Met-enk v/s+100nM Met-enk *100pM RS-ket* v/s +1nM Met-enk v/s +100nM Met-enk +1nM Met-enk v/s+100nM Met-enk *1nM RS-ket* v/s +1nM Met-enk v/s +100nM Met-enk +1nM Met-enk v/s+100nM Met-enk 10nM *RS-ket* v/s +1nM Met-enk v/s +100nM Met-enk +1nM Met-enk v/s+100nM Met-enk *100nM RS-ket* v/s +1nM Met-enk v/s +100nM Met-enk +1nM Met-enk v/s+100nM Met-enk *1μM RS-ket* v/s +1nM Met-enk v/s +100nM Met-enk +1nM Met-enk v/s+100nM Met-enk	p<0.0001 p<0.0001 p<0.0001 p=0.7215 p<0.0001 p<0.0001 p=0.2967 p<0.0001 p<0.0001 p=0.0165 p<0.0001 p<0.0001 p=0.0015 p<0.0001 p<0.0001 p<0.0001 p<0.0001 p<0.0001 p=0.0009 p<0.0001 p<0.0001	F(10,36)= 13.27 F(5,36)= 57.66 F(2,36)= 919.8 DF=36 DF=36 DF=36 DF=36 DF=36 DF=36 DF=36 DF=36 DF=36 DF=36 DF=36 DF=36 DF=36 DF=36 DF=36 DF=36 DF=36 DF=36
Fig.	**One-way ANOVA**		**Two-way ANOVA**		
	Test	**p-value**	**Test**	**p-value**	**F (DFn, DFd)**
2E, 3A			Interaction Dose Treatment **Tukey's MCT** *Basal* v/s +1nM RS-ket v/s +100nM RS-ket +1nM RS-ket v/s+100nM RS-ket *100pM Met-enk* v/s +1nM RS-ket v/s +100nM RS-ket +1nM RS-ket v/s+100nM RS-ket *1nM Met-enk* v/s +1nM RS-ket v/s +100nM RS-ket +1nM RS-ket v/s+100nM RS-ket 10nM *Met-enk* v/s +1nM RS-ket v/s +100nM RS-ket +1nM RS-ket v/s+100nM RS-ket *100nM Met-enk* v/s +1nM RS-ket v/s +100nM RS-ket	p<0.0001 p<0.0001 p<0.0001 p>0.9999 p>0.9999 p>0.9999 p=0.8660 p=0.3728 p=0.6767 p=0.0510 p=0.0047 p<0.6064 p=0.0085 p<0.0001 p=0.0218 p<0.0001 p<0.0001 p=0.0048 p<0.0001 p<0.0001 p=0.1285	F(10,36)= 12.74 F(5,36)= 505.5 F(2,36)= 92.85 DF=36 DF=36 DF=36 DF=36 DF=36 DF=36 DF=36 DF=36 DF=36 DF=36 DF=36 DF=36 DF=36 DF=36 DF=36 DF=36 DF=36 DF=36

			+1nM RS-ket v/s+100nM RS-ket *1μM Met-enk* v/s +1nM RS-ket v/s +100nM RS-ket +1nM RS-ket v/s+100nM RS-ket		
2F			Interaction Dose Treatment **Tukey's MCT** *Basal* v/s +1nM Morp v/s +100nM Morp +1nM Morp v/s+100nM Morp *100pM RS-ket* v/s +1nM Morp v/s +100nM Morp +1nM Morp v/s+100nM Morp *1nM RS-ket* v/s +1nM Morp v/s +100nM Morp +1nM Morp v/s+100nM Morp 10nM *RS-ket* v/s +1nM Morp v/s +100nM Morp +1nM Morp v/s+100nM Morp *100nM RS-ket* v/s +1nM Morp v/s +100nM Morp +1nM Morp v/s+100nM Morp	p<0.0001 p<0.0001 p<0.0001 p<0.0001 p<0.0001 p<0.0001 p<0.0001 p<0.0001 p<0.0001 p<0.0001 p<0.0001 p<0.0001 p<0.0001 p<0.0001 p<0.0001 p<0.0001 p<0.0001 p<0.0001	F(8,30)= 30 F(4,30)= 106.9 F(2,30)= 1464 DF=30 DF=30 DF=30 DF=30 DF=30 DF=30 DF=30 DF=30 DF=30 DF=30 DF=30 DF=30 DF=30 DF=30 DF=30
2G			Interaction Dose Treatment **Tukey's MCT** *Basal* v/s +1nM RS-ket v/s +100nM RS-ket +1nM RS-ket v/s+100nM RS-ket *100pM Morp* v/s +1nM RS-ket v/s +100nM RS-ket +1nM RS-ket v/s+100nM RS-ket *1nM Morp* v/s +1nM RS-ket v/s +100nM RS-ket +1nM RS-ket v/s+100nM RS-ket 10nM *Morp* v/s +1nM RS-ket v/s +100nM RS-ket +1nM RS-ket v/s+100nM RS-ket *100nM Morp* v/s +1nM RS-ket v/s +100nM RS-ket +1nM RS-ket v/s+100nM RS-ket	p<0.0001 p<0.0001 p<0.0001 p>0.9999 p>0.9999 p>0.9999 p<0.0001 p<0.0001 p=0.0002 p<0.0001 p<0.0001 p<0.0001 p<0.0001 p<0.0001 p<0.0001 p<0.0001 p<0.0001 p<0.0001	F(8,30)= 35.95 F(4,30)= 656 F(2,30)= 482.4 DF=30 DF=30 DF=30 DF=30 DF=30 DF=30 DF=30 DF=30 DF=30 DF=30 DF=30 DF=30
Fig.	**One-way ANOVA**		**Two-way ANOVA**		
	Test	**p-value**	**Test**	**p-value**	**F (DFn, DFd)**
2I			Interaction Dose Treatment **Tukey's MCT** *Basal* v/s +1nM Met-enk v/s +100nM Met-enk +1nM Met-enk v/s+100nM Met-enk *1pM RS-ket*	p<0.0001 p<0.0001 p<0.0001 p<0.0001 p<0.0001 p<0.0001 p<0.0001	F(12,42)= 14.31 F(6,42)= 35.35 F(2,42)= 3890 DF=42 DF=42 DF=42 DF=42

			v/s +1nM Met-enk	p<0.0001	DF=42
			v/s +100nM Met-enk	p<0.0001	DF=42
			+1nM Met-enk		
			v/s+100nM Met-enk	p<0.0001	DF=42
			10pM RS-ket	p<0.0001	DF=42
			v/s +1nM Met-enk	p<0.0001	DF=42
			v/s +100nM Met-enk		
			+1nM Met-enk	p<0.0001	DF=42
			v/s+100nM Met-enk	p<0.0001	DF=42
			100pM RS-ket	p<0.0001	DF=42
			v/s +1nM Met-enk		
			v/s +100nM Met-enk	p<0.0001	DF=42
			+1nM Met-enk	p<0.0001	DF=42
			v/s+100nM Met-enk	p<0.0001	DF=42
			1nM RS-ket		
			v/s +1nM Met-enk	p<0.0001	DF=42
			v/s +100nM Met-enk	p<0.0001	DF=42
			+1nM Met-enk	p<0.0001	DF=42
			v/s+100nM Met-enk		
			10nM *RS-ket*	p<0.0001	DF=42
			v/s +1nM Met-enk	p<0.0001	DF=42
			v/s +100nM Met-enk	p<0.0001	DF=42
			+1nM Met-enk		
			v/s+100nM Met-enk		
			100nM RS-ket		
			v/s +1nM Met-enk		
			v/s +100nM Met-enk		
			+1nM Met-enk		
			v/s+100nM Met-enk		
2J			Interaction	p<0.0001	F(12,42)= 30.47
			Dose	p<0.0001	F(6,42)= 1200
			Treatment	p<0.0001	F(2,42)= 354.7
			Tukey's MCT		
			Basal		
			v/s +1nM RS-ket	p>0.9999	DF=42
			v/s +100nM RS-ket	p>0.9999	DF=42
			+1nM RS-ket	p>0.9999	DF=42
			v/s+100nM RS-ket		
			100pM Met-enk	p=0.4379	DF=42
			v/s +1nM RS-ket	p=0.9842	DF=42
			v/s +100nM RS-ket	p=0.5390	DF=42
			+1nM RS-ket		
			v/s+100nM RS-ket	p<0.0001	DF=42
			1nM Met-enk	p=0.8241	DF=42
			v/s +1nM RS-ket	p<0.0001	DF=42
			v/s +100nM RS-ket		
			+1nM RS-ket	p<0.0001	DF=42
			v/s+100nM RS-ket	p<0.0001	DF=42
			10nM *Met-enk*	p<0.0001	DF=42
			v/s +1nM RS-ket		
			v/s +100nM RS-ket	p<0.0001	DF=42
			+1nM RS-ket	p<0.0001	DF=42
			v/s+100nM RS-ket	p<0.0001	DF=42
			100nM Met-enk		
			v/s +1nM RS-ket	p<0.0001	DF=42
			v/s +100nM RS-ket	p<0.0001	DF=42
			+1nM RS-ket	p<0.0001	DF=42
			v/s+100nM RS-ket		
			1μM Met-enk	p<0.0001	DF=42
			v/s +1nM RS-ket	p<0.0001	DF=42
			v/s +100nM RS-ket	p<0.0001	DF=42
			+1nM RS-ket		
			v/s+100nM RS-ket		
			10μM Met-enk		
			v/s +1nM RS-ket		
			v/s +100nM RS-ket		
			+1nM RS-ket		
			v/s+100nM RS-ket		
Fig.	**One-way ANOVA**		**Two-way ANOVA**		
	Test	**p-value**	**Test**	**p-value**	**F (DFn, DFd)**
2K			Interaction	p<0.0001	F(12,42)= 16.04
			Dose	p<0.0001	F(6,42)= 27.09
			Treatment	p<0.0001	F(2,42)= 896.4
			Sidak's MCT		
			Basal		
			v/s +1nM Morp	p=0.9998	DF=42
			v/s +100nM Morp	p<0.0001	DF=42

			+1nM Morp v/s+100nM Morp	p<0.0001	DF=42
			0.1pM RS-ket	p=0.9857	DF=42
			v/s +1nM Morp	p<0.0001	DF=42
			v/s +100nM Morp +1nM Morp	p<0.0001	DF=42
			v/s+100nM Morp	p<0.0001	DF=42
			10pM RS-ket	p<0.0001	DF=42
			v/s +1nM Morp	p<0.0001	DF=42
			v/s +100nM Morp +1nM Morp	p<0.0001	DF=42
			v/s+100nM Morp	p<0.0001	DF=42
			100pM RS-ket	p<0.0001	DF=42
			v/s +1nM Morp		
			v/s +100nM Morp	p<0.0001	DF=42
			+1nM Morp	p<0.0001	DF=42
			v/s+100nM Morp	p<0.0001	DF=42
			1nM RS-ket		
			v/s +1nM Morp	p=0.0009	DF=42
			v/s +100nM Morp	p<0.0001	DF=42
			+1nM Morp v/s+100nM Morp	p<0.0001	DF=42
			10nM *RS-ket*	p=0.0006	DF=42
			v/s +1nM Morp	p<0.0001	DF=42
			v/s +100nM Morp +1nM Morp	p=0.0021	DF=42
			v/s+100nM Morp		
			100nM RS-ket		
			v/s +1nM Morp		
			v/s +100nM Morp +1nM Morp		
			v/s+100nM Morp		
2L			Interaction	p<0.0001	F(18,60)= 35.02
			Dose	p<0.0001	F(9,60)= 185.9
			Treatment	p<0.0001	F(2,60)= 318.5
			Tukey's MCT		
			Basal		
			v/s +1nM RS-ket	p>0.9999	DF=60
			v/s +100nM RS-ket	p>0.9999	DF=60
			+1nM RS-ket v/s+100nM RS-ket	p>0.9999	DF=60
			100pM Morp	p=0.4721	DF=60
			v/s +1nM RS-ket	p=0.1095	DF=60
			v/s +100nM RS-ket +1nM RS-ket	p=0.0057	DF=60
			v/s+100nM RS-ket	p=0.8880	DF=60
			1nM Morp	p=0.0004	DF=60
			v/s +1nM RS-ket	p<0.0001	DF=60
			v/s +100nM RS-ket +1nM RS-ket	p=0.8515	DF=60
			v/s+100nM RS-ket	p=0.0331	DF=60
			3nM Morp	p<0.0078	DF=60
			v/s +1nM RS-ket		
			v/s +100nM RS-ket +1nM RS-ket	p=0.0207 p=0.0083	DF=60 DF=60
			v/s+100nM RS-ket	p<0.0001	DF=60
			10nM *Morp*		
			v/s +1nM RS-ket	p=0.1543	DF=60
			v/s +100nM RS-ket +1nM RS-ket	p=0.0008 p<0.0001	DF=60 DF=60
			v/s+100nM RS-ket		
			30nM *Morp*	p=0.5623	DF=60
			v/s +1nM RS-ket	p<0.0001	DF=60
			v/s +100nM RS-ket +1nM RS-ket	p<0.0001	DF=60
			v/s+100nM RS-ket	p<0.0001	DF=60
			100nM Morp	p<0.0001	DF=60
			v/s +1nM RS-ket	p<0.0001	DF=60
			v/s +100nM RS-ket +1nM RS-ket	p<0.0001	DF=60
			v/s+100nM RS-ket	p<0.0001	DF=60
			300nM Morp	p<0.0001	DF=60
			v/s +1nM RS-ket		
			v/s +100nM RS-ket	p<0.0001	DF=60
			+1nM RS-ket	p<0.0001	DF=60
			v/s+100nM RS-ket	p<0.0001	DF=60
			1μM Morp		
			v/s +1nM RS-ket		

			v/s +100nM RS-ket		
			+1nM RS-ket		
			v/s+100nM RS-ket		
			3μM Morp		
			v/s +1nM RS-ket		
			v/s +100nM RS-ket		
			+1nM RS-ket		
			v/s+100nM RS-ket		
Fig.	**One-way ANOVA**		**Two-way ANOVA**		
	Test	**p-value**	**Test**	**p-value**	**F (DFn, DFd)**
3B			Interaction	p<0.0001	F(10,36)= 8.631
			Dose	p<0.0001	F(5,36)= 876.2
			Treatment	p<0.0001	F(2,36)= 20.66
			Tukey's MCT		
			Basal		
			v/s +1nM RS-ket	p>0.9999	DF=36
			v/s +100nM RS-ket	p>0.9999	DF=36
			+1nM RS-ket	p>0.9999	DF=36
			v/s+100nM RS-ket		
			100pM Leu-enk	p=0.9917	DF=36
			v/s +1nM RS-ket	p=0.9391	DF=36
			v/s +100nM RS-ket	p=0.8998	DF=36
			+1nM RS-ket		
			v/s+100nM RS-ket	p=0.5010	DF=36
			1nM Leu-enk	p=0.9446	DF=36
			v/s +1nM RS-ket	p=0.6992	DF=36
			v/s +100nM RS-ket		
			+1nM RS-ket	p=0.8751	DF=36
			v/s+100nM RS-ket	p=0.4679	DF=36
			10nM *Leu-enk*	p=0.7679	DF=36
			v/s +1nM RS-ket		
			v/s +100nM RS-ket	p=0.0257	DF=36
			+1nM RS-ket	p<0.0001	DF=36
			v/s+100nM RS-ket	p=0.0256	DF=36
			100nM Leu-enk		
			v/s +1nM RS-ket	p<0.0001	DF=36
			v/s +100nM RS-ket	p<0.0001	DF=36
			+1nM RS-ket	p<0.0001	DF=36
			v/s+100nM RS-ket		
			1μM Leu-enk		
			v/s +1nM RS-ket		
			v/s +100nM RS-ket		
			+1nM RS-ket		
			v/s+100nM RS-ket		
3C			Interaction	p<0.0001	F(10,36)= 20.97
			Dose	p<0.0001	F(5,36)= 1006
			Treatment	p<0.0001	F(2,36)= 81.82
			Sidak's MCT		
			Basal		
			v/s +1nM RS-ket	p>0.9999	DF=36
			v/s +100nM RS-ket	p>0.9999	DF=36
			+1nM RS-ket	p>0.9999	DF=36
			v/s+100nM RS-ket		
			100pM Dyn A17	p>0.9999	DF=36
			v/s +1nM RS-ket	p>0.9999	DF=36
			v/s +100nM RS-ket	p=0.9992	DF=36
			+1nM RS-ket		
			v/s+100nM RS-ket	p>0.9999	DF=36
			1nM Dyn A17	p=0.8825	DF=36
			v/s +1nM RS-ket	p=0.6240	DF=36
			v/s +100nM RS-ket		
			+1nM RS-ket	p-0.1061	DF=36
			v/s+100nM RS-ket	p=0.0006	DF=36
			10nM *Dyn A17*	p=0.7439	DF=36
			v/s +1nM RS-ket		
			v/s +100nM RS-ket	p=0.0067	DF=36
			+1nM RS-ket	p<0.0001	DF=36
			v/s+100nM RS-ket	p=0.0152	DF=36
			100nM Dyn A17		
			v/s +1nM RS-ket	p<0.0001	DF=36
			v/s +100nM RS-ket	p<0.0001	DF=36
			+1nM RS-ket	p<0.0001	DF=36
			v/s+100nM RS-ket		
			1μM Dyn A17		
			v/s +1nM RS-ket		
			v/s +100nM RS-ket		

			+1nM RS-ket v/s+100nM RS-ket		
3D			Interaction Dose Treatment **Sidak's MCT** *Basal* v/s +1nM RS-ket v/s +100nM RS-ket +1nM RS-ket v/s+100nM RS-ket *100pM Met-enk* v/s +1nM RS-ket v/s +100nM RS-ket +1nM RS-ket v/s+100nM RS-ket *1nM Met-enk* v/s +1nM RS-ket v/s +100nM RS-ket +1nM RS-ket v/s+100nM RS-ket 10nM *Met-enk* v/s +1nM RS-ket v/s +100nM RS-ket +1nM RS-ket v/s+100nM RS-ket *100nM Met-enk* v/s +1nM RS-ket v/s +100nM RS-ket +1nM RS-ket v/s+100nM RS-ket *1μM Met-enk* v/s +1nM RS-ket v/s +100nM RS-ket +1nM RS-ket v/s+100nM RS-ket	p<0.0001 p<0.0001 p<0.0001 p>0.9999 p>0.9999 p>0.9999 p>0.9999 p>0.9999 p>0.9999 p>0.9999 p>0.9999 p>0.9999 p>0.9999 p=0.9988 p>0.9999 p>0.9999 p=0.5613 p=0.9522 p<0.0001 p<0.0001 p=0.0306	F(10,36)= 7.887 F(5,36)= 692.4 F(2,36)= 17.50 DF=36 DF=36 DF=36 DF=36 DF=36 DF=36 DF=36 DF=36 DF=36 DF=36 DF=36 DF=36 DF=36 DF=36 DF=36
Fig.	**One-way ANOVA**		**Two-way ANOVA**		
	Test	**p-value**	**Test**	**p-value**	**F (DFn, DFd)**
3E			Interaction Dose Treatment **Tukey's MCT** *Basal* v/s +1nM RS-ket v/s +100nM RS-ket +1nM RS-ket v/s+100nM RS-ket *100pM Leu-enk* v/s +1nM RS-ket v/s +100nM RS-ket +1nM RS-ket v/s+100nM RS-ket *1nM Leu-enk* v/s +1nM RS-ket v/s +100nM RS-ket +1nM RS-ket v/s+100nM RS-ket 10nM *Leu-enk* v/s +1nM RS-ket v/s +100nM RS-ket +1nM RS-ket v/s+100nM RS-ket *100nM Leu-enk* v/s +1nM RS-ket v/s +100nM RS-ket +1nM RS-ket v/s+100nM RS-ket *1μM Leu-enk* v/s +1nM RS-ket v/s +100nM RS-ket +1nM RS-ket v/s+100nM RS-ket	P=0.0002 p<0.0001 p<0.0001 p>0.9999 p>0.9999 p>0.9999 p=0.8915 p=0.8842 p=0.9999 p=0.7340 p=0.2327 p=0.6365 p=0.6777 p=0.0271 p=0.1639 p=0.1376 p<0.0001 p=0.0003 p<0.0001 p<0.0001 p=0.0958	F(10,36)= 4.825 F(5,36)= 983.8 F(2,36)= 27.25 DF=36 DF=36 DF=36 DF=36 DF=36 DF=36 DF=36 DF=36 DF=36 DF=36 DF=36 DF=36 DF=36 DF=36 DF=36
3F			Interaction Dose Treatment **Tukey's MCT** *Basal*	p=0.5862 p<0.0001 p<0.0001	F(10,36)= 0.8494 F(5,36)= 146.2 F(2,36)= 13.39

			v/s +1nM RS-ket	p>0.9999	DF=36
			v/s +100nM RS-ket	p>0.9999	DF=36
			+1nM RS-ket	p>0.9999	DF=36
			v/s+100nM RS-ket		
			100pM Dyn A17	p=0.7827	DF=36
			v/s +1nM RS-ket	p=0.4729	DF=36
			v/s +100nM RS-ket	p=0.8669	DF=36
			+1nM RS-ket		
			v/s+100nM RS-ket	p=0.3881	DF=36
			1nM Dyn A17	p=0.0606	DF=36
			v/s +1nM RS-ket	p=0.5646	DF=36
			v/s +100nM RS-ket		
			+1nM RS-ket	p=0.1538	DF=36
			v/s+100nM RS-ket	p=0.0283	DF=36
			10nM *Dyn A17*	p=0.7104	DF=36
			v/s +1nM RS-ket		
			v/s +100nM RS-ket	p=0.0734	DF=36
			+1nM RS-ket	p=0.0137	DF=36
			v/s+100nM RS-ket	p=0.7554	DF=36
			100nM Dyn A17		
			v/s +1nM RS-ket	p=0.0499	DF=36
			v/s +100nM RS-ket	p=0.0090	DF=36
			+1nM RS-ket	p=0.7636	DF=36
			v/s+100nM RS-ket		
			1μM Dyn A17		
			v/s +1nM RS-ket		
			v/s +100nM RS-ket		
			+1nM RS-ket		
			v/s+100nM RS-ket		
3G			Interaction	p=0.1588	F(10,36)= 1.56
			Dose	p<0.0001	F(5,36)= 129.2
			Treatment	p=0.0035	F(2,36)= 6.638
			Tukey's MCT		
			Basal		
			v/s +1nM RS-ket	p>0.9999	DF=36
			v/s +100nM RS-ket	p>0.9999	DF=36
			+1nM RS-ket	p>0.9999	DF=36
			v/s+100nM RS-ket		
			100pM Met-enk	p=0.9991	DF=36
			v/s +1nM RS-ket	p=0.9819	DF=36
			v/s +100nM RS-ket	p=0.9890	DF=36
			+1nM RS-ket		
			v/s+100nM RS-ket	p=0.9405	DF=36
			1nM Met-enk	p=0.7156	DF=36
			v/s +1nM RS-ket	p=0.8950	DF=36
			v/s +100nM RS-ket		
			+1nM RS-ket	p=0.7866	DF=36
			v/s+100nM RS-ket	p=0.5077	DF=36
			10nM *Met-enk*	p=0.8909	DF=36
			v/s +1nM RS-ket		
			v/s +100nM RS-ket	p=0.0110	DF=36
			+1nM RS-ket	p=0.0649	DF=36
			v/s+100nM RS-ket	p=0.7372	DF=36
			100nM Met-enk		
			v/s +1nM RS-ket	p=0.0317	DF=36
			v/s +100nM RS-ket	p=0.0008	DF=36
			+1nM RS-ket	p=0.3646	DF=36
			v/s+100nM RS-ket		
			1μM Met-enk		
			v/s +1nM RS-ket		
			v/s +100nM RS-ket		
			+1nM RS-ket		
			v/s+100nM RS-ket		
Fig.	**One-way ANOVA**		**Two-way ANOVA**		
	Test	**p-value**	**Test**	**p-value**	**F (DFn, DFd)**
3H			Interaction	p=0.9365	F(10,36)= 0.4028
			Dose	p<0.0001	F(5,36)= 177.9
			Treatment	p=0.1929	F(2,36)= 1.723
			Tukey's MCT		
			Basal		
			v/s +1nM RS-ket	p>0.9999	DF=36
			v/s +100nM RS-ket	p>0.9999	DF=36
			+1nM RS-ket	p>0.9999	DF=36
			v/s+100nM RS-ket		
			100pM Leu-enk	p=0.9684	DF=36
			v/s +1nM RS-ket	p=0.9149	DF=36
			v/s +100nM RS-ket	p=0.9859	DF=36

			+1nM RS-ket v/s+100nM RS-ket *1nM Leu-enk* v/s +1nM RS-ket v/s +100nM RS-ket +1nM RS-ket v/s+100nM RS-ket 10nM *Leu-enk* v/s +1nM RS-ket v/s +100nM RS-ket +1nM RS-ket v/s+100nM RS-ket *100nM Leu-enk* v/s +1nM RS-ket v/s +100nM RS-ket +1nM RS-ket v/s+100nM RS-ket *1μM Leu-enk* v/s +1nM RS-ket v/s +100nM RS-ket +1nM RS-ket v/s+100nM RS-ket	 p=0.9711 p=0.6282 p=0.7683 p=0.4379 p=0.5807 p=0.9692 p=0.4039 p=0.5249 p=0.9764 p=0.5788 p=0.2473 p=0.8075	 DF=36 DF=36 DF=36 DF=36 DF=36 DF=36 DF=36 DF=36 DF=36 DF=36 DF=36 DF=36
3I			Interaction Dose Treatment **Tukey's MCT** *Basal* v/s +1nM RS-ket v/s +100nM RS-ket +1nM RS-ket v/s+100nM RS-ket *100pM Dyn A17* v/s +1nM RS-ket v/s +100nM RS-ket +1nM RS-ket v/s+100nM RS-ket *1nM Dyn A17* v/s +1nM RS-ket v/s +100nM RS-ket +1nM RS-ket v/s+100nM RS-ket 10nM *Dyn A17* v/s +1nM RS-ket v/s +100nM RS-ket +1nM RS-ket v/s+100nM RS-ket *100nM Dyn A17* v/s +1nM RS-ket v/s +100nM RS-ket +1nM RS-ket v/s+100nM RS-ket *1μM Dyn A17* v/s +1nM RS-ket v/s +100nM RS-ket +1nM RS-ket v/s+100nM RS-ket	p=0.0061 p<0.0001 p<0.0001 p>0.9999 p>0.9999 p>0.9999 p=0.9581 p=0.2807 p=0.1751 p=0.3267 p=0.0819 p=0.7256 p=0.0320 p=0.0688 p=0.9384 p=0.0200 p=0.0170 p=0.9975 p=0.0004 p<0.0001 p=0.0511	F(10,36)= 3.097 F(5,36)= 661.5 F(2,36)= 21.44 DF=36 DF=36 DF=36 DF=36 DF=36 DF=36 DF=36 DF=36 DF=36 DF=36 DF=36 DF=36 DF=36 DF=36 DF=36
Fig.	**One-way ANOVA**		**Two-way ANOVA**		
	Test	**p-value**	**Test**	**p-value**	**F (DFn, DFd)**
4A			Interaction Dose Treatment **Sidak's MCT** *Basal* v/s +1nM R-ket v/s +100nM R-ket +1nM R-ket v/s+100nM R-ket *100pM Met-enk* v/s +1nM R-ket v/s +100nM R-ket +1nM R-ket v/s+100nM R-ket *1nM Met-enk* v/s +1nM R-ket v/s +100nM R-ket +1nM R-ket v/s+100nM R-ket	p<0.0001 p<0.0001 p<0.0001 p>0.9999 p>0.9999 p>0.9999 p<0.0001 p=0.0007 p=0.9041 p<0.0001 p<0.0001 p>0.9999 p<0.0001 p<0.0001	F(10,36)= 15.97 F(5,36)= 799.5 F(2,36)= 237.9 DF=36 DF=36 DF=36 DF=36 DF=36 DF=36 DF=36 DF=36 DF=36 DF=36 DF=36

			10nM *Met-enk*	p=0.6886	DF=36
			v/s +1nM R-ket		
			v/s +100nM R-ket	p<0.0001	DF=36
			+1nM R-ket	p<0.0001	DF=36
			v/s+100nM R-ket	p=0.2104	DF=36
			100nM Met-enk		
			v/s +1nM R-ket	p<0.0001	DF=36
			v/s +100nM R-ket	p<0.0001	DF=36
			+1nM R-ket	p=0.9179	DF=36
			v/s+100nM R-ket		
			1μM Met-enk		
			v/s +1nM R-ket		
			v/s +100nM R-ket		
			+1nM R-ket		
			v/s+100nM R-ket		
4B			Interaction	p<0.0001	F(10,36)= 78.57
			Dose	p<0.0001	F(5,36)= 1081
			Treatment	p<0.0001	F(2,36)= 680.5
			Tukey's MCT		
			Basal		
			v/s +1nM S-ket	p>0.9999	DF=36
			v/s +100nM S-ket	p>0.9999	DF=36
			+1nM S-ket	p>0.9999	DF=36
			v/s+100nM S-ket		
			100pM Met-enk	p<0.0001	DF=36
			v/s +1nM S-ket	p<0.0001	DF=36
			v/s +100nM S-ket	p=0.7893	DF=36
			+1nM S-ket		
			v/s+100nM S-ket	p<0.0001	DF=36
			1nM Met-enk	p<0.0001	DF=36
			v/s +1nM S-ket	p=0.8933	DF=36
			v/s +100nM S-ket		
			+1nM S-ket	p<0.0001	DF=36
			v/s+100nM S-ket	p<0.0001	DF=36
			10nM *Met-enk*	p=0.7748	DF=36
			v/s +1nM S-ket		
			v/s +100nM S-ket	p<0.0001	DF=36
			+1nM S-ket	p<0.0001	DF=36
			v/s+100nM S-ket	p=0.0288	DF=36
			100nM Met-enk		
			v/s +1nM S-ket	p<0.0001	DF=36
			v/s +100nM S-ket	p<0.0001	DF=36
			+1nM S-ket	p=0.0101	DF=36
			v/s+100nM S-ket		
			1μM Met-enk		
			v/s +1nM S-ket		
			v/s +100nM S-ket		
			+1nM S-ket		
			v/s+100nM S-ket		
4C			Interaction	P=0.9979	F(10,36)=0.1620
			Dose	p<0.0001	F(5,36)= 564.5
			Treatment	p=0.2502	F(2,36)= 1.440
			Tukey's MCT		
			Basal		
			v/s +1nM R-ket	p>0.9999	DF=36
			v/s +100nM R-ket	p>0.9999	DF=36
			+1nM R-ket	p>0.9999	DF=36
			v/s+100nM R-ket		
			100pM Met-enk	p=0.9483	DF=36
			v/s +1nM R-ket	p=0.9973	DF=36
			v/s +100nM R-ket	p=0.9236	DF=36
			+1nM R-ket		
			v/s+100nM R-ket	p=0.7639	DF=36
			1nM Met-enk	p=0.9366	DF=36
			v/s +1nM R-ket	p=0.5526	DF=36
			v/s +100nM R-ket		
			+1nM R-ket	p=0.7492	DF=36
			v/s+100nM R-ket	p=0.8154	DF=36
			10nM *Met-enk*	p=0.9925	DF=36
			v/s +1nM R-ket		
			v/s +100nM R-ket	p=0.4852	DF=36
			+1nM R-ket	p=0.9326	DF=36
			v/s+100nM R-ket	p=0.7040	DF=36
			100nM Met-enk		
			v/s +1nM R-ket	p=0.5442	DF=36
			v/s +100nM R-ket	p=0.9422	DF=36
				p=0.7463	DF=36

			+1nM R-ket		
			v/s+100nM R-ket		
			1μM Met-enk		
			v v/s +1nM R-ket		
			v/s +100nM R-ket		
			+1nM R-ket		
			v/s+100nM R-ket		
Fig.	**One-way ANOVA**		**Two-way ANOVA**		
	Test	**p-value**	**Test**	**p-value**	**F (DFn, DFd)**
4D			Interaction	p<0.0001	F(10,36)=40.32
			Dose	p<0.0001	F(5,36)= 1260
			Treatment	p<0.0001	F(2,36)= 356.6
			Tukey's MCT		
			Basal		
			v/s +1nM S-ket	p>0.9999	DF=36
			v/s +100nM S-ket	p>0.9999	DF=36
			+1nM S-ket	p>0.9999	DF=36
			v/s+100nM S-ket		
			100pM Met-enk	p=0.1598	DF=36
			v/s +1nM S-ket	p=0.3100	DF=36
			v/s +100nM S-ket	p=0.9186	DF=36
			+1nM S-ket		
			v/s+100nM S-ket	p<0.0001	DF=36
			1nM Met-enk	p<0.0001	DF=36
			v/s +1nM S-ket	p=0.7102	DF=36
			v/s +100nM S-ket		
			+1nM S-ket	p<0.0001	DF=36
			v/s+100nM S-ket	p<0.0001	DF=36
			10nM *Met-enk*	p=0.0001	DF=36
			v/s +1nM S-ket		
			v/s +100nM S-ket	p<0.0001	DF=36
			+1nM S-ket	p<0.0001	DF=36
			v/s+100nM S-ket	p<0.0001	DF=36
			100nM Met-enk		
			v/s +1nM S-ket	p<0.0001	DF=36
			v/s +100nM S-ket	p<0.0001	DF=36
			+1nM S-ket	p<0.0001	DF=36
			v/s+100nM S-ket		
			1μM Met-enk		
			v/s +1nM S-ket		
			v/s +100nM S-ket		
			+1nM S-ket		
			v/s+100nM S-ket		
5A			Interaction	p<0.0001	F(8,30)=27.72
			Dose	p<0.0001	F(4,30)= 629.7
			Treatment	p<0.0001	F(2,30)= 284.5
			Tukey's MCT		
			Basal		
			v/s +1nM RS-NK	p>0.9999	DF=30
			v/s +100nM RS-NK	p>0.9999	DF=30
			+1nM RS-NK	p>0.9999	DF=30
			v/s+100nM RS-NK		
			100pM Met-enk	p=0.7954	DF=30
			v/s +1nM RS-NK	p<0.0001	DF=30
			v/s +100nM RS-NK	p<0.0001	DF=30
			+1nM RS-NK		
			v/s+100nM RS-NK	p=0.0060	DF=30
			1nM Met-enk	p<0.0001	DF=30
			v/s +1nM RS-NK	p<0.0001	DF=30
			v/s +100nM RS-NK		
			+1nM RS-NK	p=0.0002	DF=30
			v/s+100nM RS-NK	p<0.0001	DF=30
			10nM *Met-enk*	p<0.0001	DF=30
			v/s +1nM RS-NK		
			v/s +100nM RS-NK	p<0.0001	DF=30
			+1nM RS-NK	p<0.0001	DF=30
			v/s+100nM RS-NK	p<0.0001	DF=30
			100nM Met-enk		
			v/s +1nM RS-NK		
			v/s +100nM RS-NK		
			+1nM RS-NK		
			v/s+100nM RS-NK		
5B	**One-way ANOVA**				
	Treatment	p<0.001; F(7,15)=154.4			
	Tukey's MCP				
	Basal v/s 1nM RS-NK	p=0.7786; DF=15			

	Basal v/s 1nM R-NK	p=0.9187; DF=15			
		p=0.6296; DF=15			
	Basal v/s 1nM S-NK	p<0.0001; DF=15			
	Basal v/s 100nM Met-enk	p<0.0001; DF=15			
	Basal v/s 100nM Met-enk+ 1nM RS-NK	p<0.0001; DF=15			
		p<0.0001; DF=15			
	Basal v/s 100nM Met-enk+ 1nM R-NK	p=0.9997; DF=15			
		p>0.9999; DF=15			
	Basal v/s 100nM Met-enk+ 1nM S-NK	p<0.0001; DF=15			
		p<0.0001; DF=15			
	1nM RS-NK v/s 1nM R-NK	p<0.0001; DF=15			
		p<0.0001; DF=15			
	1nM RS-NK v/s 1nM S-NK	p=0.9984; DF=15			
		p<0.0001; DF=15			
	1nM RS-NK v/s 100nM Met-enk	p<0.0001; DF=15			
	1nM RS-NK v/s 100nM Met-enk+1nM RS-NK	p<0.0001; DF=15			
		p<0.0001; DF=15			
	1nM RS-NK v/s 100nM Met-enk+1nM R-NK	p<0.0001; DF=15			
		p<0.0001; DF=15			
	1nM RS-NK v/s 100nM Met-enk+1nM S-NK	p<0.0001; DF=15			
	1nM R-NK v/s 1nM S-NK	p<0.0001; DF=15			
		p<0.0001; DF=15			
	1nM R-NK v/s 100nM Met-enk	p=0.8247; DF=15			
	1nM R-NK v/s 100nM Met-enk+1nM RS-NK	p=0.9987; DF=15			
		p=0.0026; DF=15			
	1nM R-NK v/s 100nM Met-enk+1nM R-NK	p=0.5009; DF=15			
		p=0.0382; DF=15			
	1nM R-NK v/s 100nM Met-enk+1nM S-NK	p=0.0009; DF=15			
	1nM S-NK v/s 100nM Met-enk				
	1nM S-NK v/s 100nM Met-enk+1nM RS-NK				
	1nM S-NK v/s 100nM Met-enk+1nM R-NK				
	1nM S-NK v/s 100nM Met-enk+1nM S-NK				
	100nM Met-enk v/s 100nM Met-enk+1nM RS-NK				
	100nM Met-enk v/s 100nM Met-enk+1nM R-NK				
	100nM Met-enk v/s 100nM Met-enk+1nM S-NK				
	100nM Met-enk+1nM RS-NK v/s 100nM Met-enk+1nM R-NK				
	100nM Met-enk+1nM RS-NK v/s 100nM Met-enk+1nM S-NK				
	100nM Met-enk+1nM R-NK v/s 100nM Met-enk+1nM S-NK				
Fig.	**One-way ANOVA**		**Two-way ANOVA**		
	Test	**p-value**	**Test**	**p-value**	**F (DFn, DFd)**

5C			Interaction	p<0.0001	F(15,48)=6.040
			Dose	p<0.0001	F(5,48)= 433.5
			Treatment	p<0.0001	F(3,48)= 28.71
			Tukey's MCT		
			Basal		
			v/s +1nM RS-NK	p>0.9999	DF=48
			v/s +1nM R-NK	p>0.9999	DF=48
			v/s +1nM S-NK	p>0.9999	DF=48
			+1nM RS-NK	p>0.9999	DF=48
			v/s+1nM R-NK	p>0.9999	DF=48
			+1nM RS-NK	p>0.9999	DF=48
			v/s+1nM S-NK		
			+1nM R-NK v/s+1nM	p>0.9999	DF=48
			S-NK	p=0.3126	DF=48
			100pM Met-enk	p=0.6104	DF=48
			v/s +1nM RS-NK	p=0.3081	DF=48
			v/s +1nM R-NK	p=0.6047	DF=48
			v/s +1nM S-NK	p=0.9556	DF=48
			+1nM RS-NK		
			v/s+1nM R-NK	p=0.2532	DF=48
			+1nM RS-NK	p=0.1064	DF=48
			v/s+1nM S-NK	p=0.5857	DF=48
			+1nM R-NK v/s+1nM	p=0.9687	DF=48
			S-NK	p=0.9309	DF=48
			1nM Met-enk	p=0.7181	DF=48
			v/s +1nM RS-NK		
			v/s +1nM R-NK	p=0.0494	DF=48
			v/s +1nM S-NK	p=0.0061	DF=48
			+1nM RS-NK	p=0.0015	DF=48
			v/s+1nM R-NK	p=0.8580	DF=48
			+1nM RS-NK	p=0.5929	DF=48
			v/s+1nM S-NK	p=0.9657	DF=48
			+1nM R-NK v/s+1nM		
			S-NK	p=0.0028	DF=48
			10nM *Met-enk*	p=0.7014	DF=48
			v/s +1nM RS-NK	p<0.0001	DF=48
			v/s +1nM R-NK	p=0.0522	DF=48
			v/s +1nM S-NK	p=0.0041	DF=48
			+1nM RS-NK	p<0.0001	DF=48
			v/s+1nM R-NK		
			+1nM RS-NK	p<0.0001	DF=48
			v/s+1nM S-NK	p=0.0296	DF=48
			+1nM R-NK v/s+1nM	p<0.0001	DF=48
			S-NK	p=0.1287	DF=48
			100nM Met-enk	p=0.0041	DF=48
			v/s +1nM RS-NK	p<0.0001	DF=48
			v/s +1nM R-NK		
			v/s +1nM S-NK		
			+1nM RS-NK		
			v/s+1nM R-NK		
			+1nM RS-NK		
			v/s+1nM S-NK		
			+1nM R-NK v/s+1nM		
			S-NK		
			1μM Met-enk		
			v/s +1nM RS-NK		
			v/s +1nM R-NK		
			v/s +1nM S-NK		
			+1nM RS-NK		
			v/s+1nM R-NK		
			+1nM RS-NK		
			v/s+1nM S-NK		
			+1nM R-NK v/s+1nM		
			S-NK		
Fig.	**One-way ANOVA**		**Two-way ANOVA**		
	Test	**p-value**	**Test**	**p-value**	**F (DFn, DFd)**
5D			Interaction	p<0.0001	F(10,36)=9.424
			Dose	p<0.0001	F(5,36)= 535.3
			Treatment	p<0.0001	F(2,36)= 99.05
			Tukey's MCT		
			Basal		
			v/s +10nM RR-HNK	p>0.9999	DF=36
			v/s +10nM SS-HNK	p>0.9999	DF=36
			+10nM RR-HNK	p>0.9999	DF=36
			v/s+10nM SS-HNK		
			100pM Met-enk	p=0.6049	DF=36
			v/s +10nM RR-HNK	p=0.6810	DF=36

			v/s +10nM SS-HNK	p=0.9917	DF=36
			+10nM RR-HNK		
			v/s+10nM SS-HNK	p<0.0001	DF=36
			1nM Met-enk	p<0.0001	DF=36
			v/s +10nM RR-HNK	p=0.3358	DF=36
			v/s +10nM SS-HNK		
			+10nM RR-HNK	p=0.0028	DF=36
			v/s+10nM SS-HNK	p<0.0001	DF=36
			10nM *Met-enk*	p<0.0001	DF=36
			v/s +10nM RR-HNK		
			v/s +10nM SS-HNK	p<0.0001	DF=36
			+10nM RR-HNK	p<0.0001	DF=36
			v/s+10nM SS-HNK	p=0.1351	DF=36
			100nM Met-enk		
			v/s +10nM RR-HNK	p<0.0001	DF=36
			v/s +10nM SS-HNK	p<0.0001	DF=36
			+10nM RR-HNK	p=0.4170	DF=36
			v/s+10nM SS-HNK		
			1μM Met-enk		
			v/s +10nM RR-HNK		
			v/s +10nM SS-HNK		
			+10nM RR-HNK		
			v/s+10nM SS-HNK		
5E			Interaction	p<0.0001	F(10,36)=96.56
			Dose	p<0.0001	F(5,36)= 2733
			Treatment	p<0.0001	F(2,36)= 1015
			Tukey's MCT		
			Basal		
			v/s +1nM RS-NK	p>0.9999	DF=36
			v/s +100nM RS-NK	p>0.9999	DF=36
			+1nM RS-NK	p>0.9999	DF=36
			v/s+100nM RS-NK		
			100pM Met-enk	p=0.0197	DF=36
			v/s +1nM RS-NK	p=0.0011	DF=36
			v/s +100nM RS-NK	p=0.5376	DF=36
			+1nM RS-NK		
			v/s+100nM RS-NK	p<0.0001	DF=36
			1nM Met-enk	p<0.0001	DF=36
			v/s +1nM RS-NK	p<0.0001	DF=36
			v/s +100nM RS-NK		
			+1nM RS-NK	p<0.0001	DF=36
			v/s+100nM RS-NK	p<0.0001	DF=36
			10nM *Met-enk*	p<0.0001	DF=36
			v/s +1nM RS-NK		
			v/s +100nM RS-NK	p<0.0001	DF=36
			+1nM RS-NK	p<0.0001	DF=36
			v/s+100nM RS-NK	p<0.0001	DF=36
			100nM Met-enk		
			v/s +1nM RS-NK	p<0.0001	DF=36
			v/s +100nM RS-NK	p<0.0001	DF=36
			+1nM RS-NK	p=0.0001	DF=36
			v/s+100nM RS-NK		
			1μM Met-enk		
			v/s +1nM RS-NK		
			v/s +100nM RS-NK		
			+1nM RS-NK		
			v/s+100nM RS-NK		
5F			Interaction	p<0.0001	F(10,36)=8.195
			Dose	p<0.0001	F(5,36)= 2048
			Treatment	p<0.0001	F(2,36)= 67.52
			Tukey's MCT		
			Basal		
			v/s +1nM R-NK	p>0.9999	DF=36
			v/s +100nM R-NK	p>0.9999	DF=36
			+1nM R-NK	p>0.9999	DF=36
			v/s+100nM R-NK		
			100pM Met-enk	p=0.4532	DF=36
			v/s +1nM R-NK	p=0.9917	DF=36
			v/s +100nM R-NK	p=0.5261	DF=36
			+1nM R-NK		
			v/s+100nM R-NK	p=0.1392	DF=36
			1nM Met-enk	p>0.9999	DF=36
			v/s +1nM R-NK	p=0.1392	DF=36
			v/s +100nM R-NK		
			+1nM R-NK	p<0.0001	DF=36
			v/s+100nM R-NK	p=0.0030	DF=36
			10nM *Met-enk*	p<0.0001	DF=36

			v/s +1nM R-NK		
			v/s +100nM R-NK	p<0.0001	DF=36
			+1nM R-NK	p=0.0611	DF=36
			v/s+100nM R-NK	p<0.0001	DF=36
			100nM Met-enk		
			v/s +1nM R-NK	p<0.0001	DF=36
			v/s +100nM R-NK	p=0.1074	DF=36
			+1nM R-NK	p<0.0001	DF=36
			v/s+100nM R-NK		
			1μM Met-enk		
			v/s +1nM R-NK		
			v/s +100nM R-NK		
			+1nM R-NK		
			v/s+100nM R-NK		
5G			Interaction	p<0.0001	F(10,36)=118.1
			Dose	p<0.0001	F(5,36)= 2622
			Treatment	p<0.0001	F(2,36)= 1044
			Tukey's MCT		
			Basal		
			v/s +1nM S-NK	p>0.9999	DF=36
			v/s +100nM S-NK	p>0.9999	DF=36
			+1nM S-NK	p>0.9999	DF=36
			v/s+100nM S-NK		
			100pM Met-enk	p=0.6284	DF=36
			v/s +1nM S-NK	p=0.2039	DF=36
			v/s +100nM S-NK	p=0.6951	DF=36
			+1nM S-NK		
			v/s+100nM S-NK	p<0.0001	DF=36
			1nM Met-enk	p<0.0001	DF=36
			v/s +1nM S-NK	p=0.9332	DF=36
			v/s +100nM S-NK		
			+1nM S-NK	p<0.0001	DF=36
			v/s+100nM S-NK	p<0.0001	DF=36
			10nM *Met-enk*	p=0.8718	DF=36
			v/s +1nM S-NK		
			v/s +100nM S-NK	p<0.0001	DF=36
			+1nM S-NK	p<0.0001	DF=36
			v/s+100nM S-NK	p=0.2290	DF=36
			100nM Met-enk		
			v/s +1nM S-NK	p<0.0001	DF=36
			v/s +100nM S-NK	p<0.0001	DF=36
			+1nM S-NK	p=0.2484	DF=36
			v/s+100nM S-NK		
			1μM Met-enk		
			v/s +1nM S-NK		
			v/s +100nM S-NK		
			+1nM S-NK		
			v/s+100nM S-NK		
Fig.	**One-way ANOVA**		**Two-way ANOVA**		
	Test	**p-value**	**Test**	**p-value**	**F (DFn, DFd)**
5H			Interaction	p<0.0001	F(10,36)=66.71
			Dose	p<0.0001	F(5,36)= 2833
			Treatment	p<0.0001	F(2,36)= 632.6
			Tukey's MCT		
			Basal		
			v/s +1nM RR-HNK	p>0.9999	DF=36
			v/s +100nM RR-HNK	p>0.9999	DF=36
			+1nM RR-HNK	p>0.9999	DF=36
			v/s+100nM RR-HNK		
			100pM Met-enk	p=0.0879	DF=36
			v/s +1nM RR-HNK	p=0.9374	DF=36
			v/s +100nM RR-HNK	p=0.0416	DF=36
			+1nM RR-HNK		
			v/s+100nM RR-HNK	p<0.0001	DF=36
			1nM Met-enk	p=0.4344	DF=36
			v/s +1nM RR-HNK	p<0.0001	DF=36
			v/s +100nM RR-HNK		
			+1nM RR-HNK	p<0.0001	DF=36
			v/s+100nM RR-HNK	p<0.0001	DF=36
			10nM *Met-enk*	p<0.0001	DF=36
			v/s +1nM RR-HNK		
			v/s +100nM RR-HNK	p<0.0001	DF=36
			+1nM RR-HNK	p<0.0001	DF=36
			v/s+100nM RR-HNK	p<0.0001	DF=36
			100nM Met-enk		
			v/s +1nM RR-HNK	p<0.0001	DF=36
			v/s +100nM RR-HNK	p<0.0001	DF=36

			+1nM RR-HNK v/s+100nM RR-HNK *1μM Met-enk* v/s +1nM RR-HNK v/s +100nM RR-HNK +1nM RR-HNK v/s+100nM RR-HNK	p<0.0001	DF=36
Fig.	**One-way ANOVA**		**Two-way ANOVA**		
	Test	**p-value**	**Test**	**p-value**	**F (DFn, DFd)**
5I			Interaction Dose Treatment **Tukey's MCT** *Basal* v/s +1nM SS-HNK v/s +100nM SS-HNK +1nM SS-HNK v/s+100nM SS-HNK *100pM Met-enk* v/s +1nM SS-HNK v/s +100nM SS-HNK +1nM SS-HNK v/s+100nM SS-HNK *1nM Met-enk* v/s +1nM SS-HNK v/s +100nM SS-HNK +1nM SS-HNK v/s+100nM SS-HNK 10nM *Met-enk* v/s +1nM SS-HNK v/s +100nM SS-HNK +1nM SS-HNK v/s+100nM SS-HNK *100nM Met-enk* v/s +1nM SS-HNK v/s +100nM SS-HNK +1nM SS-HNK v/s+100nM SS-HNK *1μM Met-enk* v/s +1nM SS-HNK v/s +100nM SS-HNK +1nM SS-HNK v/s+100nM SS-HNK	p<0.0001 p<0.0001 p<0.0001 p>0.9999 p>0.9999 p>0.9999 p=0.3216 p=0.4101 p=0.9840 p<0.0001 p<0.0001 p=0.2894 p<0.0001 p<0.0001 p=0.7646 p<0.0001 p<0.0001 p=0.2894 p<0.0001 p<0.0001 p=0.2894	F(10,36)=13.07 F(5,36)= 1334 F(2,36)= 146.5 DF=36 DF=36 DF=36 DF=36 DF=36 DF=36 DF=36 DF=36 DF=36 DF=36 DF=36 DF=36 DF=36 DF=36 DF=36
6A			Interaction Dose Treatment **Tukey's MCT** *Basal* v/s +1 nM RS-ket v/s +100 nM RS-ket *1pM DAMGO* v/s +1 nM RS-ket v/s +100 nM RS-ket *10pM DAMGO* v/s +1 nM RS-ket v/s +100 nM RS-ket *100pM DAMGO* v/s +1 nM RS-ket v/s +100 nM RS-ket *1nM DAMGO* v/s +1 nM RS-ket v/s +100 nM RS-ket *10nM DAMGO* v/s +1 nM RS-ket v/s +100 nM RS-ket *100nM DAMGO* v/s +1 nM RS-ket v/s +100 nM RS-ket *1μM DAMGO* v/s +1 nM RS-ket v/s +100 nM RS-ket *10μM DAMGO* v/s +1 nM RS-ket v/s +100 nM RS-ket	p<0.0001 p<0.0001 p<0.0001 p>0.9999 p>0.9999 p=0.9731 p=0.9813 p=0.8258 p=0.1898 p=0.1574 p<0.0001 p=0.0006 p<0.0001 p=0.0022 p<0.0001 p=0.0008 p<0.0001 p=0.0035 p<0.0001 p=0.0040 p<0.0001	F(16,81)=4.750 F(8,81)= 221.9 F(2,81)= 92.57 DF=81 DF=81 DF=81 DF=81 DF=81 DF=81 DF=81 DF=81 DF=81 DF=81 DF=81 DF=81 DF=81 DF=81 DF=81 DF=81
6C			Interaction Dose Treatment	p=0.1296 p<0.0001 p<0.0001	F(3,27)=2.056 F(3,27)= 30.85 F(1,27)= 40.09

			Sidak's MCT *10 nM Met-enk* v/s +10 nM RS-ket *100 nM Met-enk* v/s +10 nM RS-ket *1μM Met-enk* v/s +10 nM RS-ket *10μM Met-enk* v/s +10 nM RS-ket	 p=0.0682 p=0.0002 p=0.0230 p=0.1358	 DF=27 DF=27 DF=27 DF=27